no. 2

SEARS FOUNDATION FOR MARINE RESEARCH
BINGHAM OCEANOGRAPHIC LABORATORY, YALE UNIVERSITY

JAN 15 1951
LIBRARY
FISH & WILDLIFE SERVICE
PACIFIC OCEANIC FISHERY
INVESTIGATIONS

JOURNAL OF MARINE RESEARCH

VOLUME IX, 1950

NUMBER 2

ISSUED OCTOBER 1, 1950, NEW HAVEN, CONN., U. S. A.

JOURNAL OF MARINE RESEARCH

PUBLISHED BY

SEARS FOUNDATION FOR MARINE RESEARCH
BINGHAM OCEANOGRAPHIC LABORATORY, YALE UNIVERSITY

BOARD OF EDITORS

Chairman: A. E. PARR
American Museum of Natural History, New York

C. O'D. ISELIN
Woods Hole Oceanographic Institution

H. U. SVERDRUP
Norsk Polarinstitutt, Oslo, Norway

DANIEL MERRIMAN
Bingham Oceanographic Laboratory

C.-G. ROSSBY
Institut für Meteorologi, Stockholm, Sweden

THOMAS G. THOMPSON
Oceanographic Laboratories, University of Washington

MANAGING EDITOR

YNGVE H. OLSEN
Bingham Oceanographic Laboratory
Yale University
New Haven, Conn

The Journal is normally issued in three numbers per year constituting one volume, except for volume V, published in 1942–1944, and volume VI, published in 1946 and 1947. All the income derived from subscriptions is used solely to increase the volume and improve the quality of the Journal for the benefit of its subscribers and contributors.

Subscription price three dollars per volume, or one dollar per number. Sverdrup Anniversary Number (Vol. VII, No. 3) available only by purchase of complete Vol. VII at $3.00. Address all communications to the Managing Editor. See inside rear cover for Note to Authors.

SEARS FOUNDATION FOR MARINE RESEARCH
BINGHAM OCEANOGRAPHIC LABORATORY, YALE UNIVERSITY

JOURNAL OF
MARINE RESEARCH

VOLUME IX 1950 NUMBER 2

LATERAL MIXING AND WIND-DRIVEN CURRENTS IN AN ENCLOSED OCEAN

By

KOJI HIDAKA

Tokyo Uuiversity, Tokyo

ABSTRACT

The circulation of water induced by winds in an enclosed ocean comparable in size to the North Pacific is treated by using the "mass transport" instead of current velocity and by taking both horizontal and vertical mixing into account. The numerical solutions have been worked out for the wind system similar to that actually prevailing over the North Pacific, and for different intensities of lateral mixing. It is concluded that the flow pattern best agrees with the actual circulation when the numerical value of the coefficient of lateral mixing is of an order of magnitude of 10^9 c.g.s. Westward intensification of current is noticed too.

1. *Introduction.* Recently Stockmann (1946), in discussing the wind-driven currents in an enclosed sea as influenced by the lateral mixing, used "mass transport" instead of current velocity. Sometimes the former is more important than the currents themselves. However, Stockmann gave no numerical results. In the present paper the author intends to show how the lateral mixing influences the wind-driven transport in an enclosed ocean. Numerical results have been worked out for a rectangular ocean comparable in size to the North Pacific, assuming an anticyclonic wind system which corresponds roughly to the west winds and the trades of this ocean. The flow patterns for different intensities of lateral mixing are computed and discussed.

Dr. W. H. Munk, in a personal communication, has reported he has completed a similar work recently, but, since Dr. Munk's paper has not been received as yet, it is impossible to compare these results with his. It is hoped that Dr. Munk's results will advance the subject still further.

2. *Equations of Mass Transport, taking Lateral Mixing into Account.* We define the mass transport, whose x- and y-components are M_x and M_y, by

$$M_x = \int_0^d \rho u dz \text{ and } M_y = \int_0^d \rho v dz \,, \tag{1}$$

where u and v are the velocity components parallel to x- and y-axis, ρ the density of sea water, while the integration is taken from the surface ($z = 0$, z being taken vertically downward) down to a depth d, where the baroclinic distortion is considered negligible.

If we take x- and y-axis positive eastward and northward respectively, the differential equations of "mass transport" will be given on the assumption that the coefficient of lateral mixing is independent of z,

$$\left.\begin{aligned} \frac{1}{\rho}\frac{\partial}{\partial y}\left(A_l \frac{\partial M_x}{\partial y}\right) + \tau_x + 2\omega \sin\varphi M_y - \frac{\partial}{\partial x}(\rho g d \cdot \zeta + P) &= 0 \,, \\ \frac{1}{\rho}\frac{\partial}{\partial x}\left(A_l \frac{\partial M_y}{\partial x}\right) + \tau_y - 2\omega \sin\varphi M_x - \frac{\partial}{\partial y}(\rho g d \cdot \zeta + P) &= 0 \,, \\ \frac{\partial M_x}{\partial x} + \frac{\partial M_y}{\partial y} &= 0 \,, \end{aligned}\right\} \tag{2}$$

where A_l is the coefficient of lateral mixing, τ_x and τ_y the components of wind stress on the surface of the sea, ω the angular velocity of the Earth, φ the geographical latitude. Moreover, $P\,(x,y)$ is the pressure integral defined as

$$P\,(x, y) = \int_0^d p dz \,, \tag{3}$$

where p is the pressure, and ζ the elevation of the sea surface due to piled-up water by the winds.

Introducing a "transport function" $\psi\,(x, y)$, defined by

$$M_x = \frac{\partial \psi}{\partial y}; M_y = -\frac{\partial \psi}{\partial x} \,, \tag{4}$$

the equations (2) take the form:

$$\left.\begin{aligned}\frac{1}{\rho}\frac{\partial}{\partial y}\left(A_l\frac{\partial^2\psi}{\partial y^2}\right)+\tau_x-2\omega\sin\varphi\frac{\partial\psi}{\partial x}-\frac{\partial}{\partial x}(\rho g d\cdot\zeta+P)&=0\,,\\ \frac{1}{\rho}\frac{\partial}{\partial x}\left(A_l\frac{\partial^2\psi}{\partial x^2}\right)+\tau_y-2\omega\sin\varphi\frac{\partial\psi}{\partial y}-\frac{\partial}{\partial y}(\rho g d\cdot\zeta+P)&=0\,,\end{aligned}\right\}\quad(5)$$

the third equation in (2) being satisfied identically.

$\psi(x, y)$ must be constant along a solid boundary. Moreover, in a viscous fluid there can be no longshore motion directly near the coasts. Hence we may assume

$$\frac{\partial\psi}{\partial x}=\frac{\partial\psi}{\partial y}=\psi=0\ \text{(at the boundaries)}.\quad(6)$$

By cross differentiation, we can eliminate $\rho g d\cdot\zeta+P$ in (5), and thus have

$$\frac{1}{\rho}\frac{\partial^2}{\partial x^2}\left(A_l\frac{\partial^2\psi}{\partial x^2}\right)+\frac{1}{\rho}\frac{\partial^2}{\partial y^2}\left(A_l\frac{\partial^2\psi}{\partial y^2}\right)-\frac{d}{dy}(2\omega\sin\varphi)\frac{\partial\psi}{\partial x}+\left(\frac{\partial\tau_x}{\partial y}-\frac{\partial\tau_y}{\partial x}\right)=0\,.\quad(7)$$

Here, of course, it is assumed that Coriolis' parameter $2\omega\sin\varphi$ depends upon y. The equation (7) implies that wind-driven transport is independent of the baroclinic structure of the sea.

If we consider A_l as a constant, and if we introduce a length D_l similar to Ekman's "depth of frictional influence," defined as

$$D_l=\pi\sqrt{\frac{A_l}{\omega\rho}}\,,\quad(8)$$

the equation (7) becomes

$$\frac{D_l^2}{2\pi^2}\left(\frac{\partial^4\psi}{\partial x^4}+\frac{\partial^4\psi}{\partial y^4}\right)-\frac{d}{dy}(\sin\varphi)\frac{\partial\psi}{\partial x}+\frac{1}{2\omega}\left(\frac{\partial\tau_x}{\partial y}-\frac{\partial\tau_y}{\partial x}\right)=0\,.\quad(9)$$

Here the length D_l may be called tentatively the "frictional distance."

3. *Wind-driven Circulation in an Ocean Comparable in Size to the North Pacific.* Consider a rectangular ocean bounded by $x=\pm a$, $y=\pm b$, the coast $y=-b$ corresponding to the equator and $y=+b$ to the 60° N. parallel. If we compare this ocean to the North Pacific we should assume $a/b=2$. Several values of A_l have been evaluated from observations in the eastern Pacific areas (Sverdrup, et al., 1946), and it was found that they do not exceed 10^9 c.g.s. Then it follows from (8) that D_l will seldom exceed about 10^7 cm or 100 km. If the east-west dimension $2a$ of the North Pacific is estimated at about 10,000 km, a value of D_l above-cited will give

$$\left(\frac{a}{D_l}\right)^2 > 2{,}000\,.$$

However, in order to help in understanding the problems, the cases were treated in which

$$\left(\frac{a}{D_l}\right)^2 = \infty,\ 10{,}000,\ 2{,}500 \text{ and } 1{,}000,$$

the first corresponding to the absence of lateral mixing.

The wind system over the North Pacific is anticyclonic, consisting of the Trades in the horse latitudes and the West Winds in the middle latitudes. If we consider that this wind system alone is responsible for the circulation *cum sole* in this ocean, the corresponding mass transport will be given by the solution of the differential equation (9). This equation can be integrated by various methods, but we use here the approximate method of Galerkin.

For this purpose, we assume a solution of the form:

$$\psi(x, y) = \sum_{m,n} B_{mn} M_m(x) \cdot M_n(y)\,, \tag{10}$$

where B_{mn} are constants to be determined, while M_m and M_n are

$$\left.\begin{aligned} M_m(x) &= \cos\frac{\pi x}{2a}\cos\frac{m\pi x}{2a} \text{ for } m\text{: odd,} \\ &= \cos\frac{\pi x}{2a}\sin\frac{m\pi x}{2a} \text{ for } m\text{: even,} \end{aligned}\right\}$$

and

$$\left.\begin{aligned} M_n(y) &= \cos\frac{\pi y}{2b}\cos\frac{n\pi y}{2b} \text{ for } n\text{: odd,} \\ &= \cos\frac{\pi y}{2b}\sin\frac{n\pi y}{2b} \text{ for } n\text{: even.} \end{aligned}\right\} \tag{11}$$

It will be evident at once that the solution (10) satisfies the boundary conditions (6).

For elucidating the wind stresses, we assumed

$$\tau_x = T \cdot M_1(x)\, M_2(y); \quad \tau_y = -\,T \cdot M_2(x)\, M_1(y)\,, \tag{12}$$

where T is a constant. The stresses (12) represent roughly the anticyclonic wind system prevailing over the North Pacific, the trajectories being given by

$$a\cos\frac{\pi x}{2a} + b\cos\frac{\pi y}{2b} = \text{constant}\,. \tag{13}$$

The stream-lines drawn from (13) and the distribution of the magnitudes of stress are given in Fig. 1, the shaded area corresponding to the zone of strongest winds.

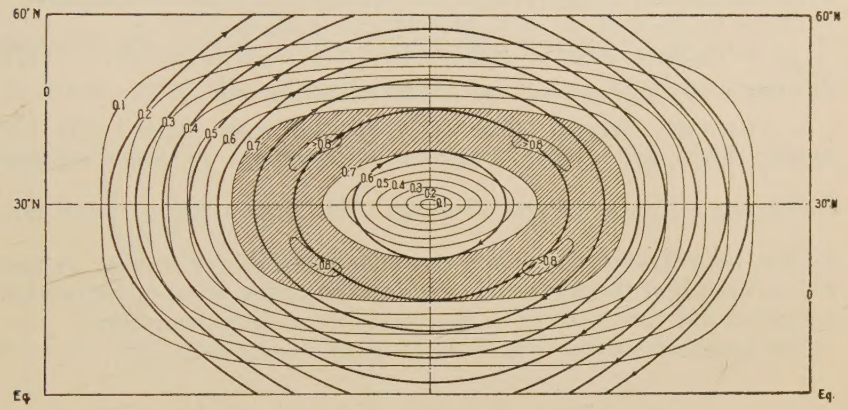

Figure 1. Distribution of wind stresses (dotted lines; unit: T) and the direction of winds (full lines with arrows). Both families of curves are not parallel, since the stress components have not been derived from one and the same function. The zone of strongest winds is shown by the shaded area.

4. *Approach by Galerkin's Method.* In the differential equation (9) we substitute, with Galerkin, the series (10). Then its left member will be of the form:

$$F\left(B_{mn}, x, y, \left(\frac{a}{D_l}\right)^2, \frac{T \cdot a}{2\omega\rho}\right). \tag{14}$$

If this quantity vanishes for all values of x and y, $\psi\,(x, y)$, as given by (10), will be the exact solution of (9). But, of course, (14) will not generally be $= 0$.

According to Galerkin we are able to obtain an approximate solution by making the integral:

$$I = \iint_{(c)} \left\{F\left(B_{mn}, x, y, \left(\frac{a}{D_l}\right)^2, \frac{T \cdot a}{2\omega\rho}\right)\right\}^2 dxdy \tag{15}$$

a minimum, where the integration should be carried out over the entire water surface of the ocean bounded by the coast lines C. For this purpose we should solve the simultaneous equations

$$\frac{\partial}{\partial B_{mn}} \iint_{(c)} \left\{F\left(B_{mn}, x, y, \left(\frac{a}{D_l}\right)^2, \frac{T \cdot a}{2\omega\rho}\right)\right\}^2 dxdy = 0\,. \tag{16}$$

In practical calculation, we confined the number of B_{mn} so as to satisfy the condition $m + n \leqq 6$. We have then

$$\begin{aligned}\psi(x,y) = {} & B_{11}M_1(x)M_1(y) + B_{12}M_1(x)M_2(y) + \ldots + B_{15}M_1(x)M_5(y) \\ & + B_{21}M_2(x)M_1(y) + B_{22}M_2(x)M_2(y) + \ldots + B_{24}M_2(x)M_4(y) \\ & + B_{31}M_3(x)M_1(y) + B_{32}M_3(x)M_2(y) + B_{33}M_3(x)M_3(y) \\ & + B_{41}M_4(x)M_1(y) + B_{42}M_4(x)M_2(y) + B_{51}M_5(x)M_1(y)\,, \qquad (17)\end{aligned}$$

the functions $M_m(x)$ and $M_n(y)$ being defined by (11).

5. *Numerical Results.* The computations were carried out for 10,000, 2,500 and 1,000. Practical observations in some eastern Pacific areas (Sverdrup and Fleming, 1941) show that $\left(\frac{a}{D_l}\right)^2$ will not be less than 2,000. However, the computations for smaller values will be useful for the theoretical explanation of the effect of horizontal mixing on the flow pattern of the wind-driven mass transport.

The relation between y and the geographical latitude φ is

$$\varphi = \varphi_0 + \frac{y}{R}\,,$$

where R is the radius of the earth and φ_0 the mean latitude of the ocean. In our case $\varphi_0 = 30°$ N and $b = \pi/6\ R$. Thus we have $d\ (\sin\ \varphi)\ /dy = \cos\ \varphi/R$.

The computed values of the coefficients B_{mn} for several values of $\left(\frac{a}{D_l}\right)^2$ are given in Table I. The diagrams in Figs. 2–4 represent the flow patterns for $\left(\frac{a}{D_l}\right)^2 = 10{,}000$, 2,500 and 1,000.

TABLE I. Numerical Values of the Coefficients B_{mn} for Several Values of $\left(\frac{a}{D_l}\right)^2$ for an Ocean Comparable in Size to the North Pacific $\left(\text{unit: } \frac{T \cdot a}{2\omega}\right)$.

$\left(\frac{a}{D_l}\right)^2 =$	∞	*10,000*	*2,500*	*1,000*
$A_l =$	*0*	*1.89 × 10⁸ c.g.s.*	*7.57 × 10⁸ c.g.s.*	*1.89 × 10⁹ c.g.s.*
B_{11}	0	+0.096	+0.249	+0.381
B_{12}	0	+0.076	+0.194	+0.233
B_{13}	0	−0.307	−0.880	−1.415
B_{14}	0	−0.084	−0.168	−0.109
B_{15}	0	+0.168	+0.255	+0.153
B_{31}	0	−0.008	−0.026	−0.050
B_{32}	0	−0.005	−0.020	−0.036
B_{33}	0	+0.027	+0.098	+0.179
B_{51}	0	−0.001	−0.004	−0.007
B_{21}	+1.349	+1.349	+1.355	+1.389
B_{22}	+0.056	+0.056	+0.062	+0.094
B_{23}	+1.220	+1.220	+1.202	+1.100
B_{24}	+0.082	+0.082	+0.070	+0.018
B_{41}	−0.136	−0.136	−0.135	−0.134
B_{42}	−0.042	−0.042	−0.041	−0.037

6. *Discussion of the Results.* The method of approach used here is an approximation, of course, and hence the solution obtained will not necessarily represent faithfully every possible detail of the motion. But we believe that more salient natures of the phenomena are represented in this solution. Figs. 2–4 give the "transport lines" for $\left(\frac{a}{D_l}\right)^2$ = 10,000, 2,500 and 1,000 as drawn by the formula (17) and the

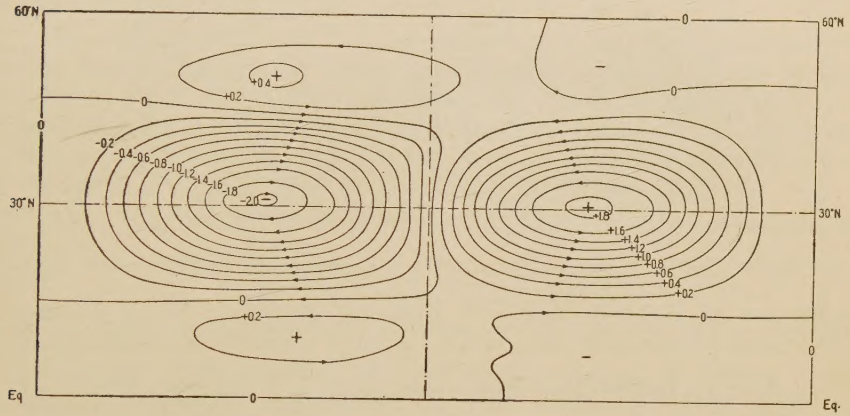

Figure 2. Transport-lines: $\psi(x,y)$ = const. $\left(\text{unit: } \frac{T \cdot a}{2\omega}\right)$ for $\left(\frac{a}{D_l}\right)^2$ = 10,000.

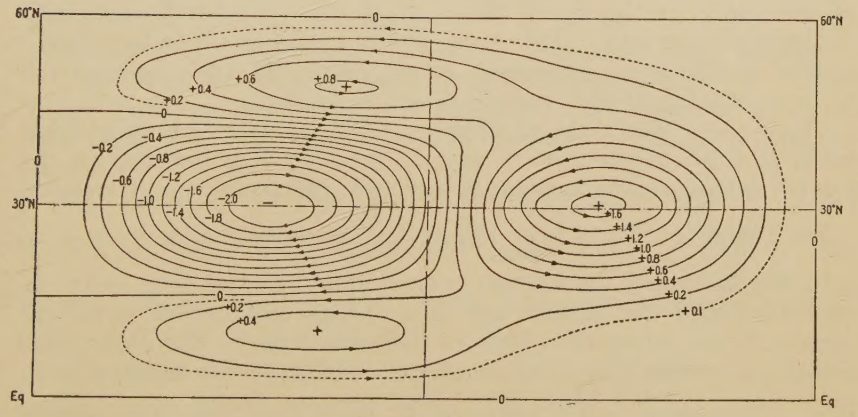

Figure 3. Transport-lines: $\psi(x,y)$ = const. $\left(\text{unit: } \frac{T \cdot a}{2\omega}\right)$ for $\left(\frac{a}{D_l}\right)^2$ = 2,500.

contents of Table I. The most conspicuous feature for the larger values of $\left(\frac{a}{D_l}\right)^2$ is the existence of two gyrals which divide the whole ocean into western and eastern halves. The dimensions of these two gyrals are nearly the same when the lateral mixing is weak, but the

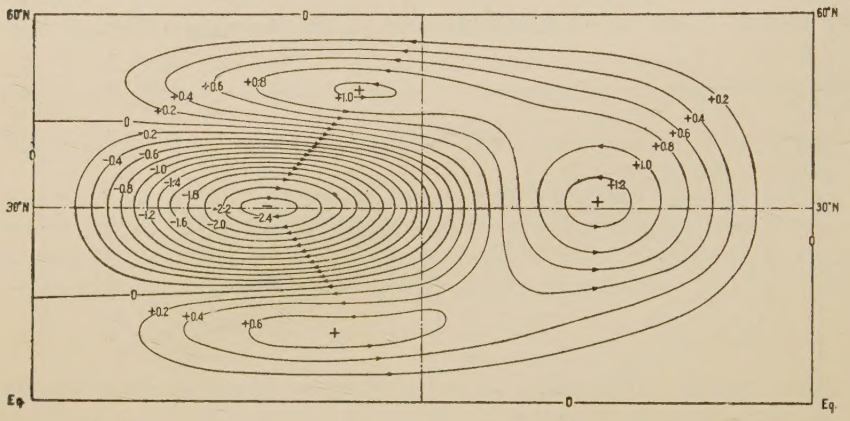

Figure 4. Transport-lines: $\psi(x,y)$ = const. $\left(\text{unit: } \frac{T \cdot a}{2\omega}\right)$ for $\left(\frac{a}{D_l}\right)^2 = 1{,}000$.

western clockwise gyral becomes larger and stronger as the lateral mixing becomes more intensive. For $\left(\frac{a}{D_l}\right)^2 = 10{,}000$, a value which we can expect in the actual ocean, the eastern gyral still exists with considerable strength. This gyral will not correspond to Sverdrup's eastern Pacific gyral (Sverdrup, et al., 1946: 723–724), because the latter is rotating in the opposite direction to ours.

These two gyrals make us expect a powerful water transport from north to south in the eastern part of the North Pacific, though the present author is quite unaware of such meridional midocean transport.

For a smaller value of $\left(\frac{a}{D_l}\right)^2$ (that is, if the order of magnitude of A_l is further increased) the western or main gyral becomes more and more intensified and the eastern one gets fainter and fainter, until the former at last covers two-thirds of the entire area of this ocean, thus forming a current system approximately similar to the actual circulation. Thus for $\left(\frac{a}{D_l}\right)^2 = 2{,}500$ or $A_l = 10^9$ c.g.s., the flow pattern agrees approximately with the circulation shown in a chart of the

surface currents of the North Pacific, though the eastern smaller gyral is not distinct in the actual ocean. For $\left(\frac{a}{D_l}\right)^2 = 1{,}000$, the eastern gyral is now so faint that there is practically no appreciable water transport in the eastern third of the ocean. This flow pattern resembles closely the distribution of surface currents in the western half of the North Pacific, where the Kuroshio System and the North Equatorial Current practically form a circulation which corresponds to our western or main gyral.

As we have just seen, the intensification of the currents occurs in the western half of the ocean only, but not necessarily close to the western coast, probably because the assumed wind system does not give the zone of the strongest winds close to the coasts. This tendency in our result may be regarded as a sort of westward intensification, though it is slightly different from that of Stommel (1948).

The center of the main gyral is about midway between the center and west coast of the ocean. In the case $\left(\frac{a}{D_l}\right)^2 = 1{,}000$, where the eastern gyral has nearly vanished, the main gyral bears a striking resemblance to the wind system. Thus, the entire aspect is as if the prevailing winds produced an oceanic circulation of similar form, though displaced considerably to the westward. This result is similar to that of Goldsbrough (1935), who solved nearly the same problem for an unbounded ocean on a rotating globe, but without taking lateral mixing into account.

There are two more weak anticlockwise gyrals to the north and south of the main gyral. However, it is not certain whether these gyrals are really significant. If they have meaning, then they might correspond to the Oyashio and Equatorial Counter Current. But it would be dangerous to strain our imagination with such details of the flow pattern, because our method of approach is actually an approximation.

The agreement of the theoretical flow pattern with the actual circulation seems to be better for smaller values of $\left(\frac{a}{D_l}\right)^2$. This implies that we must consider a value of A_l equal or larger than 10^9 c.g.s. for the entire North Pacific.

In his book "The Oceans," Sverdrup (1946: 483) points out that the coefficient of lateral mixing increases with the areal dimension of the sea considered. This probably explains why the average coefficient of lateral mixing over an ocean comparable in size to the North Pacific

is of an order of magnitude much larger than the estimates hitherto obtained from the hydrographic observations in small areas.

Acknowledgments. Finally, the author wishes to thank Walter H. Munk and Robert O. Reid of the Scripps Institution of Oceanography and Yngve H. Olsen of the Sears Foundation for Marine Research for their generous assistance and advice.

REFERENCES

Goldsbrough, G. R.

1935. On ocean currents produced by winds. Proc. roy. Soc. London, A–*148* (863): 47–58.

Stockmann, W. B.

1946. Equations for a field of total flow induced by the wind in a non-homogeneous sea. C. R. (Doklady) Acad. Sci. U. R. S. S., *54* (5): 403–406.

Stommel, Henry

1948. Westward intensification of wind-driven ocean currents. Trans. Amer. geophys. Un., *29* (2): 202–206.

Sverdrup, H. U. and R. H. Fleming

1941. The waters off the coast of southern California March to July, 1937. Bull. Scripps Inst. Oceanogr., *4* (10): 261–378.

Sverdrup, H. U., M. W. Johnson and R. H. Fleming

1946. The Oceans. 2nd Ed., Prentice-Hall, Inc., New York. 1087 pp.

A NOTE ON THE VEGETATION OF A NEW COASTAL UPWELLING AREA OF BAJA CALIFORNIA

By

E. YALE DAWSON

Allan Hancock Foundation
University of Southern California
Los Angeles, California

ABSTRACT

Series of surface temperature observations and bathythermograms made during the late summer of 1948 and the spring of 1949 along the Central Pacific Coast of Baja California have revealed the presence of an area of inshore upwelling centering in the vicinity of Isla San Roque and Isla Ascunción. Supporting evidence is furnished by the fact that all but five of the 30 known species in the intertidal vegetation of these islands are characteristic of cool water localities to the north in California.

Following McEwen's (1916: pl. 9) initial report of upwelling along the coast of northwestern Baja California, studies of plants and animals and of temperature data collected in recent years have indicated the presence of a number of low temperature inshore areas along this coast. Collections of marine algae from the vicinity of Punta Descanso and Cabo Colnett established the first correlation of vegetation with low shore-water temperatures in this region (Dawson, 1946). The writer's recent survey of the marine flora of Pacific Mexico has provided further confirmation to the presence of these and other upwelling areas of Baja California (Dawson, 1949). A similar correlation between the low temperatures and the distribution of marine animals, particularly fishes, has been indicated by Hubbs (1948), and this problem is being studied currently on an expanded scale by him and his associates.

During an Allan Hancock Expedition to the Gulf of California in the spring of 1949, several series of surface temperature observations and some bathythermograms were made in inshore waters along the Central Pacific Coast of Baja California south of Punta Eugenia in an effort to locate still more southerly areas of upwelling in which rich algal floras might be expected. Although the season was early and the thermoclines not yet well developed, two series of observations made on courses between Bahía San Cristobal and Bahía San Hipolito gave evidence of a distinct inshore area of cold water centering between Isla San Roque and Isla Ascunción. These series (on March 7 and April 6) showed that surface temperatures in the vicinity of these

inshore islands were as much as 2.4° C. lower than those north of Punta San Pablo or a few miles seaward to the southwest.

In following up these preliminary observations, examination of a series of bathythermograms made by the PAOLINA T. during a favorable period of well developed thermoclines in late September and early October of 1948 and kindly loaned for this study by J. D. Cochrane of the Hydrographic section of the Scripps Institution, revealed a quite conclusive demonstration of the occurrence of upwelling in this locality. These records represent two longshore courses, each of which passes through the Isla San Roque-Isla Ascunción area (Fig. 1). The sections presented in Figs. 2 and 3 show graphically the presence of low surface temperatures in the water bathing these two islands.

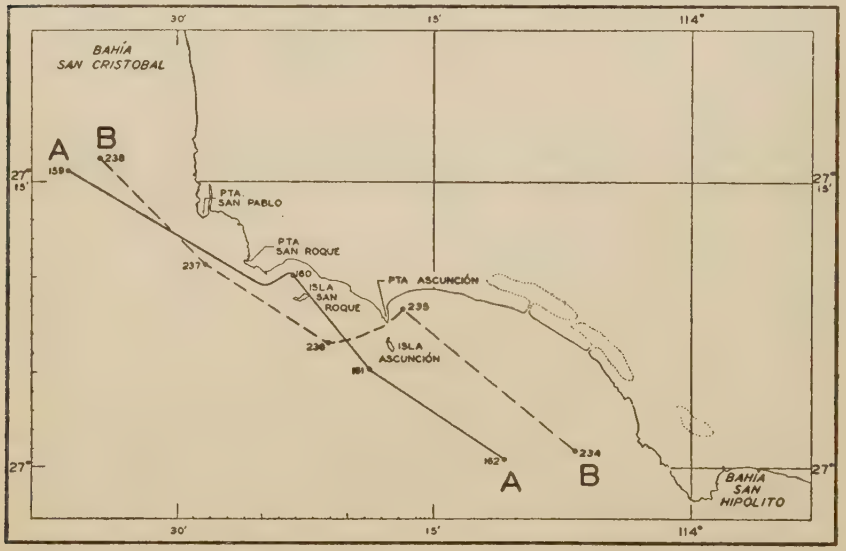

Figure 1. The Isla San Roque-Isla Ascunción upwelling region showing bathythermograph stations along courses A and B made by the PAOLINA T.

Although it was not possible to obtain samples of marine plants in this area in 1949, two small collections, obtained on an expedition sponsored by Guanos y Fertilizantes de Mexico in September 1946, have been contributed by B. F. Osorio-Tafall. These collections from Isla San Roque and Isla Ascunción are in excellent agreement with the detection of cool water conditions in this region, since all but five of the plants are characteristic of northern rather than southern

waters. With the exception of *Padina Durvillaei*, *Bryopsis muscosa*, and three apparently local species, all of the plants are well known in central or southern California. In a large majority of cases their occurrence at these islands represents a southward extension of range.

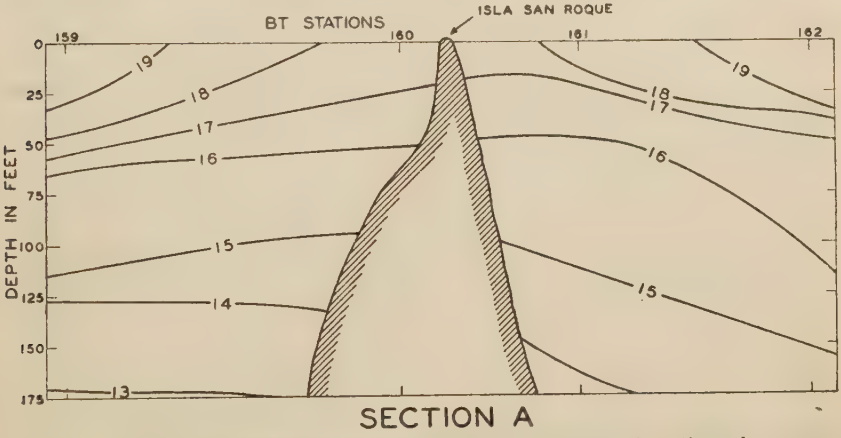

Figure 2. Temperature section drawn from four bathythermograph stations along course A of Fig. 1, September 23–24, 1948.

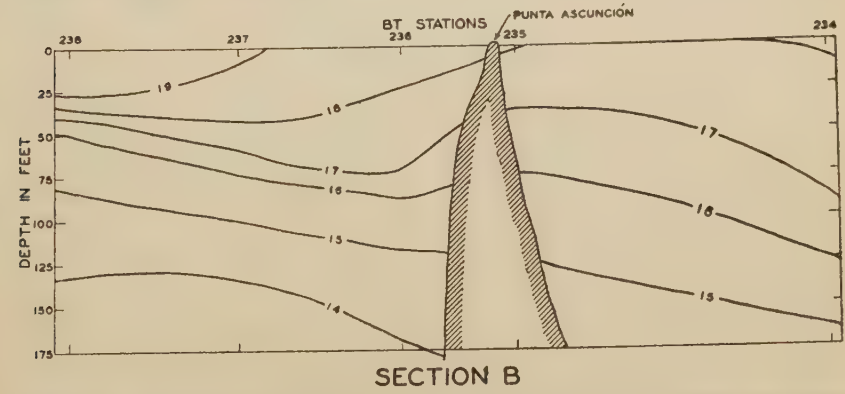

Figure 3. Temperature section drawn from five bathythermograph stations along course B of Fig. 1, October 2–3, 1948.

Vegetation of Isla San Roque as known from collections made September 1, 1946

Bryopsis muscosa Lamouroux, prox.; *Pachydictyon Binghamiae* (J. Agardh) Dawson; *Padina Durvillaei* Bory; **Halidrys dioica* Gardner; **Cystoseira osmundacea* (Menzies) C. Agardh; *Colpomenia sinuosa* (Roth) Derbès and Solier; *Porphyra perforata* J. Agardh; *P.*

naiadum Anderson, forma; **Gelidium Coulteri* Harvey; **G. cartilagineum* var. *robustum* Gardner; **Zanardinula linearis* (Kylin) Papenfuss; *Callophyllis violacea* J. Agardh; *Melobesia mediocris* (Foslie) Setchell and Mason; *Plocamium pacificum* Kylin; *Gymnogongrus* sp.; **Gigartina serrata* Gardner; **G. canaliculata* Harvey; **Rhodoglossum affine* (Harvey) Kylin; *Rhodoglossum* sp.; *Chondria californica* (Collins) Kylin; **Cryptopleura crispa* Kylin; *Ceramium Eatonianum* (Farlow) G. B. De Toni; **Polysiphonia acuminata* Gardner, prox.; **Pterochondria Woodii* (Harvey) Hollenberg; **Pterosiphonia Baileyi* (Harvey) Falkenberg; **Phyllospadix Scouleri* Hooker.

Vegetation of Isla Ascunción as known from collections made September 1, 1946

Pachydictyon Binghamiae (J. Agardh) Dawson; **Halidrys dioica* Gardner; **Cystoseira osmundacea* (Menzies) C. Agardh; *Macrocystis pyrifera* (Linneaus) C. Agardh; **Gelidium Coulteri* Harvey; **G. cartilagineum* var. *robustum* Gardner; **Zanardinula linearis* (Kylin) Papenfuss; *Porphyra naiadum* Anderson, forma; *Melobesia mediocris* (Foslie) Setchell and Mason; **Polyopes Bushiae* Farlow; *Gracilaria* sp.; **Gigartina canaliculata* Harvey; *Ceramium Eatonianum* (Farlow) G. B. De Toni; **Pterochondria Woodii* (Harvey) Hollenberg; **Phyllospadix Scouleri* Hooker; **P. Torreyi* S. Watson.

LITERATURE CITED

Dawson, E. Y.

1946. Marine algae associated with upwelling along the northwestern coast of Baja California, Mexico. Bull. Sth. Calif. Acad. Sci., *44* (2): 57–71.

1949. Resultados preliminares de un reconocimiento de las algas marinas de la costa pacifica de Mexico. Rev. Soc. Mex. Hist. Nat., *9* (3–4): 215–255.

Hubbs, C. L.

1948. Changes in the fish fauna of western North America correlated with changes in ocean temperature. J. Mar. Res., *7* (3): 459–482.

McEwen, G. F.

1916. Summary and interpretation of hydrographic observations made by the Scripps Institution for Biological Research of the University of California, 1908–1915. Univ. Calif. Publ. Zool., *15* (3): 255–356.

*Indicates southward extension of range.

NATURAL SLICKS ON THE OCEAN

By

ROBERT S. DIETZ and EUGENE C. LAFOND

U. S. Navy Electronics Laboratory
San Diego 52, California

ABSTRACT

Slicks are smooth glassy streaks or patches on the ocean. Prominent slicks are confined largely to near-shore areas where organic production is high. Experiments and observations are described which show that slicks are contaminate films of organic oil, probably derived primarily from diatoms which contain droplets of oil in their cells to assist in flotation and/or as an emergency food supply. Slicks are discernible because of their damping effect on small wavelets. The parallel slicks that develop in light to moderate winds result because the contaminate films pile up at the top of convergences in the homogeneous, wind-stirred layer above the thermocline.

INTRODUCTION

Slicks are smooth glassy patches or streaks on the surface of oceans or lakes which render a heterogeneous aspect to the water surface (Fig. 1). They are extremely common in coastal waters, bays, and lakes, often covering a large percentage of the surface, and they are most prominent when light breezes ripple the surface, the slicks damping out the small wavelets and forming a calm patch in water of higher surface roughness. Although observable from shipboard or from shore, they are most striking when viewed toward the sun from an airplane.

Although natural slicks are extremely common and widespread phenomena, they seem to have received little scientific consideration, since almost no reference is made to them in oceanographic literature. It is well known, of course, that artificial slicks form in harbor waters contaminated with refuse and oil; in some harbors these slicks create a serious fire hazard. In the open sea the wakes of ships are frequently marked by a slick for a considerable length of time after the passage of the vessel. In addition, artificially produced slicks formed by pouring oil on the water have been used by ships in distress, with doubtful success, in an attempt to prevent heavy seas from breaking over them. It is apparent even to the casual observer, however, that artificially produced slicks are grossly insufficient quantitatively to account for the great profusion of slicks encountered on the ocean. Frequently petroleum slicks can be distinguished from natural slicks because they often display high order interference colors.

Inquiries made of persons familiar with the sea produced no general conformity of opinion regarding the origin of natural slicks. Fisher-

men commonly ascribe them to local calm areas where the wind does not strike the surface; this opinion is held widely by yachtsmen also, many of whom, when racing sailboats, assiduously avoid these areas of supposed calm.[1] However, photographs of true slicks at short time intervals reveal that this "calm-spot" theory is untenable, because the slicks are persistent features which drift along with the surface current and change form rather slowly. Another common opinion is that they are related to oil seeps on the sea floor. It is true that extensive slicks, such as the one at Coal Oil Point near Santa Barbara, California, are produced locally by seeps, but obviously this does not serve as a plausible explanation for slicks in general.

Prior to undertaking the present study, it was the writers' belief that natural slicks were possibly films of oil derived from organisms in the sea, and because of the dearth of recorded scientific information on these interesting and widespread phenomena, it seemed worthwhile to investigate them further. This paper summarizes a few observations concerning the distribution and origin of natural slicks.

DISTRIBUTION OF NATURAL SLICKS

For the past few years the writers have recorded the distribution of slicks observed during rather extended journeys over the seas, and it was hoped that a study of their geographic distribution would yield significant information as to their cause. For example, if slicks are films of animal or vegetable oil, one would expect them to be most prominently developed in regions of high organic production, such as in coastal and insular water where upwelling and runoff supply the euphotic zone with nutrients. The following observations on the distribution of slicks demonstrate that this distribution actually was found to exist.

On a cruise to the Antarctic in December of 1946, rather prominently developed slicks were observed in the coastal waters of California, but they disappeared when the blue oceanic water was reached. Slicks were noted once again when the ship passed the Marquesas Islands, the only landfall en route to the Antarctic. As a general rule slicks were not observed in oceanic water, but some were faintly discernible in the South Pacific at Lat. 30° 48′ S and Long. 152° 24′ W when unusually smooth sea conditions prevailed. Upon reaching the

[1] In this respect slicks are apparently confused with true wind streaks or "cat paws." It should be noted here that smooth slick-like areas, such as those from tide rips and rip currents, frequently develop over turbulent water. The wake of a vessel is often smooth due to this surface turbulence as well as to the formation of an artificial slick from the ships' oil and refuse.

Figure 1.

Aerial photos of slicks in the Gulf of California taken with infra-red film, which accents the streaks. *A*. A prominent irregular pattern of slicks under quiet conditions in the lee of an island. *B*. The typical linear pattern of slicks under conditions of light wind. Official U. S. Navy photographs.

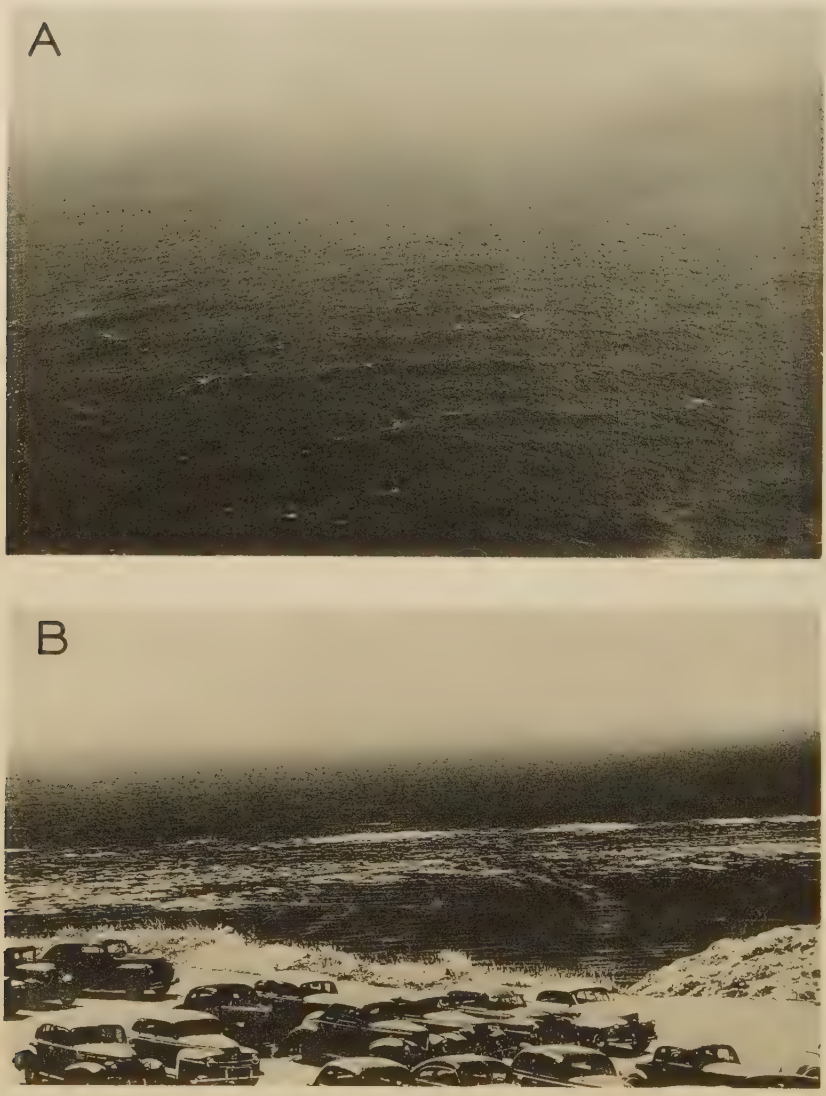

Figure 2.
Photographs of slicks off southern California. *A*. Slicks marking Cortes Bank, 100 miles off southern California. Note that slicks have lined up parallel to the wind direction. Incipient white caps show that sea state is Beaufort 3. With a further increase in sea state the slicks would be destroyed. *B*. Photo taken with infra-red film shows slick patches near San Diego, marking kelp beds which are formative areas for prominent slicks. Note also parallel slicks moving inshore from the kelp beds. Official U. S. Navy photographs.

green Antarctic water, where organic production is notably high in summer, prominent well developed slicks were frequently observed, especially near the ice pack. Aerial observers who were questioned reported generally good development of slicks in the near-shore waters. Slicks were seen but once on the high seas during the homeward passage; but these, found in a subtropical area (Lat. 20° S and Long. 175° W) under unusually calm conditions, were only faintly discernible. However, well developed slicks were found in Australian coastal waters, and especially striking slicks were seen in the insular waters of American Samoa. When the coastal waters of California were reached, prominent slicks were found again.

On a round trip flight from California to New Zealand in February 1949, the sea surface was examined for slicks whenever visibility permitted. They were noted from San Francisco Bay to a distance of 60 miles off the coast. They appeared again in the coastal waters around the southeastern Hawaiian Islands, especially on the leeward side, in the vicinity of the Samoan and Fiji islands, and near the New Zealand Coast. In only one oceanic area, between Lat. 25–30° S, were slicks strongly developed.

A cruise from San Francisco to the Hawaiian Islands and thence to the Aleutian Islands in July 1947 revealed an almost complete absence of slicks in the open Pacific. A moderate development of slicks was sometimes observed in the Bering Sea and, on the return passage along the coast, well developed slicks were observed in the Gulf of Alaska.

Throughout the coastal waters off southern California, where the writers have made numerous cruises and flights, slicks are widespread, but they are most prominent near the coast, especially in the lee of the kelp beds and around the islands. On one flight, a large bank (Cortes Bank) which rises to within a few fathoms of the surface was found to be marked by slicks (Fig. 2A). This suggests the possibility that slicks might sometimes furnish an indication of the presence of shoals.

Slicks are by no means entirely confined to the open ocean, because bays and fresh water lakes typically display the most prominent slicks. It is interesting to note, however, that during a recent flight across Great Salt Lake in Utah no prominent slicks were observed. This may be related to an unusually low organic productivity in this lake due to its high salinity.

It seems apparent, then, that prominent slicks are confined to the coastal and inshore waters and are largely absent from the deep oceanic waters where organic production is generally believed to be about one per cent of that of coastal water.

NATURE AND ORIGIN OF SLICKS

In order to ascertain whether slicks are contaminate films on the surface of the ocean, several surface tension measurements were made with duNouy surface tension apparatus, which measures the force required to pull a platinum wire ring off the surface of a liquid. The samples tested were collected from water surrounding the slicks, from water a meter below the slicks, and from water at the surface of the slicks themselves. It was found that all of the samples, when allowed to stand without agitation for at least several minutes, gave readings slightly less than the reported values for pure sea water; the water from the slicks gave the lowest values. It appears that sea water is generally covered with at least a monomolecular contaminate film and that piles of such a layer exist in slicks, thus forming a skin many molecules thick.

While collecting the water samples it was noted that slicks are typically marked by foam and that bubbles, formed by stirring the water, persisted for a much longer period than they did in the water outside of the slick. This further demonstrates the presence of a film. Further examination of the slicks reveals that they are found at zones of converging or descending water which are appreciably warmer than the surrounding water and which are marked by a considerable amount of floating sea weed and small particulate detritus.

In order to determine what substances in the ocean might produce slicks, the following experiment was performed. A chemically clean white enamel pan was filled with distilled water, the surface of which was then lightly sprinkled with talc. The surface thus prepared was touched with droplets of various crushed organic substances, including kelp, fish, zooplankton, and phytoplankton. In all cases, when the droplet touched the water, the talc-covered portion of the water in the immediate vicinity was rapidly repelled, showing displacement by the formation of a surface film. This indicates that a wide variety of organisms in the sea are potential slick producers. A crushed mixture of phytoplankton consisting largely of diatoms gave a particularly strong reaction. This is not surprising, for diatoms are known to synthesize droplets of oil in their cells to provide a food reserve and to assist in flotation (Sverdrup, Johnson, and Fleming, 1942: 765; Cupp, 1943: 26). Also, analyses of diatom lipids (Clarke and Mazur, 1941) show the abundant presence of free fatty acids and other substances that are potential slick producers. Because of the quantitative importance of phytoplankton in the ocean, it is believed that they are largely responsible for the production of slicks. Of course marine animals may also contribute oil to form slicks. In fact, the writers

have noted that the spot where a whale has surfaced is marked by a faint but quite persistent slick. However, marine animals probably are quantitatively unimportant as compared to phytoplankton, and in any case, much of their oil results from grazing upon the diatoms.

It is interesting to note here that although the best slicks off California are associated with the kelp beds (Fig. 2), a sample of the giant kelp *Macrocystis* gave only a weak slick-producing reaction in the talc-covered water. It is likely, therefore, that the slicks associated with kelp beds may not be produced directly by the kelp but rather by the attached diatoms and other forms that abound in the kelp.

Droplets of oil released by organisms which are lighter than and immiscible with water must rise to the surface. Because water has a higher surface tension than that of any other naturally occurring liquid, many oils spread into a thin film. Any oil with a molecular structure which possesses a polar group and a nonpolar portion capable of self cohesion will tend to spread into a monomolecular layer if the sum of the air-oil tension plus the water-oil tension is less than the air-water tension. The rapidity with which the film spreads is proportional to the amount by which the air-water tension exceeds the sum of the air-oil tension plus the water-oil tension. The calming effect of an oil film on capillary waves increases with the air-oil tension. Lamb (1932: 631) quotes earlier writers as saying that the calming effect of oil on water waves is due to the *variations* of tensions caused by the extensions and contractions of the oil film.

Under completely calm conditions, the entire surface of the ocean appears smooth and glassy. Slicks are not readily distinguishable until small wavelets, which require a critical wind speed of about 110 cm/sec (two miles per hour) and essentially a zero fetch, are generated. Although slicks can sometimes be distinguished from the surrounding water by a slight difference in texture and color, they show up primarily when the damping out of small wavelets causes a smooth glassy patch on an otherwise rough surface. When light winds prevail, slicks have a patchy form, but as the winds increase they tend to line up into evenly spaced streaks parallel to the wind (Fig. 2). These parallel streaks apparently develop when the slick material collects along small wind-induced convergences associated with the helical circulating cells of water in the homogeneous layer above the thermocline (Langmuir, 1938; Woodcock, 1944).[2] If the

[2] Subsequent to the transmittal of this paper for publication, Ewing (1950) has given evidence to show that the slick bands form at convergences above the troughs of internal waves. However, since internal waves may be induced in large part by wind-induced circulation, Ewing's observations are not necessarily in conflict with the belief that the slicks form along wind-induced convergences.

sea state increases to three or higher, the slicks appear to be destroyed by the mixing associated with the formation of white caps.

ACKNOWLEDGMENTS

The writers are indebted to E. G. Meyer of the University of New Mexico, John A. Spangler of San Diego State College, and John Knauss, for making certain measurements in connection with this study. The writers are also indebted to D. A. Wilson of the U. S. Navy Electronics Laboratory, R. W. Raitt of the Marine Physical Laboratory of the University of California, and to Marston Sargent and Walter Munk of the Scripps Institution of Oceanography for their critical consideration of the manuscript.

REFERENCES

Clarke, H. T. and Abraham Mazur
1941. The lipids of diatoms. J. biol. Chem., *141:* 283–289.

Cupp, E. E.
1943. Marine plankton diatoms of the west coast of North America. Bull. Scripps Inst. Oceanogr., *5* (1): 221 pp.

Ewing, G. C.
1950. Relation between band slicks at the surface and internal waves in the sea. Science, *111:* 91–94.

Lamb, Horace
1932. Hydrodynamics. Dover Publications, New York. 6th ed. 738 pp.

Langmuir, Irving
1938. Surface motion induced by wind. Science, *87:* 119–123.

Sverdrup, H. U., M. W. Johnson, and R. H. Fleming
1942. The Oceans. Prentice-Hall, Inc., New York. 1087 pp.

Woodcock, A. H.
1944. A theory of surface water motion deduced from the wind-induced motion of the *Physalia.* J. Mar. Res., *5* (3): 196–205.

SUBSURFACE PELAGIC *SARGASSUM*[1]

By

ALFRED H. WOODCOCK

Woods Hole Oceanographic Institution

ABSTRACT

Observations are given which indicate that the presence of *Sargassum* below the sea surface is associated with lines of convergence of surface waters and with wind speeds in excess of about 4 m sec^{-1}. It is suggested that descending currents under the convergence lines carry the plants down.

Measurements of compression and of rates of rise of *S. natans* of various densities were made at Bermuda. Results of these measurements indicate that these plants may be carried down by descending currents in excess of 4.5 to 7.2 cm sec^{-1}, and that the plants can maintain positive buoyancy, for short periods of time at least, under pressures equal to 100 m of sea water.

The pressure of the gases in the spherical bladders on *S. natans* was found to change diurnally.

INTRODUCTION

The author has often noted that *Sargassum* tends to spread out close to the sea surface during light winds and calm, whereas the plants float deeper in the water with fewer leaves thrust through the surface during winds of force 3 or greater. This phenomenon seems to indicate that descending currents, occurring during higher winds, maintain a sustained drag on the plants, thus reducing their apparent buoyancy below that of plants which are not influenced by vertical currents. During higher winds the author has seen a great many *Sargassum* plants at various depths beneath the sea surface; on one occasion more than ten per cent of the plants seen were below the surface.

The purpose of this paper is to present some observations which indicate that subsurface *Sargassum* is carried downward by descending currents under lines of convergence of surface waters. The presence of these phenomena in surface waters of a lake and ocean has been shown by Langmuir (1938) and Woodcock (1944). It is suggested that plants may remain below for a time and then return to the surface as the speed of the converging and descending currents diminishes. Also presented are data showing the compression and rates of rise of *Sargassum* of varying densities. These measurements were made in order to estimate the depths at which water pressure would cause a

[1] Contribution No. 489 of the Woods Hole Oceanographic Institution, and Contribution No. 152 of the Bermuda Biological Station for Research.

plant to lose all positive buoyancy[2] and to estimate the speeds of currents necessary to draw plants downward. Pressure changes in the gas bladders supporting the plants were also measured, because, as suggested by Parr (1939: 9), such changes might modify the rates of rise, assuming some elasticity of bladder walls. A diurnal cycle of gas pressure was found in these bladders.

Previously questions concerning pelagic *Sargassum* beneath the surface of the North Atlantic have been given scant attention. Murray and Hjort (1912: 336) suggested that these plants have a negative buoyancy due to fragmentation by wave action. Winge (1923: 11) stated that subsurface *Sargassum* is probably burdened with an excess growth of epizoans, or that it has too few floats to maintain positive buoyancy. Parr (1939: 9) made net tows for a distance of 24 nautical miles, using five *Sargassum* nets simultaneously at different levels from the surface downward. The results of this tow and of direct observations from the deck of the ship led him to doubt that the sinking of whole plants takes place in "quantitatively significant" amounts.

SOME PHYSICAL CONDITIONS UNDER WHICH *SARGASSUM* IS SEEN BENEATH THE SEA SURFACE

Sargassum below the sea surface is almost always beneath floating plants which are formed into lines (see Fig. 1) that lie approximately parallel to the wind direction at the time of observation. Winge (1923: 11) attributed this alignment to a differential sailing which caused slower plants to be drawn into the wake of those that were more exposed to wind drag. Langmuir (1938) explained the weed lines as "wind induced" zones of convergence of surface waters which are parts of systems of left and right helical vortex pairs lying with their long axis parallel with the wind (see Fig. 2). Measurements among similar lines on Lake George (Langmuir, 1938) showed water descending (2 to 3 cm sec^{-1}) under the convergence lines and ascending in the divergent regions. Later Woodcock (1944) showed that drift bottles having a positive buoyancy of one gram, when placed 2 m apart on the sea surface and in a line normal to the wind, always reformed into lines lying parallel with the wind. This indicated that the convergence of surface waters into lines parallel with the wind also occurs on the open sea.

[2] The terms "positive buoyancy" and "negative buoyancy" refer to the sign of the buoyant force, which is the weight of the water displaced minus the weight of the immersed plant.

In view of the work cited above, it is reasonable to assume that plants seen in lines are carried there by converging surface waters and that those under these lines are carried down by converging and descending waters. However, no direct measurements have been made of descending currents under lines of *Sargassum.*

The observations in Fig. 3 suggest that the presence of *Sargassum* beneath the sea surface under lines of convergence is related to wind speed. Records were made of the occurrence and nonoccurrence of subsurface plants together with attending wind and thermal conditions.[3] The plus signs denote a period of observation (from the ship's bow or mast) of ten minutes or more when *Sargassum* was plentiful and when it was seen on the surface only.[4] The circle indicates a similar period during which surface plants were plentiful and during

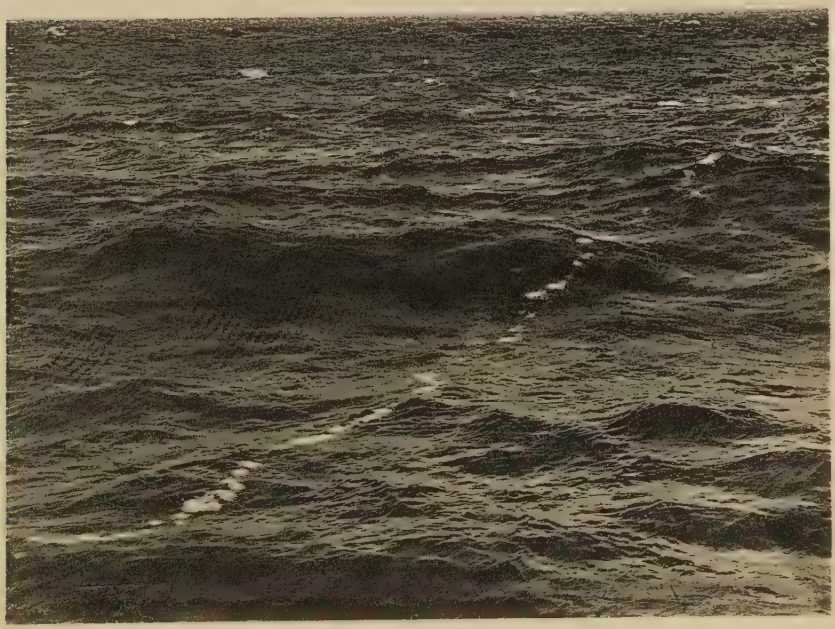

Figure 1. A photograph of a line of *Sargassum* on the sea surface.

[3] These observations were all made in Central Atlantic waters within a few hundred miles of Bermuda and over a period of several years.

[4] Only those plants free from the influence of the ship's hull were included in these data.

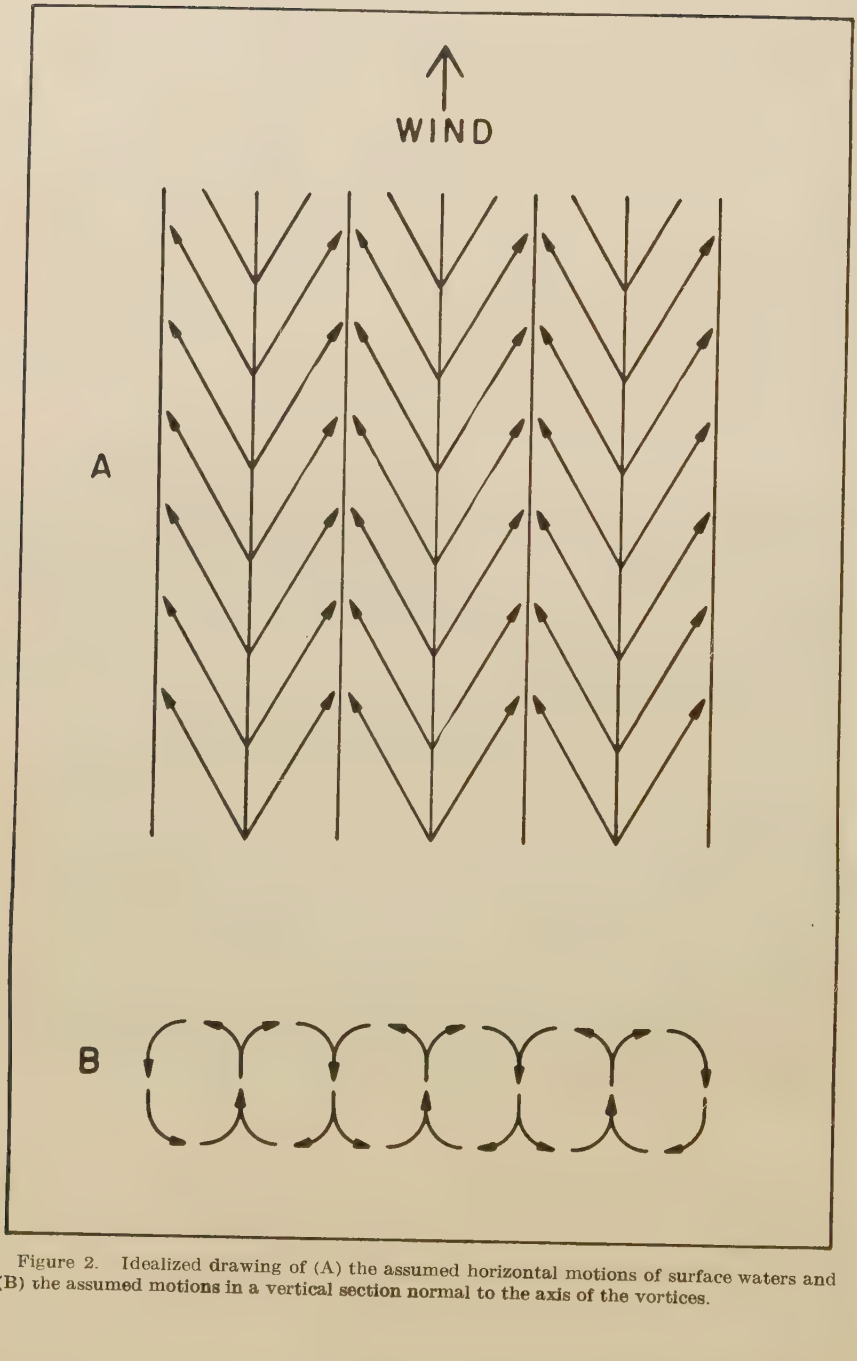

Figure 2. Idealized drawing of (A) the assumed horizontal motions of surface waters and (B) the assumed motions in a vertical section normal to the axis of the vortices.

which they were seen at an estimated depth of a meter or more below the surface. In Fig. 3 these symbols are plotted against wind speed and $e_s - e_3$ values.[5] This was done because these variables are, under average oceanic conditions, among the major factors determining changes in the rate of heat and water loss from surface waters

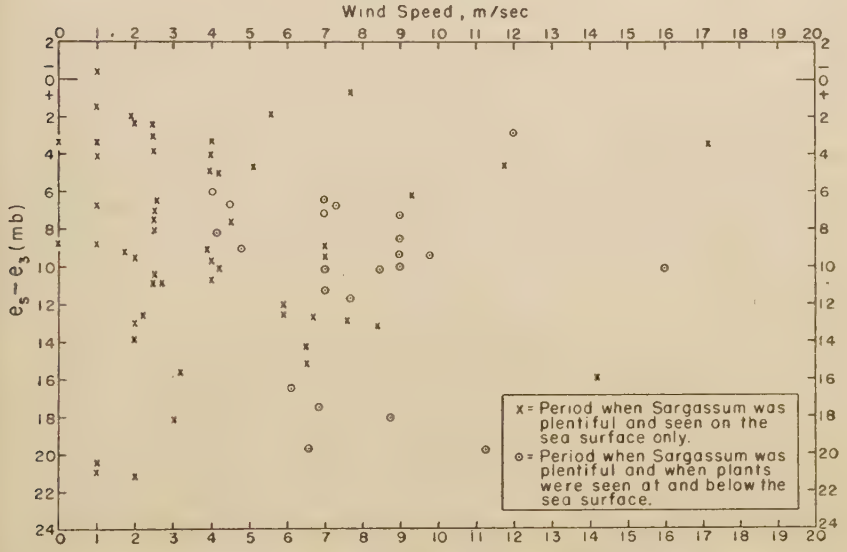
Wind Speed, m/sec
$e_s - e_3$ (mb)
x = Period when Sargassum was plentiful and seen on the sea surface only.
o = Period when Sargassum was plentiful and when plants were seen at and below the sea surface.

Figure 3. Showing symbols representing the occurrence and nonoccurrence of subsurface *Sargassum* at various wind speeds and at various values of $e_s - e_3$.

(Montgomery, 1941: 19). During higher winds and higher values for $e_s - e_3$, more rapid descending motions would be expected because greater volumes of relatively heavy water are being produced by evaporation and cooling at the surface. The locations of the circles in Fig. 3 show that no *Sargassum* is seen beneath the surface at wind speeds less than 4 m sec^{-1}. There is no indication in these data that evaporation, as expressed by $e_s - e_3$, has any effect on the occurrence of subsurface plants.

During many observation periods with higher winds, no subsurface plants were visible (see x symbols at wind speeds above 4 m/sec in Fig. 3). It is assumed that at such times stronger vertical currents

[5] e_s = the saturation pressure of aqueous vapor over sea water at sea surface temperatures. e_3 = partial pressure of aqueous vapor at a height of about 3 meters above the sea.

had carried the subsurface plants to depths at which they were not visible.

Fig. 3 and the remarks about wind-induced vortices in surface waters suggest that the *Sargassum* seen below the sea surface is drawn down by local descending currents which are associated with higher winds.[6] Thus, decreasing positive buoyancy, due to fragmentation by wave action or to an excessive burden of epizoans, may not be the factor which finally brings about sinking of the *Sargassum*. Sinking is probably caused by descending surface waters that carry downward those plants which have the lowest positive buoyancy.

At what depths will the water pressure compress plants to a density in excess of that of ambient water? What velocities are necessary to draw *Sargassum* downward? Can these plants modify the gas pressure in their bladders, thus perhaps changing their density and rate of rise? These questions have led the author to make some exploratory measurements of compression, rate of rise and bladder gas pressure of *Sargassum*.

DENSITY, COMPRESSION, RATE OF RISE AND BLADDER PRESSURES

Sargassum natans, used in these experiments, is present in the Bermuda region in greater numbers than any other form (Parr, 1939: 65). All of the plants used appeared to be in healthy growing condition with a moderate accumulation of attached colonial epizoa. Unattached organisms were removed from experimental plants.

Density. This portion of the study was performed in order to obtain an approximation of the pressure required to compress a plant to the sinking point in sea water. As was expected, this pressure increased with decreasing initial plant density. The method used to determine density will be discussed first.

The damp-dry plants were weighed and placed in sea water and ballasted with brass weights until the addition of a final 2 to 5 mg

[6] It is of interest to note that Parr's subsurface tow of *Sargassum* nets was made at a time when the average wind was force 2 (1 to 2 m sec^{-1}, see ATLANTIS log for Feb. 9, 1935, on file at the Woods Hole Oceanographic Institution, Woods Hole, Mass.). The nets caught no subsurface plants, and Parr (1939: 10) suggested that this fact indicated the absence of quantitatively significant amounts of subsurface *Sargassum*. However, at these wind speeds no subsurface weed has been seen by the author (see Fig. 3).

It should not be judged that these observations indicate serious errors in Parr's quantitative studies of the distribution of *Sargassum*, which were based upon surface collections. The observations indicate the possibility of error in surface collections during winds of 4 m sec^{-1} or more.

weight caused sinking. Thus the combined weights of the immersed plants plus the ballast were brought to a weight very nearly equal to the weight of the displaced sea water. Density (S_d) was then derived in the following manner:

$$S_d = \frac{S_w}{\frac{S_w + b}{d_t} - b_v}, \qquad (1)$$

where S_w = plant weight in air (g), b = ballast weight (g), d_t = density of ambient sea water, and b_v = ballast volume at sea water temperature. When the volume of a plant is determined, as shown by the term in the denominator of equation (1), plant density can be modified a known amount by adding or subtracting small ballast weights. Thus,

$$S_d = \frac{S_w + b}{S_v + b_v}, \qquad (2)$$

where S_v = plant volume [derived in denominator of equation (1)].

Table I gives an example of the numerical steps used to derive the density of a plant and of the plant plus various weights of ballast. The figure at the top of column E gives the density of the unballasted *Sargassum;* the accuracy of this value depends in major part upon the accuracy of the determination of plant weight. The figure at the bottom of column E is obviously the same as the density of the ambient sea water. In this case the *Sargassum* was experimentally ballasted until the weight of the plant plus the brass was equal to the weight of the displaced water (within 2 to 5 mg).

The damp-dry condition of the plants for weighing was achieved by spreading them between layers of absorbent diaper cloth which had been dampened with sea water, after which the cloth was pressed gently on all sides for about three minutes in order to bring most of the plant surfaces into contact with the cloth. Plant weighing errors were not determined. Lowndes (1942) found up to 8% error in the weighing of live marine organisms. A positive error of 8% in the weighing of the plant would cause an error of about + 0.0075 in the computed unballasted plant density given in Table I (cf., top figures of columns E and F). Since this error approaches zero as ballast is added, and since the density of plant plus ballast approaches that of the ambient water (see column F), the densities derived here are to be regarded as carefully determined approximations, the accuracy becoming greater as the density approaches that of sea water. These densities serve the desired purpose of indicating the general nature of the relationship between plant density, compression, and rate of rise.

TABLE I.—An Example of the Method Used to Derive the Density of a *Sargassum* Plant and the Attached Ballast. The Weight of This Plant Was 177.8 Grams; Ambient Sea Water Temperature 22.2–22.5° C; Salinity 36.40 °/₀₀; Density 1.0252; Pressure, About One Atmosphere

A	*B*	*C*	*D*	*E*	*F*
Ballast weight	Sargassum *weight plus ballast weight**	*Ballast volume*	*Volume of* Sargassum *plus ballast*	*Density of* Sargassum *plus ballast*	*Column E corrected for 8% positive weighing error*
b	$S_w + b$	b_v	$S_v + b_v$	$\frac{S_w + b}{S_v + b_v}$	$\frac{S_w - (S_w .08) + b}{S_v - \left(\frac{S_w .08}{1.0252}\right) + b_v}$
grams	grams	cm³	cm³	g cm⁻³	g cm⁻³
0.0	177.8	0	191.342†	0.9292	0.9217
8.05	185.85	0.95	192.296	0.9665	0.9619
12.05	189.85	1.43	192.773	0.9848	0.9817
15.05	192.85	1.79	193.131	0.9986	0.9965
17.05	194.85	2.03	193.369	1.0077	1.0063
18.55	196.35	2.21	193.547	1.0145	1.0136
19.05	196.85	2.27	193.607	1.0168	1.0161
19.55	197.35	2.33	193.668	1.0190	1.0185
20.05	197.85	2.38	193.726	1.0213	1.0210
20.55	198.35	2.44	193.785	1.0236	1.0235
20.92	198.72	2.49	193.835	1.0252‡	1.0252

* Buoyancy corrections in air were not made.

† This volume is determined as shown by the term in the denominator of equation (1); all volume and density values in this table are based upon this value.

‡ This density is empirically established by ballasting the plant to neutral buoyancy in sea water of this density. The maximum error (5 mg) in this ballasting produces an insignificant weighing error of about 2×10^{-5} grams per gram.

Compression. Ballasted and unballasted plants, their densities established as described previously, were tested for compression in a pressure chamber which was large enough to test a whole plant and which had a lucite viewing port at the top. Plants were placed in sea water, after which the top of the chamber was sealed. By forcing more sea water into the chamber, the internal pressure was slowly increased until the enclosed plant was observed to sink slowly, at which point the water pressure was read from a gauge of known error. Compression of these plants was then expressed as the change in density with pressure, this change in density being approximately

equal to the density of the ambient sea water[7] minus the initial density of the plant.

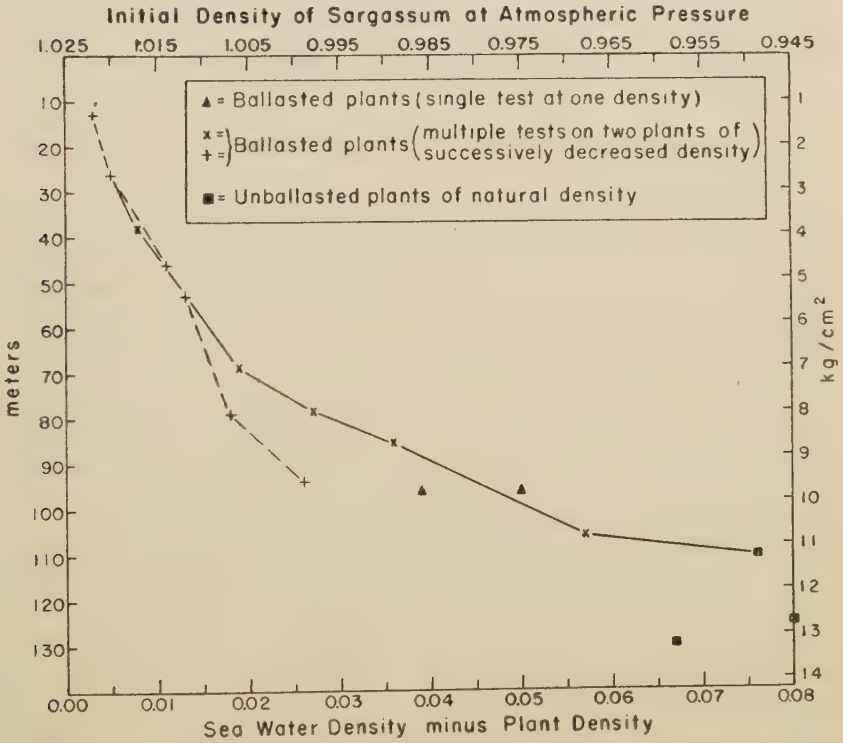

Figure 4. The effects of increasing hydrostatic pressure on the indicated initial densities of ballasted and unballasted *Sargassum*. The symbols indicate the sinking points of plants.

Fig. 4 gives the results of numerous compression tests on *Sargassum* of various initial densities and shows the effect of pressure in increasing these densities. The symbols represent the pressures or depths at which the plants of known initial density (top scale) were so compressed that they sank very slowly in sea water. The lower scale shows the approximate increase in plant density due to compression. The general trend of the points suggests a marked change in the rate of compression of the plants as the pressure is increased above

[7] Sea water densities were taken from Knudsen's (1901) tables. Salinities were determined by titration of chlorides with silver nitrate [the Oxner (1920) method].

about 7 kg cm^{-2}. This change in rate is attributed to the beginning of the implosion of the gas-filled bladders.

Plants represented in Fig. 4 were held at the higher pressures for a few minutes only. Other *Sargassum* plants of natural buoyancy (i. e., density unmodified by the addition of weight) were subjected to a sustained pressure of 5 kg cm^{-2} for a period of 90 minutes. These plants retained their positive buoyancy at this pressure and at atmospheric pressure. Other plants were held at a pressure of 2.2 kg cm^{-2} for a period of three days without apparent effect upon their buoyancy or general condition.

Rate of Rise. Regarding the speed at which water must descend to draw a plant beneath the surface, a current must have a rate of flow exceeding the plant's rate of rise. Hence measurements showing the rates of rise of *Sargassum* of various densities can be used also to estimate the current speeds which will draw these plants beneath the surface.

Fig. 5 shows the variations in the rising rates of *Sargassum* in sea water as the density of plants was made to approach the density of the ambient sea water. As shown in the given equation, plant densities were determined and artificially modified. In a tank about

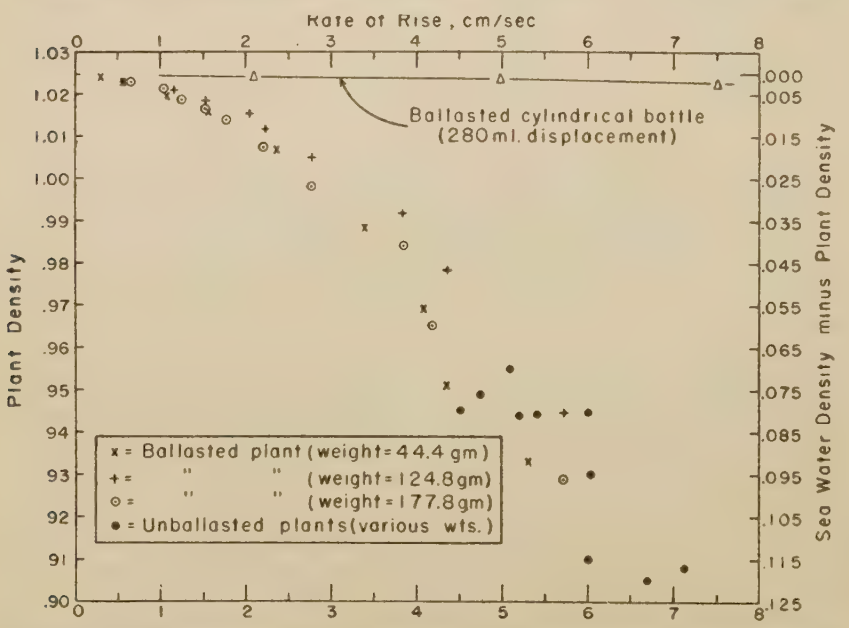
Rate of Rise, cm/sec
Plant Density
Sea Water Density minus Plant Density
Ballasted cylindrical bottle
(280 ml. displacement)
x = Ballasted plant (weight = 44.4 gm)
+ = " " (weight = 124.8 gm)
⊙ = " " (weight = 177.8 gm)
• = Unballasted plants (various wts.)

Figure 5. Showing the rates of rise of *Sargassum* of various natural and modified densities.

one meter square with a large window in one side, plants were released in sea water at an average depth of 80 cm and their rates of rise were timed after they reached terminal velocity. The black dots in Fig. 5 represent the densities and rates of rise of *Sargassum* of natural density. The other symbols represent three plants whose weights are shown in the legend. As the density of these plants was caused to approach that of sea water, the rate of rise decreased in the manner indicated.

Varying numbers of attached organisms on the experimental plants (i. e., gooseneck barnacles, bryozoa, etc.) seemed to have no effect upon rates of rise, except as they modified density. It is assumed, therefore, that the effect of ballasting on plant density is similar to the effects caused by the weights of attached organisms.

Thus, for plants having the natural range of density found in the Bermuda area, the data shown in Fig. 5 indicate that descending currents in excess of about 4.5 to 7.2 cm sec^{-1} would be required to draw them downward. The comparative effects of density change upon the rate of rise of a bottle is shown also in Fig. 5.

Bladder Gas Pressures. Parr (1939: 9) suggested that measurements of the gas pressures in *Sargassum* bladders might prove to be of interest in studying the sinking of plants. Results of some measurements of bladder pressures, with a brief description of the methods, are now given.

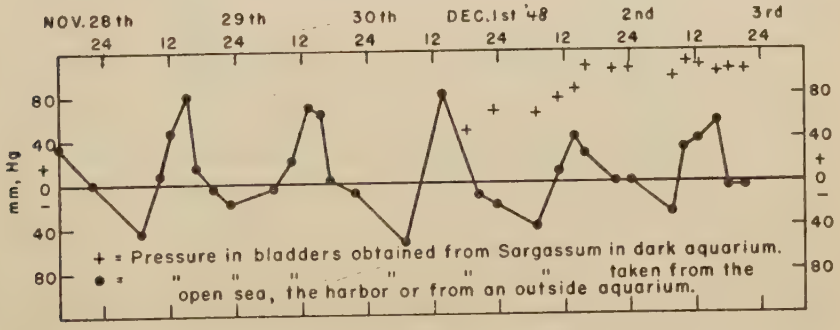

Figure 6. Variations with time of the gas pressure in *Sargassum* bladders.

Fig. 6 shows the pressures in bladders of *S. natans* during five days. Each point represents the average pressure of from 5 to 15 bladders taken from several plants. For each observation period fresh plants were taken from the sea, harbor or open-air aquarium. Pressures shown in Fig. 6 have been corrected for the effects of small water

temperature variations and atmospheric pressure changes. (During the five-day period, sea-water temperature varied between 20° and 22.6° C, and atmospheric pressure varied from 760 to 768 mm.) *S. natans* shows a diurnal pressure cycle similar to, but of greater amplitude than, that found by Frye (1915) in kelp bladders. From the results of Damant (1937) with rockweed (*Ascophyllum nodosum*) bladders, it is supposed that the *Sargassum* was secreting oxygen inside the bladders, thus increasing the gas pressure during the day. However, continuous darkness in an aquarium caused an increase in and a maintenance of a positive pressure in *Sargassum* bladders. The plus symbols in Fig. 6 show the pressures in bladders from these plants, and a marked variation from the usual diurnal pressure cycle is evident. Positive pressure is constant in an environment of continuous darkness whereas alternating positive and negative pressures occur with day and night alternations. Thus *Sargassum* should be added to the list of marine algae whose bladder gases show diurnal pressure fluctuations.

Fig. 7 shows the simple apparatus used to measure the pressures. Bladders were taken from plants immersed in sea water and were placed upon the glass micropipette (B in Fig. 7). The penetration of the micropipette tip[8] through the bladder wall, which could be felt readily, coincided with the sudden movement of bladder gas displacing the liquid (mineral oil) in the glass micropipette. Pressure was then applied on the syringe (A) until the gases were forced back into the bladder and the oil meniscus was barely visible outside the bladder wall. The pressure necessary to do this was then read from the scale beside the mercury tube (C). When bladder pressures were less than atmospheric, the pressure was suddenly reduced manually at A the instant the oil-filled needle penetrated the bladder wall. Gas was withdrawn from the bladders by this technique. As before, the pressure needed to hold the oil meniscus just outside the bladder wall was measured by the displacement of the mercury at C.

The accuracy of this method of measuring bladder pressures was not determined. The same basic method has been used by Damant (1937), by Robert Chambers (personal communication) and others. The author has found no evidence to indicate that the pressures are seriously in error. The sign of the pressures was shown to be correct by inserting the tips of glass micropipettes partly filled with water into bladders and noting whether this water flowed into or out of the

[8] Methods used in making micropipettes are described by Chambers and Grant in the 1948 edition of Encyclopaedia Britannica, under the title "Micromanipulation."

bladders. This was done with average pressures of − 20 mm and + 50 mm of mercury.

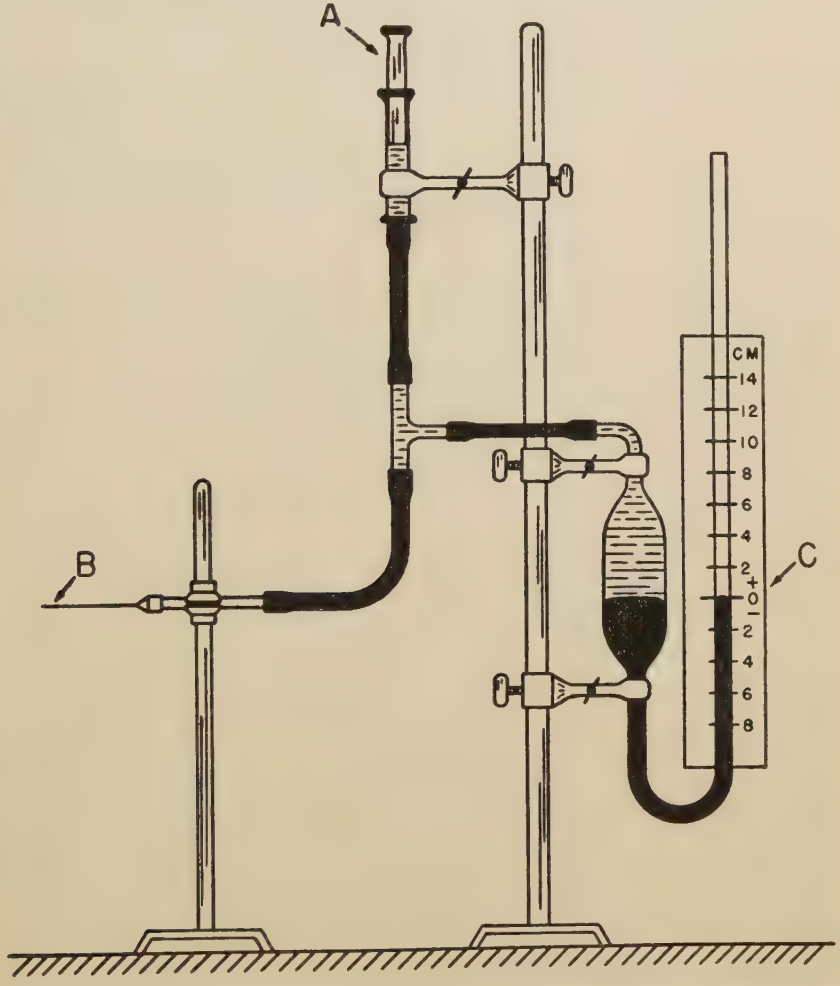

Figure 7. Diagramatic sketch of the apparatus used to determine the gas pressures in the bladders of *Sargassum*.

SUMMARY AND REMARKS

A beginning having been made in answering some of the questions about subsurface *Sargassum*, the following summary and remarks seem pertinent at this stage in the study.

1. The presence of *Sargassum* beneath the sea surface is associated with higher winds. These plants are probably drawn downward by descending currents under lines of convergence of surface waters.

2. Descending currents of 4.5 to 7.2 cm sec^{-1} would be necessary to draw *S. natans* beneath the sea surface, assuming a natural density range (0.905 to 0.955 g ml^{-1}) and rate of rise like that found among plants near Bermuda (Fig. 5). However, greater densities and lower rates of rise probably occur among pelagic *Sargassum*. A descending current of 3 cm sec^{-1} (the maximum rate measured by Langmuir [1938] in a lake) would carry downward any plants with a density greater than about 1.0 (Fig. 5).

3. Compression in *S. natans* is so low that plants of the natural density found at Bermuda could descend to depths greater than 100 meters without losing all positive buoyancy (Fig. 4). It seems probable that some plants in the regions of water convergence are drawn down to a depth at which a diminishing descending rate in the water becomes equal and opposite to the plant's rate of rise. Here the plants might remain until a further change occurred in the water motion or in the plants themselves. If cell-like water motions are associated with lines of convergence, other plants may move in trajectories which are closed circuits about the areas of descent within the cells, as pointed out by Stommel (1949).

4. A change in gas pressure within *Sargassum* bladders is associated with changes in light (Fig. 6). If these pressure changes cause the bladders to expand and contract, a diurnal variation in plant density and rate of rise may occur.

5. Subsurface *Sargassum* may be of interest to oceanographers and biologists in studying sound-scattering organisms. The nearly spherical gas bubbles in the bladders have radii ranging from 0.02 to 0.17 cm. At pressures of two to five atmospheres, air bubbles in the above size range are resonant to sound frequencies of 5 to 20 kilocycles (Anon., 1946: 463). There are several hundred of these bladders on an average plant.[9] Near atmospheric pressure the plants have been found to scatter sound markedly at a frequency of 26 kc (Smith, personal communication).

Suggestions for further study of subsurface Sargassum

In view of the foregoing measurements and observations, we may ask:

[9] It should be noted, however, that effects of the bladder walls upon resonance of the enclosed bubble are unknown.

a. What is the rate of rise and density of plants actually present under convergence lines at sea? How do these quantities vary in plants collected during different wind speeds?

b. Does the diurnal pressure change in bladders of *S. natans* significantly modify plant density and rate of rise?

c. What happens when a plant becomes neutrally buoyant at a depth of near-zero vertical motion?

d. What is the annual variation of the average density and rate of rise of *Sargassum* occurring on the sea surface?

e. How is the gas pressure in the bladders affected by long sustained hydrostatic pressures of several atmospheres?

Pelagic *Sargassum* is adapted, through long periods of time, to survival on the surface of the central North Atlantic Ocean (Parr, 1939). It is the author's opinion that a thorough study of the motions of this plant on and within the upper layers of the sea will add to an understanding of the water motions in this important part of the sea.

The author wishes to thank Alfred C. Redfield, George L. Clarke and Albert E. Parr for their helpful criticism.

REFERENCES

Anonymous
1946. Physics of sound in the sea. Research Analysis Group, National Research Council, Div. 6, National Defense Research Committee. Summary, Tech. Rep., *8* (4): 441–546.

Damant, G. C. C.
1937. Storage of oxygen in the bladders of the seaweed *Ascophyllum nodosum* and their adaptation to hydrostatic pressure. J. exp. Biol., *14:* 198–209.

Frye, T. C.
1915. Gas pressures in *Nereocystis.* Publ. Puget Sd. Mar. (biol.) Sta., *1:* 85–88.

Knudsen, Martin
1901. Hydrographische Tabellen. G. E. C. Gad, Kopenhagen. 63 pp.

Langmuir, Irving
1938. Surface motion of water induced by wind. Science, *87:* 119–123.

Lowndes, A. G.
1942. The displacement method of weighing living aquatic organisms. J. Mar. biol. Ass. U. K., *25:* 555–574

Montgomery, R. B.
1941. Transfer of heat and water across the sea surface. Woods Hole Oceanographic Institution, Woods Hole, Mass. Unpublished.

Murray, John and Johan Hjort
1912. The depths of the ocean. Macmillan and Co., London. 821 pp.

Oxner, Miczyslaw
1920. Chloruration par la methode de Knudsen. Bull. Comm. int. Explor. Mediterr., No. 3: 1–36.

Parr, A. E.
1939. Quantitative observations on the pelagic sargassum vegetation of the western North Atlantic. Bull. Bingham oceanogr. Coll., *6* (7): 1–94.
Stommel, Henry
1949. Trajectories of small bodies sinking slowly through convection cells. J. Mar. Res., *8:* 24–29.
Winge, Øjvind
1923. The Sargasso Sea, its boundaries and vegetation. Rep. Danish oceanogr. Exp. 1908–10. *3,* Misc. Pap. 2: 1–34.
Woodcock, A. H.
1944. A theory of surface water motion deduced from the wind-induced motion of the Physalia. J. Mar. Res., *5:* 196–205.

SOME CURRENT METERS DESIGNED FOR SUSPENSION FROM AN ANCHORED SHIP[1]

By

WILLIAM S. von ARX

Woods Hole Oceanographic Institution

ABSTRACT

Current velocities measured by means of instruments suspended from shipboard may err significantly if the ship's motion at anchor is permitted to tow the instruments through the water while observations are in progress. Two current meter designs are described which employ a propeller linkage by electromagnetic induction to permit continuous observation of current velocity through, and to determine the extent of, the periods when the anchored ship is essentially at rest. The motions of an anchored ship are described.

Current velocity measurements made by means of instruments suspended from shipboard may err significantly if the ship's motion at anchor is permitted to shift the position of the instruments in the water while observations are in progress. On occasion, the ship's motions have been eliminated by mounting the current meter in a bottom frame, reduced by employing anchors at the bow and stern, or have been corrected by allowing the ship to drift a measurable distance and direction while current measurements are being made. When these methods are impractical it is still possible to make intermittent current measurements from an anchored ship during certain phases of the ship's motion when the acceleration is great but the velocity small. Continuous indication current meters permit the incoming velocity signals to be sorted into categories of ship's motion and water velocity. Once the rhythm of the ship's motions at anchor has been found, this technique allows observations to be made at predictable intervals. The method has been found useful on the continental shelf and in surveys of sheltered waters.

Current meters of several experimental designs which employ electromagnetic induction as the link between the propeller and the registering equipment have been built to provide continuous indications of current velocity to an observer on deck.[2] The link by electromagnetic induction between the propeller and the signal circuit

[1] Contribution No. 509 from the Woods Hole Oceanographic Institution.

[2] Some general interest in these instruments has prompted the preparation of working drawings of present designs, prints of which may be obtained from the Woods Hole Oceanographic Institution.

involves no moving parts save the propeller itself. To form this link, the propeller is fitted with a small Alnico V magnet at the tip of one blade, and a small coil of wire is housed on the propeller guard. Each turn of the propeller causes the flux of the magnet to cut the turns of the wire coil. This induces a momentary pulse of electromotive force in the coil and causes an electric current to flow in a closed circuit. When this circuit is closed through the indicating or recording apparatus on deck, measurements of the current speed can be obtained by counting, recording, or integrating these pulses as they are generated. The signal is transmitted to the deck by a two-conductor rubber-insulated cable. The cable also serves as a suspension to support the current meter over the bottom.

The pulses, generated in the coil by the passing magnet and transmitted by the cable, have the form with respect to time shown in Fig. 1a. Each wave corresponds to a turn of the propeller. These

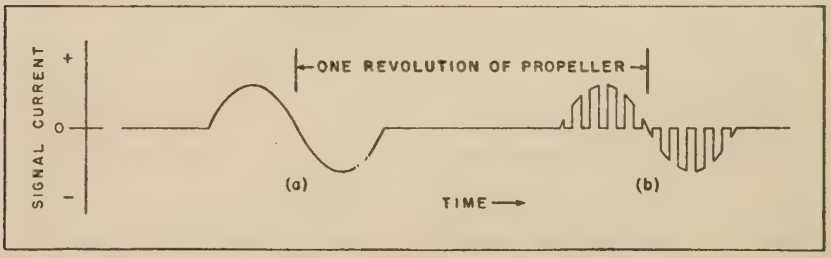

Figure 1a. The signal generated by the propeller-tip magnet as it passes the pick-up coil. Figure 1b. The signal of the following revolution of the propeller shown interrupted at an audible frequency.

waves represent enough power to operate an indicating or recording microammeter or a pair of headphones, provided impedances are reasonably well matched. The pulsing of the signal wave is subaudible, but when interrupted at an audible frequency, a signal having the form shown in Fig. 1b can be heard in phones over the background noise of wind, waves, and ordinary ship's machinery. Interruption is most simply accomplished by means of a battery-driven reed vibrator.

The energy of the electrical signal is derived from that given the propeller by the passing water. Thus there is an intermittent drag during part of each rotation of the propeller which may produce a "toe" on the calibration curve at speeds below one-quarter knot. The intermittent magnetic drag may equal the energy imparted by the water passing at a speed of 0.05 knot (2.5 cm/sec). This, combined

with propeller bearing friction, usually places the minimum detectable water speed in the neighborhood of 0.15 knot (7.5 cm/sec).

The magnetic and electric circuits used to detect the propeller rotation are shown in Fig. 2.[3] The electrical characteristics of these circuits may be varied within wide limits. Three kinds of circuits have been utilized:

1. Direct recording of the propeller rotation signal on the tape of a recording 0–1.0 milliammeter (Esterline Angus). The signal should be rectified through a Selenium rectifier bridge before it enters the recorder so that both swings of the signal wave have the same sign.

2. Visual detection of the rate of propeller rotation through the replacement of the above recorder by a slow response microammeter. Very low rates of rotation will be indicated by separate kicks of the needle, which can be counted, and higher rates will produce a steady deflection.

3. Acoustic detection of the propeller rotation signal by headphones. Pulses are counted over an interval of time, usually one minute. With a little practice, high pulse rates may be counted by threes, fours, sixes, or even tens, up to the rate of 600 pulses per minute.

Sufficient signal strength for all of these circuits can be obtained if the magnetic link is composed of from 10 to 15 grams of Alnico V magnet stock (having a cross section 0.5 cm^2 and length 1.0 cm) mounted on the tip of one propeller blade so that it passes the pick-up coil with a gap of less than 0.5 cm. The pick-up coil may be coreless and should have an inductance near 1.0 henry and resistance to match that of the cable plus either the headphones, microammeter, or milliammeter recorder. The smallest coil at hand, a "sound level recorder clutch coil" made by Sound Apparatus Co., New York City, was used in the first of these induction current meters. Other equivalent coils of larger physical size have been used but with no conspicuous change in performance. The "clutch coils" have an inductance of 0.8 henry and a resistance of 2000 ohms. They are fragile, but when packed in grease in the propeller guard housing no harm seems to come to them even when the rest of the current meter is rather badly battered from hard use.

Two styles of underwater units have been designed which employ the induction link. The earliest is the "Model I" current meter which is designed to indicate only current speed, the direction being observed visually. This is a practical arrangement for the clear water of the tropics and for shoal observations in coastal water. In tideways and

[3] Western Electric IN34 rectifiers have greater current capacity and are recommended in place of the IN22 rectifiers specified.

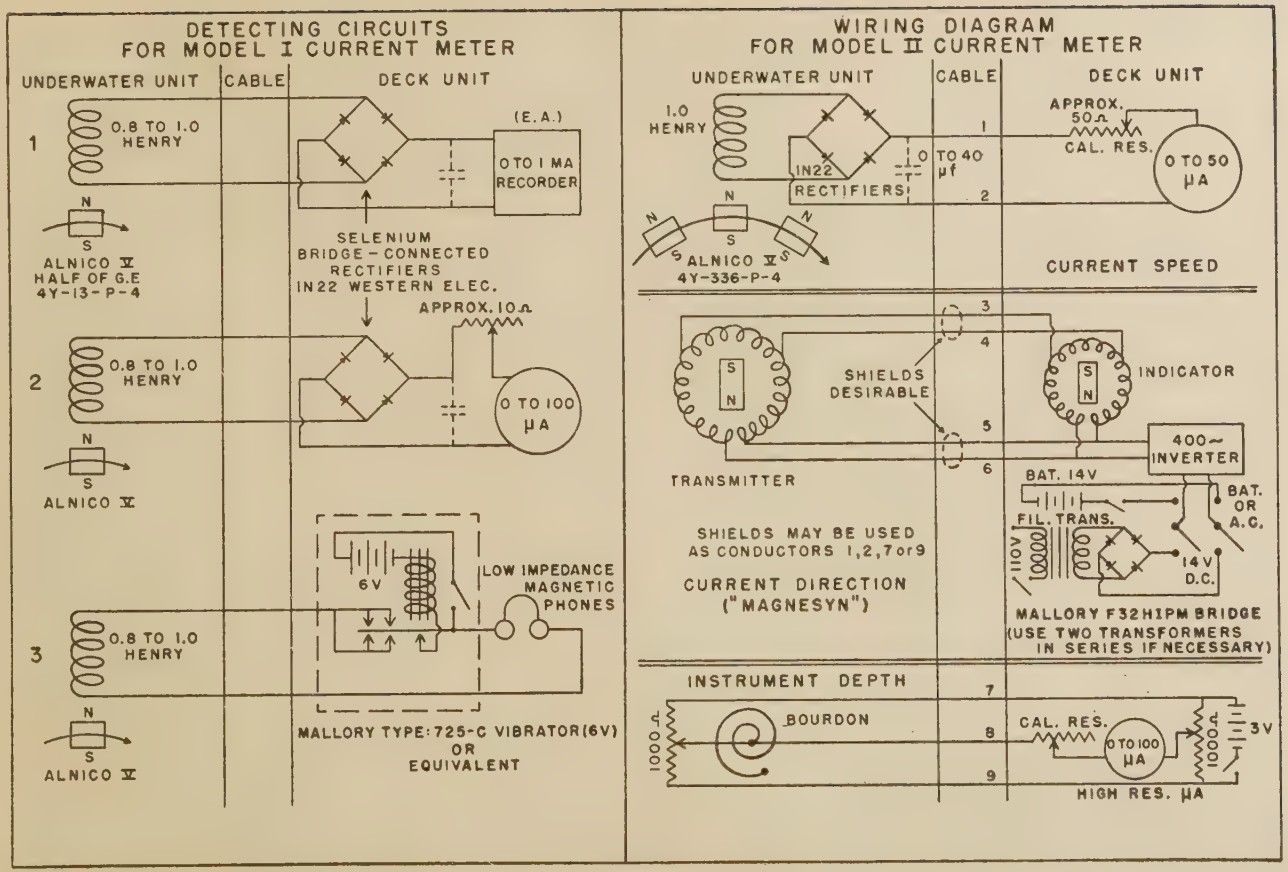
DETECTING CIRCUITS
FOR MODEL I CURRENT METER
UNDERWATER UNIT
CABLE
DECK UNIT
1
0.8 TO 1.0 HENRY
N
S
ALNICO V HALF OF G.E 4Y-13-P-4
(E.A.)
0 TO 1 MA RECORDER
SELENIUM BRIDGE-CONNECTED RECTIFIERS IN22 WESTERN ELEC.
APPROX. 10Ω
2
0.8 TO 1.0 HENRY
ALNICO V
0 TO 100 μA
6V
LOW IMPEDANCE MAGNETIC PHONES
3
0.8 TO 1.0 HENRY
ALNICO V
MALLORY TYPE: 725-C VIBRATOR (6V) OR EQUIVALENT
WIRING DIAGRAM
FOR MODEL II CURRENT METER
UNDERWATER UNIT
CABLE
DECK UNIT
1.0 HENRY
IN22 RECTIFIERS
.1
TO 40 μf
APPROX. 50Ω
CAL. RES.
0 TO 50 μA
ALNICO V 4Y-336-P-4
CURRENT SPEED
SHIELDS DESIRABLE
INDICATOR
400~ INVERTER
TRANSMITTER
BAT. 14V
BAT. OR A.C.
FIL. TRANS.
110V
14V D.C.
SHIELDS MAY BE USED AS CONDUCTORS 1,2,7 or 9
CURRENT DIRECTION ("MAGNESYN")
MALLORY F32H1PM BRIDGE
(USE TWO TRANSFORMERS IN SERIES IF NECESSARY)
INSTRUMENT DEPTH
BOURDON
1000Ω
CAL. RES.
0 TO 100 μA
3V
HIGH RES. μA

Figure 2.

rivers, wherever the current direction is known to remain nearly constant from top to bottom, useful data may be obtained even when the meter is lowered out of sight. In some sediment motion studies, for which direction is unimportant, these meters have been used in bottom frames for prolonged periods of observation. The "Model II" current meter is equipped with a remote reading magnetic compass and a bourdon-operated depth-indicating circuit, for when a current meter is lowered in swift water, wire angles become large and the depth of measurement is uncertain.

The Model I Current Meter is illustrated in Fig. 3A. It has been found most practical to use the acoustic method for detecting the propeller turns so that the observer's vision is free to attend to direction. An underwater viewing box or glass port in the bottom of a skiff is essential when the current meter is deeper than two meters. In the clearest water the Model I meter can be seen in full daylight to depths as great as 40 meters. At night it is possible to observe the current direction to roughly the same depth if the scene is illuminated by a reflector photoflood lamp (R-2) lowered to a depth of about 10 meters. To protect the glass envelope from thermal shock, the lamp should not be lighted until it is under water.

The Model I current meter is not affected by pressure. The only cavity in the instrument, the pick-up coil housing, is packed with stiff grease; the ambient sea water pressure is admitted through the grease fitting.

Cables for Model I current meters have been adapted from those used for underwater demolition. These cables have steel strands in each of the copper conductors. In lengths greater than a few meters, their resistance to torsion is low enough so that they do not influence the direction of the current meter and their strength is so great that they will survive several years of ordinary use. It is convenient to store the current meter cable on a reel, and since it is inconvenient to have the current meter attached to the stored cable, the coupling shown in Fig. 3B has been used. This is built of ordinary 1-inch pipe-fittings and is filled with light grease when the connection is made. When disconnected, the components may be protected with a nipple and cap. A plug-in receptacle on the cable reel, Fig. 3C, permits the first turn of the cable to be spooled inside, thus eliminating one of the free ends.

The Model II Current Meter is illustrated in Fig. 4. This current meter has been supported by an experimental nine-conductor cable designed to have low resistance to torsion. The barrel of the instrument is designed to withstand pressure at 300 meters. The pressure

case contains a Magnesyn compass transmitter to report direction to the deck, a bourdon-operated microtorque potentiometer to report instrument depth, and a pick-up coil with Selenium rectifiers to supply a microammeter in the deck panel that indicates as a current speedometer. To smooth the microammeter action, the signal impulse rate of this instrument has been increased by mounting several smaller magnets separately on the tip of each propeller blade instead of having a larger magnet mounted on only one blade. This change improves the microammeter action and its response at low current speeds, but it removes the possibility of counting individual propeller revolutions at the lowest current speeds.

The Model II meter, through its ability to indicate continuous values of velocity and depth, has been used in a qualitative study of: (1) the value of Garbell fins for directional oceanographic instruments, and (2) the motions of an anchored ship.

(1) When the Model II meter was built it was fitted with both the conventional streamline fin and an experimental pair of Garbell fins,[4] shown in Figs. 4A and 4B respectively. The remarkable feature of Garbell fins is the high directional sensitivity they impart to a "short" instrument having greatly reduced rotational inertia. The amount of toe-in (negative angle of attack) of the fins influences both the drag and directional sensitivity. If the fins are designed to stall easily, the amount of toe-in can be reduced to a few degrees, the drag materially decreased, and the directional sensitivity markedly increased. The modified airfoil sections which have been used to approximate Garbell hydrofoils have given good experimental results. When fitted with these Garbell fins the instrument is steady at all speeds up to six knots, the highest tested, responds quickly in turbulent water, and develops wire angles of the same order of magnitude as those developed when the common fin is attached. The short impingement time lag and high sensitivity to the direction of flow afforded by Garbell fins extends the period of observation available from an anchored ship.

(2) Fig. 5 shows how an anchored ship, unless secured by several anchors, is constantly in motion, yawing from side to side and riding to and fro the anchor. Yaw is the principal motion. At the end of each yaw there is a period when the ship swings off on the opposite tack, and during the swing a certain point in the ship's length is temporarily at rest with respect to the bottom. The location of this point is usually well forward of amidships and varies with the size and shape of the ship. If the current meter suspension is led over

[4] Garbell, M. A. Fins for aerological instruments. J. Meteorology, *4* (3): 82–90, 1947.

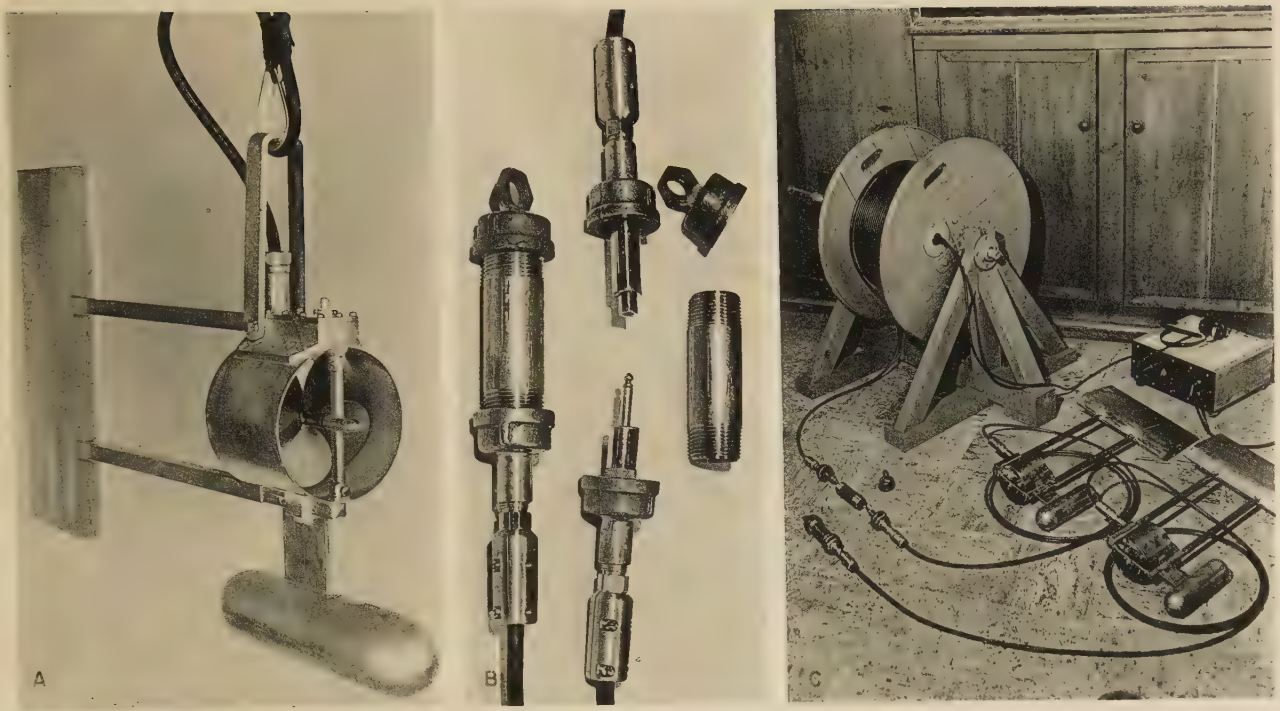

Figure 3. *A*. Model I current meter for measuring current speed. Current direction, under favorable conditions, can be observed visually to a depth of 40 meters. *B*. Cable connectors permit Model I current meters to be detached from the cable drum for storage or to be interchanged in the field. *C*. The Model I current meters used at Bikini, together with the cable drum, interrupter box and phones. These two instruments have been in use since 1946 and, though battered, still function reliably. The propeller and cable attachment details have been changed in more recent instruments illustrated in Fig. 3A.

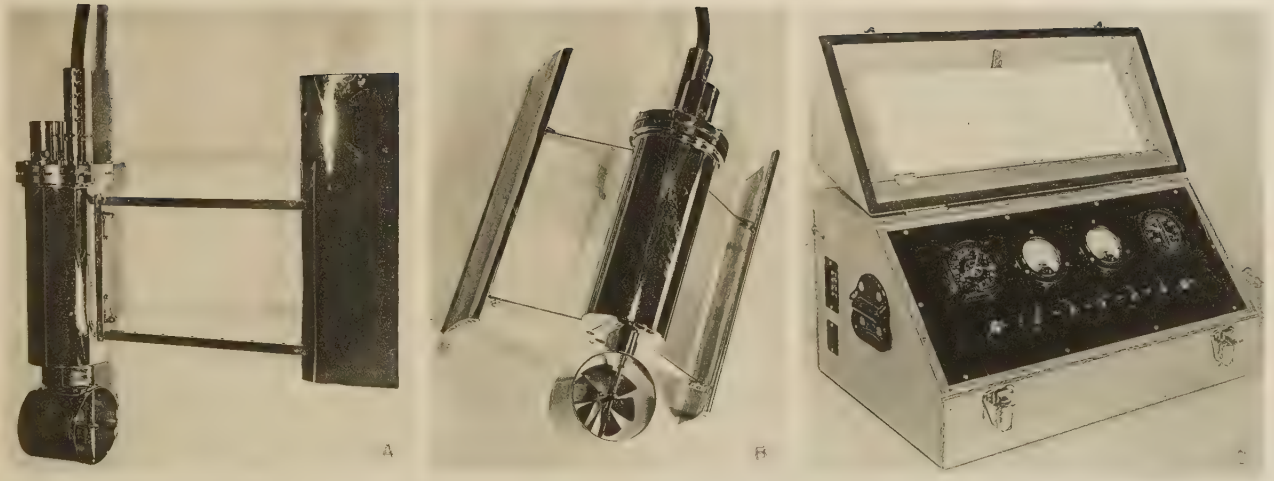

Figure 4. *A.* Model II current meter fitted with the ordinary streamline fin. The pick-up coil is housed in the strut connecting the pressure body with the propeller guard. The cylinder forward of the cable clamp houses the oil-filled sylphon which communicates the sea pressure to the bourdon inside the pressure case. *B.* Model II current meter fitted with Garbell fins. Behind the pressure case there is a streamline fairing to reduce the turbulence and improve the action of the fins. *C.* Model II current meter deck unit. From left to right the dials indicate: Time, current speed, instrument depth, and current direction. The knobs and switches (from left to right) control: Battery – A.C. power supply, current speed range, depth indicator range, depth zero adjustment, depth calibration adjustment, Magnesyn inverter current, and Magnesyn on-off. The Jones plug receptacles on the left end of the box feed the depth and current speed circuits (above), and the Magnesyn (below). On the right-hand end of the box there is a receptacle which permits A.C. operation. The current speed calibration curve is protected under lucite in the cover.

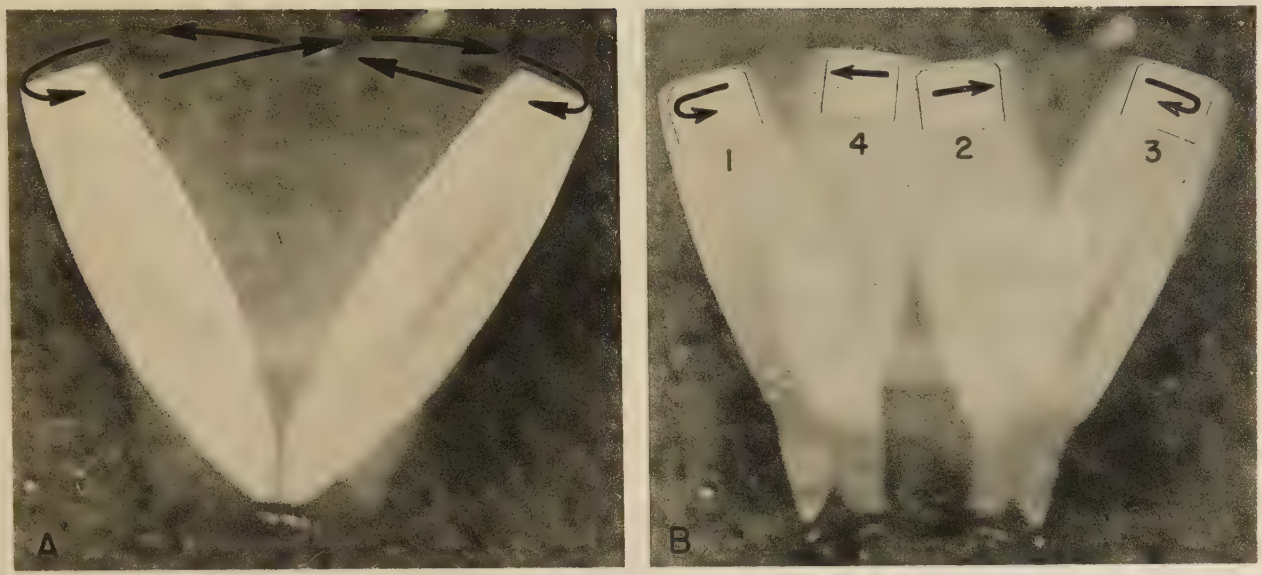

Figure 5. *A*. Multiple exposure photograph of a model ship at anchor with a scope of 3. The arrows indicate the motion of the stern in response to the combined forces of wind and current. *B*. Multiple exposure photograph of the same model showing the initial and final positions of the swings 4-1 and 2-3 and the character of the yawing motion 1-2-3-4.

the rail into the water at this center of rotation, the upper end of the current meter cable will be held at rest with respect to the bottom for a matter of seconds or minutes, depending on the size of the ship. During this time, measurements can be made with some degree of reliability provided the time is long enough for the current meter and cable to come to equilibrium. At equilibrium during these stationary intervals the indicated current speed is minimum, the indicated rate of change of direction is maximum, and the indicated depth maximum. The speed observed during the motionless period and the average of the directions observed on the preceding and succeeding yaws is taken to be the current velocity. Since this technique permits the ship to lie at only one anchor it is possible to make reasonably reliable measurements of current velocity in all depths at which a single anchor can reach and hold. Whenever possible, however, a second anchor should be placed under foot without scope. This second anchor will snub the motion of the bow considerably and thereby reduce both the ride and yaw.

THE OCCURRENCE OF PRONOUNCED SALINITY VARIATIONS IN LOUISIANA COASTAL WATERS

By

RICHARD A. GEYER

Humble Oil & Refining Company

ABSTRACT

The chloride-ion contents of more than 700 sea water samples from the coastal waters of western Louisiana were converted to salinity values and were used in a study of the salinity characteristics. These data were gathered from seven drilling platforms during a period of 14 months in a zone paralleling the coast for about 60 miles, approximately 6 to 8 miles offshore and in depths varying between 40 and 50 feet. The chloride-ion content was determined by the standard chemical titration method in connection with quality control of salt water drilling mud used in the drilling of offshore oil wells.

An independent check of the validity of these data by means of salinity values derived from temperature and density determinations corroborate the existence of marked short and long range changes in salinity. In conclusion, it is pointed out that the existence of these salinity variations also means that other chemical and physical properties of sea water in the areas studied must be varying in essentially the same manner. Therefore, the marine organisms in these areas are subjected to a constantly changing ecological environment and must be continually making the physiological adjustments necessary to cope with these changes.

The analysis of the chloride-ion concentration data clearly demonstrates the existence of a wide salinity variation in any one area. The variations may be classified into long seasonal and shorter daily and even hourly types. A well defined correlation exists between the seasonal variations in salinity and the variations in the amount of water discharged by the Mississippi River. These data demonstrate that this is the major factor in determining the long term salinity characteristics of this area. However, available information also indicates that salinity variations in a given area are affected as well by local drainage patterns and current characteristics.

Results of the statistical summary show that the greatest variations occur from January through March and the least during summer months. This is further evidence in support of the argument that variation in the discharge of the Mississippi River is the major factor responsible for the pronounced long term salinity changes.

INTRODUCTION

It has long been suspected, and certain isolated bits of information have indicated, that the discharge of the Mississippi River and the westward moving littoral current are responsible for the marked decrease in salinity in the offshore coastal waters of Louisiana west of the delta. The only readily available published data on this subject are incorporated in papers by Riley (1937) and Parr (1935); for salinity

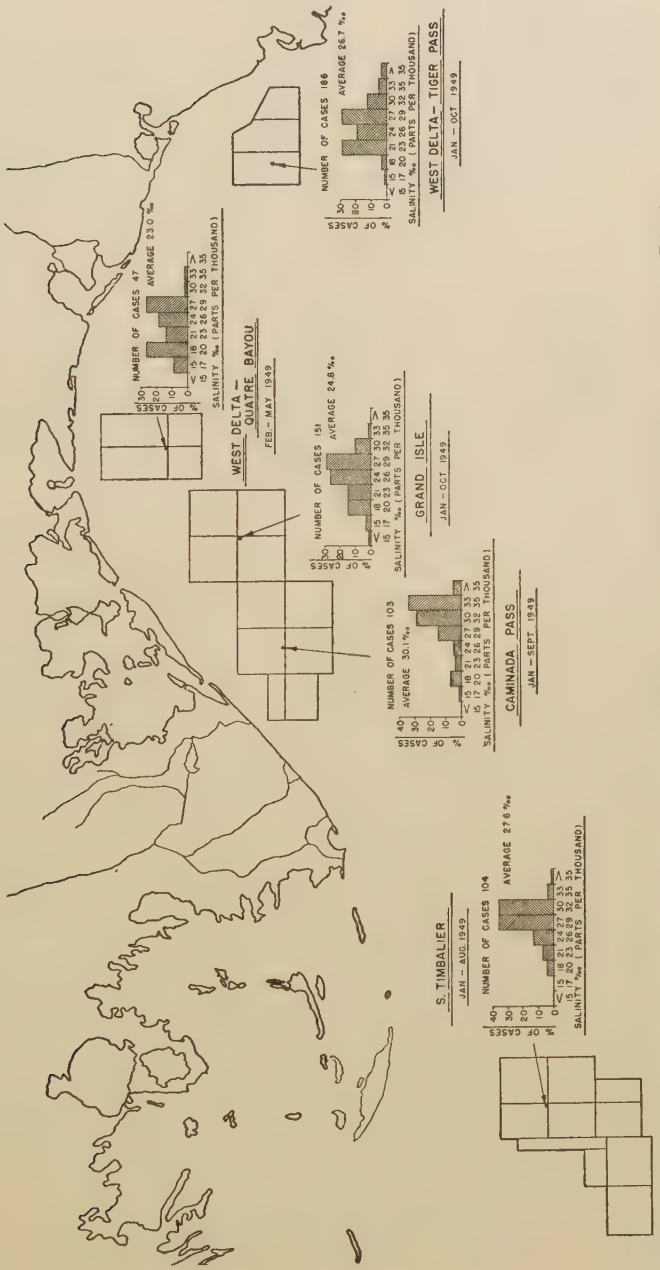

Figure 1. Frequency distribution of salinity values at drilling locations in Grand Isle District.

and phosphate distribution, see Riley (1937: figs. 20, 21). With the advent of the offshore drilling era it became feasible to obtain sufficient information to arrive at certain definite conclusions regarding the relationship between the discharge of the Mississippi River and salinity variations in the offshore coastal waters. Permanent observation platforms, extending as far as 24 miles offshore, are now available in this area. The data discussed in this report have been obtained from a series of platforms located west of the delta starting near Long. 89° 30′ W and continuing 90° 30′ W (about 60 miles) in a zone paralleling the shore line at a distance of approximately 6–8 miles offshore. The absence of fresh water in this area, together with the cost of barging from inland points, necessitates the use of salt water in the drilling mud. As one phase in maintaining good quality control of this type of drilling mud, the chloride-ion content of both the mud and the sea water is frequently analyzed by means of the conventional and universally accepted titration method. This procedure constitutes the basic source of the data discussed in this report.

DISCUSSION OF DATA

Seasonal Variations. The chloride-ion contents of approximately 700 sea water samples, obtained from a mean depth of about 10 feet below the surface, were compiled and analyzed. They represent observations made at seven platforms over a fourteen-month period from September 1948 through October 1949. These data were converted to salinity values by using the standard formula given by Sverdrup, et al. (1946: 51). Because of the proximity of several of these platforms to one another, the region under discussion is reduced to five areas which are treated as distinct units in the analysis of these data. The locations of these areas with respect to the shore line and the land drainage pattern are shown in Fig. 1. In addition, a histogram, which summarizes the percentage frequency distribution and range of salinity values observed for a representative period of approximately 10 months, was compiled and plotted on this figure for each of the areas. The salinity over the entire region ranges from about 14 to 35°/$_{oo}$ or more, although the percentage frequency distribution of the observed salinities varies appreciably from one area to another and from month to month. These variations between areas and months undoubtedly represent the combined effects of the proximity to the mouth of the Mississippi River and other drainage outlets in the more immediate vicinity and of the prevailing current characteristics.

Another series of histograms was constructed to show the variation of percentage frequency distribution and range of observed salinities

by months. These again reflect the effect of the above mentioned factors. The greatest range in salinity, varying from 14 to 38°/₀₀, is observed during the spring months, whereas in June and July, for example, the range is limited between 21 and 37°/₀₀. Thus, with the beginning of summer the range not only decreases but the values are concentrated in the higher salinity class intervals. These relationships are illustrated in Fig. 2.

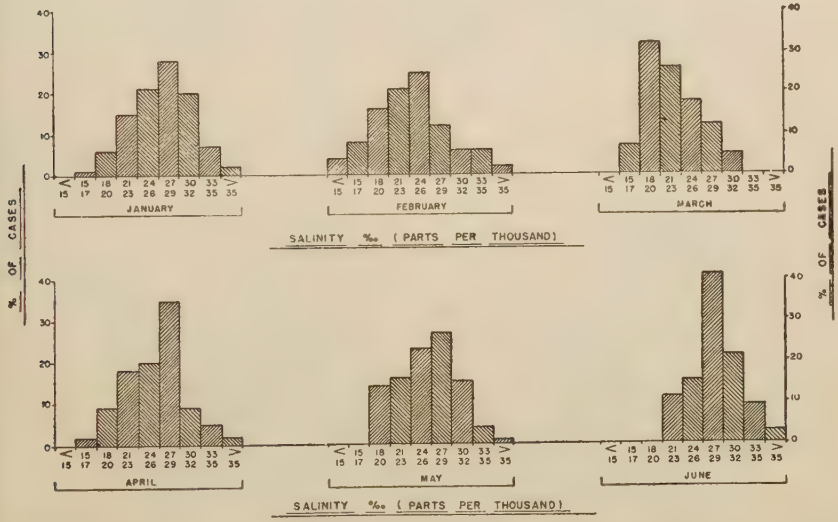

Figure 2. Frequency distribution of salinity values for a six-month interval in the Grand Isle District.

An analysis of the average salinity values by months for September 1948 through October 1949 for the entire region is shown in the bar graph in Fig. 3; shown also is the average monthly discharge of the Mississippi River for the same period. This graph demonstrates that the effect of the discharge of the Mississippi River on the salinity of the offshore coastal waters dominates salinity characteristics of the entire region. For example, a minimum average salinity of 22.6°/₀₀ is observed during March when the river is carrying off the melting snows and spring rains. The average monthly salinity then continues to increase throughout the remainder of the late spring and summer, reaching a maximum of 34.1°/₀₀ in November. These changes correspond closely with the marked decrease in the discharge of the Mississippi River, reflecting summer rainfall and runoff conditions. Although data for only a portion of the second year's record are

available, it is evident from Fig. 3 that the cycle is beginning to repeat itself, although the absolute values are somewhat less.

Short Term Variations. The evidence presented thus far demonstrates that a wide variation in salinity occurs in these coastal waters each year and that this variation shows pronounced seasonal effects which reflect primarily the seasonal variations in the amount of water discharged by the Mississippi. The remainder of the discussion will show that the salinity in this region varies markedly in each area over a shorter period of time, of the order of days, and even fractions of

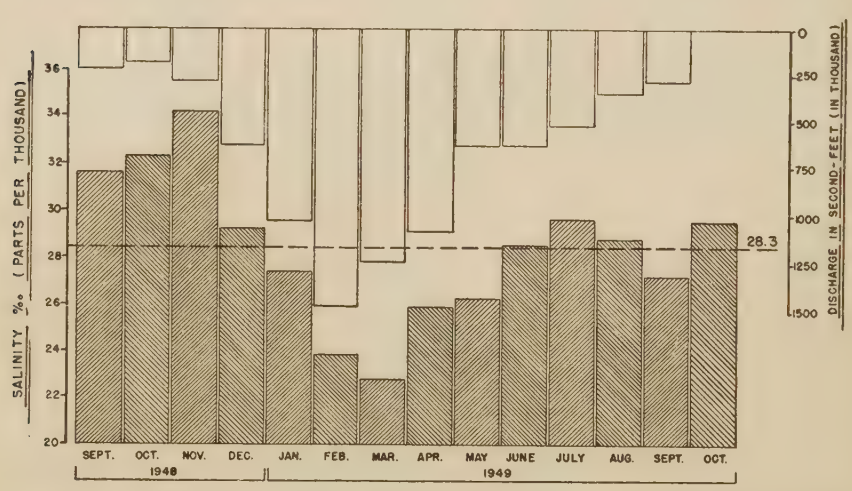

Figure 3. Comparison of monthly average salinity values with discharge in sec./ft. of the Mississippi River at Vicksburg.

days. Examples of these marked and frequent salinity variations are plotted in Fig. 4 for four of the areas. This illustration demonstrates that salinity variations of as much as 19°/$_{oo}$ can occur in a matter of one to two days. These occurrences are characteristic of the areas studied rather than isolated. In addition to the marked short period variations, the seasonal trends are also evident in these graphs.

The values plotted in Fig. 4 are primarily one-a-day observations. However, for one location a series of observations is available for a two-month period during which the chloride-ion content was measured as often as three times a day. These data, plotted in Fig. 5, indicate that even shorter period variations of the order of several hours exist in addition to the seasonal and daily variations of salinity.

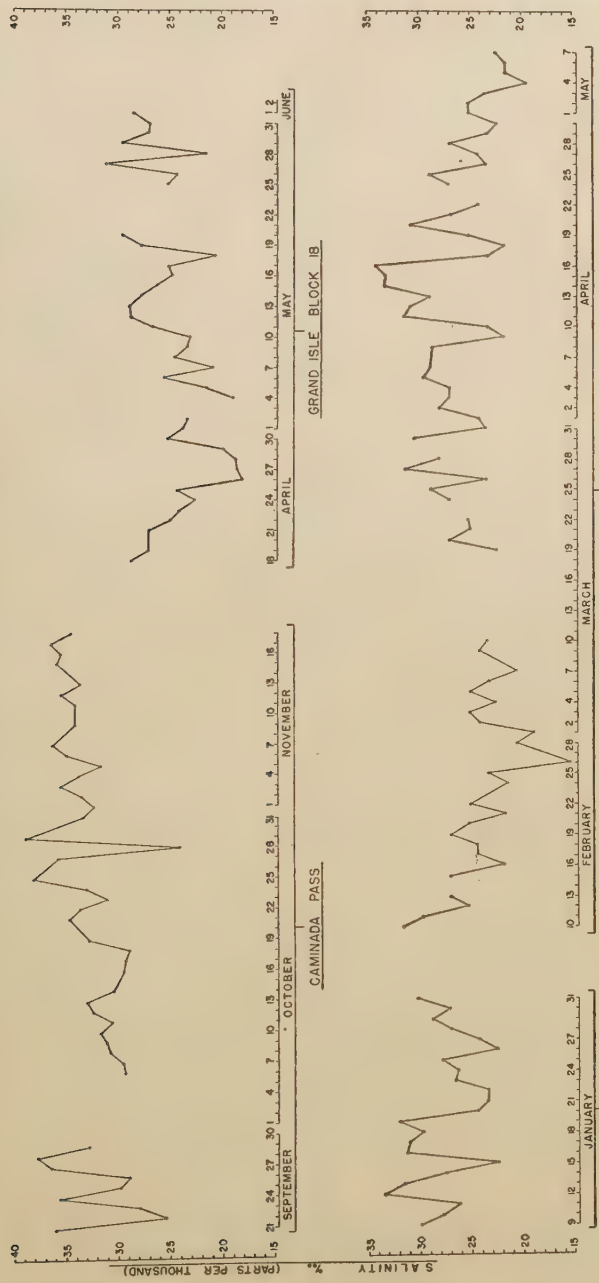

Figure 4. Example of frequent salinity variations in the Grand Isle District, 1948–1949.

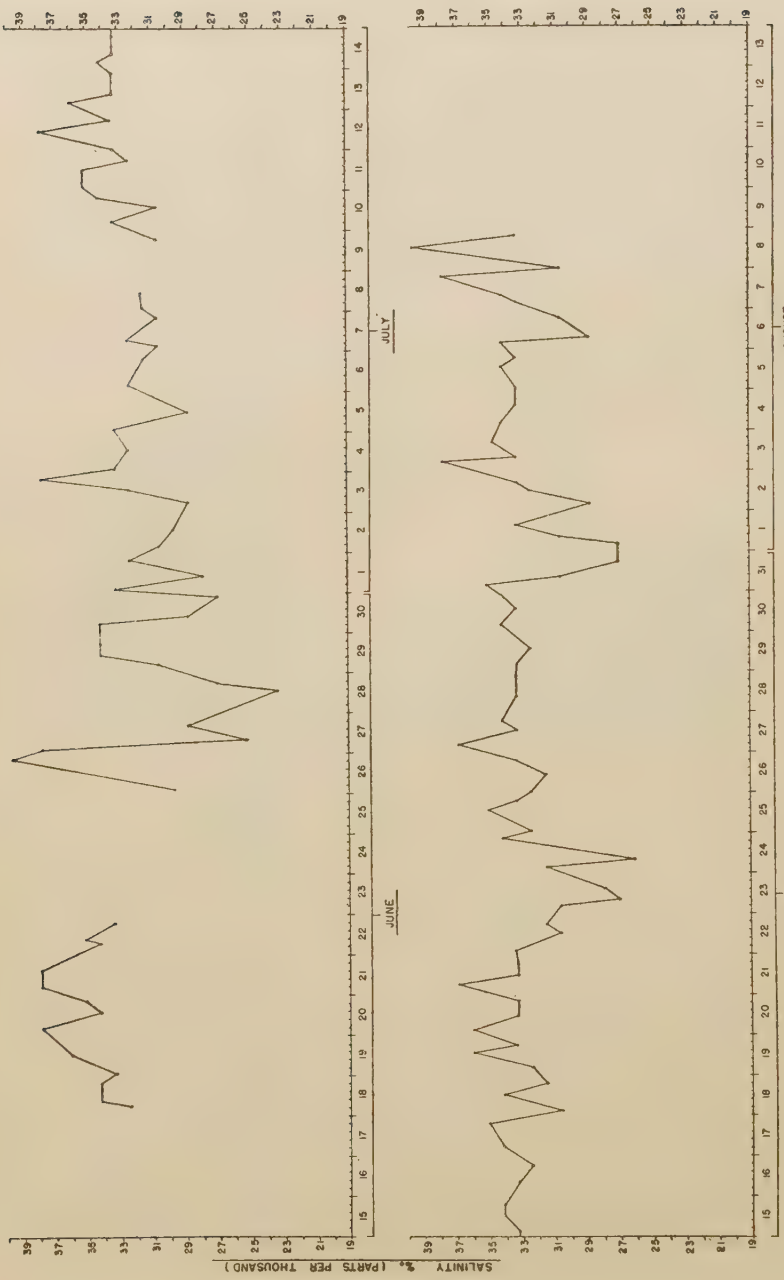

Figure 5. Short and long period salinity variations in the Caminada Pass area from June 18 to August 9, 1949.

A statistical quantitative analysis of the daily salinity variations for the five different areas is summarized in Table I.

TABLE I. Percentage Frequency Distribution of Observed Daily Changes in Salinity and Maximum Range for Each of the Areas Studied

Area	*Less Than 2 ppm* (%)	*2–5 ppm* (%)	*Greater Than 5 ppm* (%)	*Maximum Range* (*ppm*)
Tiger Pass	57	30	13	11
Quatre Bayou	43	38	19	10
Grand Isle	61	25	14	10
Caminada Pass	64	25	11	19
S. Timbalier	57	31	12	12
Average	56	30	14	12
Maximum Difference Between Areas	18	13	8	9

This table demonstrates that the Caminada Pass area has the least variation in day to day salinity whereas Quatre Bayou has the greatest. More than half of all observations for this latter area show variations of more than 2°/₀₀ and almost one out of every five greater than 5°/₀₀. Analyzing the data as a whole, Table I also shows that day to day variations of more than 2°/₀₀ occur for almost half the observations and more than 5°/₀₀ for 14% of the observations. The appreciable difference in the degree of day to day salinity variations for the five areas studied indicates that they are affected also to an appreciable extent by their locations with respect to local drainage patterns and current characteristics.

An analysis of the observed daily changes in salinity for all of the areas by months for a representative period starting in June and continuing into August 1949 is presented in Table II.

This summary, expressed in terms of the percentage frequency distribution, indicates that the greatest variations with respect to time of year occur during the months of January through March, the least during the summer months; for example, for at least one-half of the time during the spring months there are variations of more than 2°/₀₀ in salinity, and in January one out of every four observations shows a day to day variation of more than 5°/₀₀. This is again in agreement with the previous facts demonstrating that the variation in the discharge of the Mississippi River is the major factor responsible for these changes in salinity.

Independent Check of Validity of Data. These data were obtained initially in the form of the chloride-ion content of sea water and were

TABLE II. Average Salinity, Percentage Frequency Distribution of Observed Daily Changes in Salinity, and Maximum Range by Months for January–August 1949 for All Areas

Month	*Average Salinity (ppm)*	*Less Than 2 ppm (%)*	*2–5 ppm (%)*	*Greater Than 5 ppm (%)*	*Maximum Range (ppm)*
January	27.3	47	27	26	19
February	23.9	57	31	12	9
March	22.6	44	42	14	10
April	25.9	58	26	16	11
May	26.2	59	27	14	13
June	28.4	64	23	13	10
July	29.6	67	33	0	5
August	28.7	72	21	7	10
Average	26.6	58	28	14	
Maximum Difference	7.0	33	21	26	

converted to salinities by the standard conversion formula. This is the first appreciable amount of information available from this region and it is characterized by pronounced as well as rapid short and long period variations. It was felt, therefore, that a verification of these phenomena with evidence obtained by an entirely different method would add significantly to the validity of the observations and their interpretation. An official U. S. Coast and Geodetic Survey tide gauge station is located on the Grand Isle platform, and at this station daily reports are made of the temperature and density of a sample of sea water taken from or near the surface. These observations for a representative two-month period were converted to salinity values by the standard method discussed by Adams (1942: 585). The corresponding salinities were then plotted as illustrated in Fig. 6. The same characteristics as those found in the other graphs (Figs. 4, 5) are evident. Thus, two independent lines of corroborative evidence are available.

CONCLUDING REMARKS

In view of the frequent and marked salinity changes, other chemical and physical properties of the sea water must be changing also in essentially the same manner. This statement is based on the fact that the salinity changes actually reflect the movement of water masses as a unit rather than as a specific isolated change of one particular physical characteristic. Thus, if the salinity changes at one location, then the whole water mass changes in that area, such change being attended by variations in other factors such as oxygen and

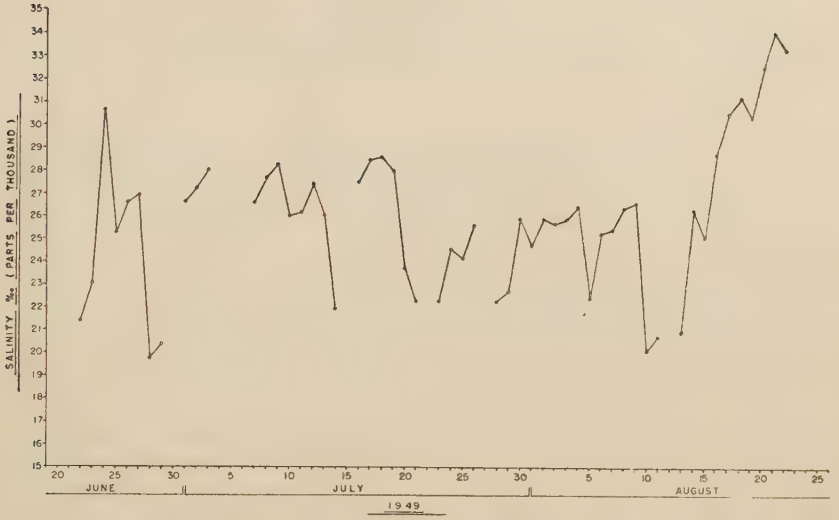

Figure 6. Salinity data for Grand Isle platform computed from hydrometer and temperature measurements of sea water at surface.

hydrogen-ion content and in nutrient material, i. e. phosphates, nitrates, and nitrites, necessary for the life of marine organisms. Therefore, any attached marine organisms living in the areas from which these salinity data have been obtained are constantly subjected to a changing ecological environment and must be making continual physiological adjustments to cope with these changes. It is hoped that additional information may be obtained in the future, possibly including some of the other physical characteristics of the water masses.

ACKNOWLEDGMENT

The writer wishes to express his appreciation to Humble Oil & Refining Company for permission to publish this report and to those members of the Petroleum Engineering Division who made the actual observations, to Miss Mary Jo Clark for helping in the analysis of the data, and to George Boer for his assistance in preparing the illustrations. In addition, the use of unpublished data on the mean monthly discharge for the Mississippi River, obtained from the personnel in the district office of the U. S. Geological Survey at Jackson, Mississippi, is gratefully acknowledged.

REFERENCES

Adams, K. T.
1942. Hydrographic Manual. Spec. Publ. U. S. Cst. geod. Surv., No. 143. 940 pp.

Parr, A. E.
1935. Report on hydrographic observations in the Gulf of Mexico and the adjacent Straits made during the Yale Oceanographic Expedition on the "Mabel Taylor" in 1932. Bull. Bingham oceanogr. Coll., *5* (1): 1–93.

Riley, G. A.
1937. The significance of the Mississippi River drainage for biological conditions in the northern Gulf of Mexico. J. Mar. Res., *1:* 60–74.

Sverdrup, H. U., M. W. Johnson and R. H. Fleming
1946. The Oceans. Prentice-Hall, Inc., New York. 1087 pp.

ON THE ORIGIN OF INTERNAL TIDE WAVES IN THE OPEN SEA[1,2]

By

ALBERT DEFANT

Institute of Meteorology and Geophysics, University of Innsbruck, Austria

ABSTRACT

Several mechanisms are examined which might explain the observed preponderance of internal waves of tidal period. It is concluded that the effect of the earth's rotation on the velocity of internal waves is an important factor in favoring the generation of such internal waves.

The phenomenon of internal waves with periods of the tide generating forces, designated briefly as internal tides, occurs not only in shallow seas and straits but in the open ocean as well. The amplitude of these internal tides and the water transport connected with them are much larger than those of the normal surface tides. These internal tides exert a much greater influence on the thermohaline structure of the oceans than do normal tides. Fr. Nansen and Bj. Helland-Hansen were the first to notice the existence of such internal waves, but Otto Pettersson was the first to associate these large periodic displacements of water masses with the tide generating forces. Such internal tides have been observed during all subsequent oceanographic expeditions where anchor stations were made in deep water. The anchor stations of the METEOR in the North and South Atlantic oceans have been discussed in the METEOR publications, and those of the SNELLIUS Expedition have been elaborated by Dr. Lek. The later cruises of the METEOR (1937, 1938) in the North Atlantic and in the area between the Cape Verde and Canary islands, the observations of the ALTAIR at anchor stations in the mean current of the Gulf Stream north of the Azores, the many cruises of the ATLANTIS in the western North Atlantic, the observations of the DANA Expedition, etc., *all* have shown that internal tides are as common as tides at the surface of the ocean.

Recent observations, taken on the Marine Life Research cruises of the Scripps Institution of Oceanography, have shown again very definitely that the influence of internal tides is great in this area also. This influence can be very disconcerting when attempting to obtain

[1] Contribution from the Scripps Institution of Oceanography, New Series, No. 471.

[2] I should like to draw attention to a paper by Haurwitz (1950) which appeared while this paper was in press. The conclusions reached in Haurwitz' paper are similar to the ones presented here.

the mean distribution of oceanographic elements, and therefore knowledge of the behavior of internal tides is required in order to eliminate their influence (Defant, 1950). However, aside from a practical application, the rising and sinking of immense water masses is in itself one of the interesting phenomena of dynamic oceanography; in fact, it is every bit as interesting as normal tides at the surface.

By theoretical and experimental research we are well informed concerning the physical nature of internal waves. Early theoretical models treated two-layered bodies of water with a physical discontinuity between them. Later the problem of internal waves of tidal periods in water masses of continuous density variations with depth were studied, especially by Fjeldstad (1933) and Groen (1948).

Although we know what internal waves with tidal periods are, there still are many difficulties on how such internal waves with large amplitudes develop and why they are so frequent, i. e., why they occur everywhere and at all times. Although observations at anchor stations, up to the present time, do not give accurate data about the velocity of internal tides in the open ocean, they do show clearly and distinctly that internal tides are related to tides at the surface. But the form of this coupling is not the same everywhere, though it seems to remain fixed with time at a fixed locality. This coupling leads to the assumption that internal tides are *forced* waves. If that is so, then they travel with a velocity about 100 times that of the theoretical velocity of *free* internal waves.

Free internal waves with tide periods, once they are generated, will soon lose every connection with the tide at the surface, and the coupling between the two wave systems would vary with time and distance. Since the generation of internal waves requires but little energy, the internal tides generated at different points would spread freely in all directions, the result being a chaos of internal tides in the ocean and the impossibility of finding a suitable method of eliminating their influence. But this is not the case, for internal tides are very regular and are strictly coupled to normal tides at the surface. With the latter they form a well determinated wave system. This has been shown clearly by the observations of the Marine Life Research program

In work with the Meteor data I have already dealt with the question of the generation of internal tides, but at that time it was not possible to give a satisfactory answer. Now, in connection with the Marine Life Research observations, I have been occupied again with this problem, and I would like to submit a few points of view which might make this question clearer. In the following discussion I will work mostly with a model of two superposed water bodies.

In the case of tidal waves in deep water, the entire water masses

will be moved with the same periodic tidal velocity; there will be no change of current with depth. If the lower water mass lies on a rough bottom, friction will decrease the intensity of tidal currents and will change the phase of these currents. This influence makes itself felt up to a certain height above the bottom, this height depending on the turbulence of the tidal current. If the lower water mass is not too deep, as on an ocean shelf, then the friction will influence the total underlayer to some extent. On the boundary, shearing stresses will occur which can force a dislocation of the boundary layer. These will produce internal waves or, if they are already present, they will affect amplitude.

The theoretical solution, given previously in the METEOR work (Defant, 1932), is

$$\frac{\zeta_2}{\zeta_1} = 1 - \frac{1}{(h_2/h_1)\, M + 1}, \tag{1}$$

where h_1 designates the height of the upper homogeneous water mass and ρ_1 its density; the corresponding values for the bottom layer are h_2 and ρ_2; $\Delta\rho$ is $(\rho_2 - \rho_1)/\rho$; ζ_1 and ζ_2 are the displacements of the surface and of the boundary; at most they are the amplitudes of the corresponding waves. The function M is given by

$$M = 1 - \frac{tgh(1+i)\beta_2 h_2}{(1+i)\beta_2 h_2},$$

where $\beta_2 = \sqrt{\sigma/2\nu_2}$, and ν_2 is the eddy viscosity of the lower layer. Since M is always slightly less than 1, ζ_1 is larger than ζ_2. Therefore this process is incapable of increasing the amplitude of internal waves of tidal character.

A second point of view may be illustrated by the following problem. Let the upper water mass move with constant velocity U_1, the lower with the constant velocity U_2, both parallel to the undisturbed discontinuity layer. A tide generating force,

$$X = f\, e^{i(\sigma t - \kappa x)}, \tag{2}$$

acting in a horizontal direction on the whole system, will produce tide waves at the surface and on the discontinuity layer. The frequency is denoted by σ, the wave number by κ; the velocity of propagation $c = \sigma/\kappa$ is determined by the force. Under which conditions then will real internal waves, whose amplitudes are much larger than the amplitudes at the surface, be generated?

The solution is not difficult to find, since the vertical motion in both layers can be neglected, according to the first approximation in tide

theory. In the equations for the amplitudes of the surface and of the boundary layer, the expression

$$c(c-U_1)[(c-U_2)^2\omega_1\omega_2+(c-U_1)^2\rho_1/\rho_2]-[(c-U_2)^2\omega_1+(c-U_1)^2\omega_2\rho_1/\rho_2 + c(c-U_1)\omega_1\Delta\rho].g/k+\Delta\rho g^2/k^2 = D_1 \quad (3)$$

always appears as denominator, wherein $\omega_1 = ctgh\ \kappa h_1$ and $\omega_2 = ctgh\ \kappa h_2$. But this expression, when set equal to zero, is the equation which determines the velocity of the *free* waves of the system. For $U_1 = U_2 = 0$ this equation becomes the well known equation of the velocity of free waves with the wave number κ:

$$c^4(\omega_1\omega_2+\varphi_1/\rho_2)-c^2(\omega_1+\omega_2)g/\kappa+\Delta\rho g^2/\kappa^2 = D_2 = 0\,. \quad (4)$$

The two solutions of this equation for long waves are

$$c_1 = \sqrt{g(h_1+h_2)} \quad \text{and} \quad c_2 = \sqrt{\Delta\rho g\, h_1h_2/(h_1+h_2)}\,. \quad (5)$$

The velocity c_1 is valid for waves at the surface, which are associated with displacements of the boundary layer of smaller amplitudes than those at the surface. c_2 is the velocity of free internal waves.

In the case of *forced* waves the case of *resonance* corresponds to $D_2 = 0$. Theoretically the amplitude of forced waves will be infinitely large. Note that the internal waves will be infinitely large if the condition $c = c_2$ is exactly fulfilled. But this never occurs, since the magnitude of c for tidal waves in the oceans is about 200 m/sec and that of c_2 only 2 m/sec. The same is true for the more general equation (3) which also contains the influence of steady currents. For values of c, U_1 and U_2 that occur in nature, D_1 is a very large number, so that the generated internal waves will remain small—much smaller than those at the surface. Consequently they are not internal waves in a strict sense.

The same conclusions follow from the computation of the ratio of the amplitudes of the two generated tide waves. One finds with good approximation:

$$\frac{\zeta_1}{\zeta_2} = 1 - \frac{(c-U_2)^2\, h_1/h_2}{gh_1\Delta\rho - c(c-U_1)\,\rho_1/\rho_2}\,. \quad (6)$$

Since internal waves have larger amplitudes on the boundary layer:

$$\Delta\rho g h_1 - c(c-U_1)\rho_1/\rho_2 \geqq (c-U_2)^2 h_1/h_2\,.$$

Since $c >> U_1$ and U_2,

$$c^2 \leqq \Delta\rho g\, h_1h_2/(h_1+h_2)\ ;$$

in other words, c must be smaller than the velocity of *free* internal

waves. However, this is never the case. We see that this factor does not contribute to the generation of large internal waves. This factor has been considered in greater detail by Haurwitz (1948), who arrives at essentially the same conclusion.

The condition $D_1 = 0$ has another significance which needs a few words of explanation. The solution (3) for c leads to a few difficulties. Since we want internal waves for which amplitudes of contemporary waves at the surface are extremely small, we may take, with good approximation, this amplitude equal to zero. Then we replace the surface by a rigid horizontal plane, in which the vertical motions are zero. The solution for c is then:

$$c = \frac{\rho_1 U_1 \omega_1 + \rho_{22} U \omega_2}{\rho_1 \omega_1 + \rho_2 \omega_2} \pm \sqrt{\frac{g}{\kappa} \frac{\rho_2 - \rho_1}{\rho_2 \omega_2 + \rho_1 \omega_1} - \rho_1 \rho_2 \omega_1 \omega_2 \left(\frac{\rho_2 - \rho_1}{\omega_2 \rho_2 + \omega_1 \rho_1} \right)^2} . \quad (7)$$

The first term on the right side is the convection velocity which corresponds approximately to a mean velocity of two currents. The first term below the root is the velocity of free internal waves; the second term with the negative sign, which always decreases the stability of the internal waves, gives the velocity of inertial waves. Dynamic instability will occur if this term is larger than the first, and therefore the condition for dynamically unstable internal waves will be:

$$(U_2 - U_1)^2 > \frac{g}{\kappa} (\rho_2 - \rho_1)[1/\rho_1 \omega_1 + 1/\rho_2 \omega_2] . \quad (8)$$

This criterion of stability is discussed in all its details by Bjerknes, et al. (1933) from the point of view of the generation of cyclones in the atmosphere. Here we are interested with the question as to when dynamic instability occurs in the ocean. The condition for this is:

$$(U_2 - U_1) > \sqrt{\frac{\rho_2 - \rho_1}{\rho_1 \rho_2} (\rho_2 h_1 + \rho_1 h_2) g} . \quad (9)$$

If h_2 is large, which is the case in the open sea, the inequality is reduced to $(U_2 - U_1) > \sqrt{\Delta\rho \, g h_2}$. The quantity on the right-hand side is always large, since h_2 is large, even with small $\Delta\rho$. Such steady currents will not occur in nature, and the inequality (9) is never fulfilled. Hence internal tide waves are always stable in the open ocean. But on shelf water or in shallow straits internal waves may easily become unstable. If $h_1 = h_2$, we have

$$U_2 - U_1 > \sqrt{g h_1 \frac{\rho_2^2 - \rho_1^2}{\rho_1 \rho_2}} , \quad (10)$$

with $h_1 = 100 - 150$ m, $U_2 - U_1 > \frac{1}{2}$ to 1 m/sec. This velocity difference is easily reached by steady currents. In fact, observations at anchor stations in straits have shown that normal stable internal waves can become unstable (Defant, 1948). The observations at anchor stations by the DANA Expedition in the Strait of Gibraltar during the spring of the year show distinctly that large internal waves will be unstable, thus leading to internal surf. Also, internal waves on the shelf off the West African Coast tend towards instability and formation of internal surf. This surf may destroy the thermocline, and only in this case will the phenomenon of upwelling of cold water develop off the coast. The instability of internal waves is still more pronounced in the Strait of Messina, where it produces the famous eddies of Scylla and Charybdis (Mazarelli, 1938; Defant, 1940). When the boundary layer between the converging tidal currents in the two water masses is brought to the surface on one side of the Strait by Coriolis' force, the instability of the internal waves will generate a large eddy. Undoubtedly these eddies are nothing but the effect of dynamic instability of internal waves in this shallow Strait.

The two points of view just discussed lead to negative results. I will now discuss a third point of view, which may account in part at least for the generation of internal tide waves. Until now we have neglected the Coriolis' force. Perhaps this force can be neglected in the first approximation in small regions or in narrow straits, but in the open ocean this is surely not permissible. Since we have already shown that the steady current in the two superposed water masses does not lead to large internal waves, we can disregard those currents. By working with long waves we can neglect the vertical accelerations; the equations of motion of the system are:

$$\frac{\partial u_1}{\partial t} = \lambda v_1 - g\frac{\partial \zeta_1}{\partial x} + X\,, \qquad \frac{\partial u_2}{\partial t} = \lambda v_2 - g\frac{\rho_1}{\rho_2}\frac{\partial \zeta_1}{\partial x} - g\Delta\rho\frac{\partial \zeta_2}{\partial x} + X\,,$$
$$\frac{\partial v_1}{\partial t} = -\lambda u_1 - g\frac{\partial \zeta_1}{\partial y}\,, \qquad \frac{\partial v_2}{\partial t} = -\lambda u_2 - g\frac{\rho_1}{\rho_2}\frac{\partial \zeta_1}{\partial y} - g\Delta\rho\frac{\partial \zeta_2}{\partial y}\,, \tag{11}$$

where X is given by (2) and $\lambda = 2\Omega \sin\varphi$ is the Coriolis' parameter; the influence of friction is neglected. To these dynamic equations must be added the equation of continuity for both layers:

$$\frac{\partial \zeta_1}{\partial t} + h_2\left[\frac{\partial u_2}{\partial x} + \frac{\partial v_2}{\partial y}\right] + h_1\left[\frac{\partial u_1}{\partial x} + \frac{\partial v_1}{\partial y}\right] = 0$$
$$\frac{\partial \zeta_2}{\partial t} + h_2\left[\frac{\partial u_2}{\partial x} + \frac{\partial v_2}{\partial y}\right] = 0\,. \tag{12}$$

If we take

$$\frac{u_1}{v_1} = \frac{U_1}{V_1} e^{i(\sigma t - \kappa x)}, \quad \frac{u_2}{v_2} = \frac{U_2}{V_2} e^{i(\sigma t - \kappa x)} \quad \text{and} \quad \frac{\zeta_1}{\zeta_2} = \frac{Z_1}{Z_2} e^{i(\sigma t - \kappa x)},$$

then the previous system of equations gives six equations for computing the six unknowns U, V, Z. With

$$\frac{\sigma^2 - \lambda^2}{\kappa^2} = \varepsilon^2, \tag{13}$$

we have as denominator of all these quantities the expression:

$$\varepsilon^4 - (h_1 + h_2)g\varepsilon^2 + \Delta\rho g^2 h_1 h_2 = D_3. \tag{14}$$

It has the same form as the relation (4), transformed for tidal waves. But instead of being the velocity of forced waves, c enters the influence of the earth's rotation through the quantity ε. Whereas c has the magnitude of 200 m/sec and the quantity D_2 is a large number, as shown before, under certain conditions ε can be small or nearly equal to the velocity of free internal waves. With these values, however, D_3 will be zero. If T_i is the period of inertial waves (equal to 12 pendulum hours), then

$$\varepsilon^2 = c^2[1 - (T/T_i)^2]. \tag{15}$$

For the diurnal tide wave, $T = 24$ hours and ε will be zero at 30° latitude, but for the semidiurnal lunar wave, $T = 12.43$ hours and ε will be zero at 74° latitude.

For small ε equation (14) has, in the first approximation, the form:

$$D_4 = \Delta\rho g^2 h_1 h_2 - g(h_1 + h_2)\varepsilon^2.$$

D_4 will be zero for

$$\varepsilon^2 = \Delta\rho g\, h_1 h_2/(h_1 + h_2). \tag{16}$$

When $\varepsilon = c_2$ = the velocity of free internal waves, then *resonance* exists for forced internal waves. In other words, the amplitudes of internal tide waves will be very large at these latitudes. This is not the case for the normal tides at the surface, for which

$$D_5 = \varepsilon^2[\varepsilon^2 - g(h_1 + h_2)]. \tag{17}$$

D_5 remains a large number when $\varepsilon = c_2$.

Therefore, the rotation of the earth provides a factor which is able to increase the amplitudes of internal waves, and internal waves will thus be a larger wave motion than the tide at the surface.

If we add steady currents to the two superposed layers, the denominator assumes, for forced internal waves, the form

$$(c - U_2)^2\left[1 - \frac{\lambda^2}{(\sigma - \kappa U_2)^2}\right]h_1 + \frac{\rho_1}{\rho_2}(c - U_1)^2\left[1 - \frac{\lambda^2}{(\sigma - \kappa U_1)^2}\right]h_2 - \Delta\rho g h_1 h_2 = D_6 . \quad (18)$$

The term with Coriolis' parameter will be changed only insofar as we have $(\sigma - \kappa U)^2$ instead of σ^2. The influence of this change goes in the desired direction of increasing the resonance, but the effect is very small.

In the foregoing results there is one difficulty, which I wish to discuss. The width of the resonance area is very small, at most 2 to 3 degrees of latitude. Outside this small strip, D_3 is always large and the amplitudes of internal waves will not be influenced greatly by the rotation of the earth. This surprising result, however, is the consequence of the way the problem has been formulated. The difficulties are the same as those in the theory of surface tides, and they can be removed if the boundary conditions are taken into account.

Finally, the equations of the problem show directly that the rotation of the earth must have a great influence upon internal wave motion. We will suppose in this case that the density increases in an arbitrary manner with depth. Eliminating pressure from the equation of motion,

$$\begin{aligned} \frac{\partial \rho}{\partial x} &= \frac{\lambda}{g}\frac{\partial \rho v}{\partial z} - \frac{1}{g}\frac{\partial \rho \dot{u}}{\partial z} \\ \frac{\partial \rho}{\partial y} &= -\frac{\lambda}{g}\frac{\partial \rho u}{\partial z} - \frac{g}{g}\frac{\partial \rho \dot{v}}{\partial z} , \end{aligned} \quad (19)$$

where the z-axis is positive downwards. If $u = u_0 \sin \sigma t$ and $v = v_0 \cos \sigma t$ designate tidal currents, then (19) gives

$$\begin{aligned} \frac{\partial \rho}{\partial x} &= \frac{\sigma}{g}\left[s\frac{\partial \rho v_0}{\partial z} - \frac{\partial \varphi u_0}{\partial z}\right]\cos \sigma t , \\ \frac{\partial \rho}{\partial y} &= \frac{\sigma}{g}\left[\frac{\partial \rho v_0}{\partial z} - s\frac{\partial \rho u_0}{\partial z}\right]\sin \sigma t , \end{aligned} \quad (20)$$

where $s = \lambda/\sigma$. To these equations we must add the equation of continuity, and, as shown by Fjeldstad in his theory of internal waves, we obtain equations for u and v in which the denominator is again the quantity ε. With the same values of T, resonance will occur in the same latitudes. But the equations (20) already show clearly that internal waves are also associated with a variation of the density gradient with depth. If internal waves exist only in the y-direction, then $\partial\rho/\partial x = 0$, and we have $u_0 = s\, v_0$; in other words, the tidal current u in the x-direction will then be

$$\frac{\partial \rho}{\partial y} = \frac{\sigma}{g} \epsilon^2 v_0 \frac{\partial \rho}{\partial z} \sin \sigma t \,, \tag{21}$$

provided the tidal current v is independent of z, as in the case of simple tidal waves. This means that every change in density with depth is followed by a periodical sinking and rising of isopycnals across the tidal current. As a numerical example, take $v_0 = 1$ m/sec, $\sigma_s = 1.45 \times 10^{-4}\,\mathrm{sec}^{-1}$, and $\lambda = 0.7 \times 10^{-4}\,\mathrm{sec}^{-1}$ and $\Delta\rho/\Delta z = 4 \times 10^{-3}$ g cm^{-3} per 30 m $= 1.33 \times 10^{-6}$ g cm^{-4}. This gives $\Delta\rho/\Delta y = 1.52 \times 10^{-11}$ g cm^{-4}; that is, the isopycnals show an elevation of 5.7 m over a distance of 500 km. The range of internal waves is 11.4 m. Therefore, strong tidal current must always be connected with large internal waves, and it is not surprising that the oceanographic observations at anchor stations in the open ocean always show large internal waves. If we wish to eliminate these waves from the observations of oceanographic surveys, we must know the law to which they are subjected. But we are still far from this aim.

REFERENCES

Bjerknes, V., B. Bjerknes, H. Solberg and T. Bergeron
1933. Physikalische Hydrodynamik. Julius Springer, Berlin. 797 pp.

Defant, Albert
1932. Die Gezeiten und innere Gezeitenwellen des Atlantischen Ozeans. Wiss. Ergebn. dtsch. Atlant. Exped. Meteor, *7* (1): 1–318.
1940. Scylla und Charibdis und die Gezeitenströmungen in der Strasse von Messina. Ann. Hydrog., *68:* 145–157.
1948. Über interne Gezeitenwellen und ihre Stabilitatsbedingungen. Arch. Met. Geophys. Bioklim., (A) *1* (1): 39–61.
1950. Reality and illusion in oceanographic surveys. J. Mar. Res., *9* (2): 120–138.

Fjeldstad, J. E.
1933. Interne Wellen. Geofys. Publ., *10* (6): 1–35.

Groen, Pier
1948. Contribution to the theory of internal waves. Meded. ned. met. Inst., (B) 2, no. 11.

Haurwitz, Bernhard
1948. The effect of ocean currents on internal waves. J. Mar. Res., *7* (3): 217–228.
1950. Internal waves of tidal character. Trans. Amer. geophys. Un., *31* (1): 47–52.

Mazzarelli, G.
1938. I vortici, i tagli e altri fenomeni delle correnti dello Stretto di Messina. Atti Accad. peloritana, *40.*

REALITY AND ILLUSION IN OCEANOGRAPHIC SURVEYS[1]

By

ALBERT DEFANT[2]

ABSTRACT

Care must be exercised in selecting time intervals and spacings between stations along oceanographic profiles in order to avoid erroneous conclusions regarding the mean circulation. By proper combinations of time intervals and spacings, the effect of internal waves of tidal periods, which are the source of these errors, can be suppressed. The application of these principles to the Marine Life Research cruises of the Scripps Institution is discussed.

INTRODUCTION

Generally oceanographic surveys are made by one or several ships occupying a series of oceanographic stations along specific profiles according to a predetermined plan. To obtain the best possible synoptic picture of the various oceanographic factors, the profiles and the stations along them should be spaced as closely as possible, and in order to obtain data that is as homogeneous as possible, the distances and the time intervals should be kept constant. Bjørn Helland-Hansen (1939) has indicated in his work with the Armauer Hansen in the Norwegian Sea how difficult it is to fulfill these conditions of a quasisynoptic survey and how careful one must be in interpreting such observations.

With a single ship at disposal, it is difficult to reach a satisfactory compromise between two confiicting requirements. To fulfill the requirement of a *synoptic* survey the area under investigation should be covered in the least possible time. To obtain great *accuracy*, the number of stations in the area should be as numerous as possible. It is only by working a great number of ships simultaneously that the conflicting requirements can be met to a certain extent.

There is still another difficulty which is of no less importance but which has been neglected hitherto; in fact, it can even make the observations of an oceanographic survey completely worthless and meaningless. Here we refer to the difficulties associated with periodic variations of temperature and salinity (as well as other oceanographic factors). Although these variations occur in a more or less regular

[1] Contribution from Scripps Institution of Oceanography, New Series, No. 478.

[2] Professor at the University and Director of the Institute for Meteorology and Geophysics of Innsbruck, Austria.

form, nevertheless they are capable of completely confusing the picture. In the following simple case I will discuss this problem more thoroughly.

THEORETICAL COMPUTATIONS

Let temperature (respectively salinity) at any point in an ocean vary periodically with time in such a manner that

$$T = T_o + a_1 \cos \frac{2\pi}{24} (t - \varepsilon_1) + a_2 \cos \frac{2\pi}{12} (t - \varepsilon_2) , \qquad (1)$$

where t is time in hours. The time variations of T result from a superposition of two waves, one of which is diurnal (period = 24 hours), the other semidiurnal (period = 12 lunar hours). The temperature T_o, the amplitudes a_1 and a_2, and the phases ε_1 and ε_2 (expressed in hours) depend upon the position x, y and the depth z. We do not have to specify the origin of these variations; for instance, they may be internal waves with a tidal period, or in the case of large horizontal temperature and salinity gradients they may be caused by the advection of different water bodies by the periodic tidal currents.

Let a ship occupy a profile along the x-axis starting at time $t = 0$ from a point x_o; at specific intervals there will be oceanographic stations (serial observations). If c denotes the average speed of the ship in knots, taking into account the duration of the stations, the position at time t is given by

$$x = x_o + c\,t . \qquad (2)$$

Should the ship register the temperature continuously, the observed variations would be given by

$$T = T_o + a_1 \cos \frac{2\pi}{24c} (x - x_o - \varepsilon_1 c) + a_2 \cos \frac{2\pi}{12c} (x - x_o - \varepsilon_2 c) . \qquad (3)$$

Therefore the observed temperature distribution of the profile would be periodic, although the mean temperature distribution does not show periodicities. The lengths of these simulated temperature waves would be 24 c n.m. and 12 c n.m. respectively. Should the ship occupy intermittent oceanographic stations (serial observations) at the points x_n, which are at constant distances from each other, the temperature T_n observed there will be given by

$$T_n = T_o + a_1 \cos \frac{2\pi}{24c} (x_n - x_o - \varepsilon_1 c) + a_2 \cos \frac{2\pi}{12c} (x_n - x_o - \varepsilon_2 c) . \qquad (4)$$

The observed temperatures are critically dependent on the selection of x_n, and it might prove difficult to disentangle the temperature distribution thus obtained.

One might then raise the question: Is it possible to select x_n in such a manner that the effect of the semidiurnal tide vanishes or is at least greatly reduced? One would expect the former to be the case if the condition

$$\frac{2\pi}{12c}(x_n - x_o - \varepsilon_2 c) = (2n-1)\frac{\pi}{2} \tag{5}$$

be fulfilled. In this case the position of the stations would be given by

$$x_n = 3c\,(2n-1) + (x_o + \varepsilon_2 c)\,, \tag{6}$$

or the distance between two successive stations by

$$x_{n+1} - x_n = 6c\,, \tag{7}$$

provided ε_2 remains constant along the profile. Therefore, the spacing of the stations depends *only* upon the speed of the ship c. For instance, with a ship speed of 8 knots the required distance of the stations is 48 n.m., a typical distance for oceanographic surveys.

From (1) and (2) it follows that stations will be occupied at times

$$t_n = \varepsilon_2 + 3\,(2n-1)\,, \tag{8}$$

so that the time interval between two stations equals

$$t_{n+1} - t_n = 6^h\,. \tag{9}$$

At the start of the profile, the phase ε_2 is not generally given, and it is not possible to indicate beforehand the station times required for the complete elimination of the semidiurnal wave. If $t_n - \varepsilon_2 = 3^h, 9^h, 15^h$, etc., the semidiurnal wave will vanish; if $t_n - \varepsilon_2 = 0^h, 6^h$, etc., the semidiurnal wave will remain unchanged. If the time of the stations is selected freely, the probability that the effect of the semidiurnal wave in the values will be reduced to ¼, to ½ and to ⅔ is 17, 33 and 67 per cent. Therefore, in the case of a succession of stations with intervals of 6 hours, a more or less large portion of the semidiurnal wave will remain in the station values.

If one wishes to eliminate the semidiurnal wave *completely*, this can be done only if all stations are occupied at the same phase-time of this wave; i. e., the difference in time must be independent of the speed of the ship c, and must always be 12 hours. In this case the values at *all* stations differ from the mean value by the same constant amount; there will be no oscillating disturbance.

If one takes the stations at intervals of more than 6 hours (about 7 or 8), the effect of the semidiurnal wave increases gradually from small amounts to larger according to the value of ε_2, and after having reached a maximum it decreases again. In this case, for instance, it would be

possible that the effect of the semidiurnal wave is small in the first part of the profile but large in the second, or vice-versa.

In assuming that there are stations at a time interval of 6 hours, it follows from (4) that there will be at stations x_n, besides the reduced semidiurnal wave, a diurnal effect in the form:

$$T_n = T_o + a_1 \cos \frac{\pi}{4} (2n - 1) - \frac{\varepsilon_1 - \varepsilon_2}{3}. \tag{10}$$

It is remarkable that these values are independent of the speed of the ship. Every *fourth* station will show a maximum of temperature so that local variations of temperature are simulated. However, they have nothing to do with the actual temperature distribution in the ocean. Such errors are present in all oceanographic observations, and they can become extremely important if the tidal influence on the oceanographic factors is large. In such cases phenomena are simulated which depend exclusively upon the speed of the ship and the distance between stations.

Until now we have supposed, in a special case, that ε_1 and ε_2 are constant; i. e., that the tide waves have a direction of propagation perpendicular to the profile. But for the general case, the cotidal lines of the semidiurnal wave cut the direction of the profile by an angle α, and ε_2 is dependent upon x. To determine ε_2 we have to consider only the component $c'/\sin \alpha$ of the velocity of the tidal wave in the direction of the ship movement. Analagous with the Doppler effect, it is easy to show that the time interval between stations required for the complete elimination of the semidiurnal wave is

$$t_{n+1} - t_n = 12 / \left(1 - \frac{c}{c'} \sin \alpha\right). \tag{11}$$

The value of c' is approximately 150 knots and the ratio c/c' a small number. The effect in all cases is small, especially since profiles are mostly perpendicular to coast lines, α thus being a small angle.

In the following example let ε_2 have a constant value of 3 hours. A ship takes oceanographic stations every 6 hours at a distance of 40 n.m. The average speed of the ship is 40/6 knots. According to equation (8) the effect of the semidiurnal tide wave will be completely eliminated if the times at the stations are 0^h, 6^h, 12^h, 18^h; it is reduced by 50 per cent if the station times are 5^h, 11^h, 17^h, 23^h. In addition there will be a considerable influence of the diurnal wave, especially if the diurnal wave is large compared to the semidiurnal wave. In the observations, highest and lowest temperatures occur at an interval of 4 stations. These influences thus simulate local disturbances in the

temperature (and salinity) field. Dynamic computation based on such temperature and salinity values are subject to similar errors.

THE CRUISES OF THE MARINE LIFE RESEARCH PROGRAM

The Marine Life Research Program[3] of the Scripps Institution of Oceanography, University of California, includes an oceanographic survey of the west coast of America between 25° and 43° N. Cruises involving three ships have been made at regular intervals of about a month since February 1949. Each cruise lasts about 15 days and is composed of 12 profiles perpendicular to the coast about 140 n.m. apart. At each station the normal serial observations extend to a depth of 1,200 m. For each survey, charts of the horizontal distribution of all oceanographic factors are given, among them a chart of the dynamic height of the sea surface relative to the 1,000 decibar surface, with an interval of 5 dyn cm (S.I.O., 1949).

The main purpose of this extensive oceanographic survey is to obtain an insight into the circulation variations in this area, which is characterized by the California Current. During my visit at the Scripps Institution of Oceanography the various quasisynoptic charts of the oceanographic elements of the first profiles were submitted to me for discussion. In general they showed the California Current running southward. Moreover, on the maps surprising disturbances in the form of cyclonic and anticyclonic eddies seemed to be superimposed upon the California Current.

A close inspection of the dynamic topographies of the surface showed that these eddies succeed each other along the profiles at approximately equal intervals. Similar intervals exist in the corresponding disturbances in the temperature and salinity distribution. This made me suspect that these eddies are simulated disturbances rather than real. This idea was supported by the fact that the average time interval from one station to another is about 6 hours, whereas the distances between the stations was 40 n.m. Consequently the average speed of the ship is 40/6 knots, and this value fulfills in a remarkable way equation (7). This corresponds to the case discussed previously, and the occurring eddies at an interval of about 4 stations (160 n.m.) would be due to the influence of a diurnal wave. Any possible influence of a semidiurnal wave would be weakened by the selected spacing of stations and the speed of the ship. In fact, most of the profiles scarcely showed the influence of the semidiurnal wave. Aside

[3] This program represents part of the Cooperative Sardine Investigation of the west coast, the latter including two other state agencies of California and a division of the U. S. Fish and Wildlife Service.

from the fact that the station spacing and ship speed would naturally favor the diurnal over the semidiurnal wave, as they appear in the observations, there are reasons why the diurnal wave should be of larger amplitude in the ocean off the California Coast. One reason is that the tide observations along this coast show a pronounced diurnal character. Another reason follows from the theory of internal waves (Defant, 1940; Sverdrup, et al., 1942), according to which the period T of free internal oscillations is given by relation

$$T = \frac{T_e}{\sqrt{1 + T_e^2/T_o^2}}. \tag{12}$$

Here T_o is the period of free oscillations on a nonrotating earth, and $T_e = 12/\sin\zeta = \frac{1}{2}$ pendulum day is the period of the inertia oscillations. For the ocean region under consideration, the magnitude of T_o is 150–200 hours, so that $T_e/T_o = 0.1$ and $T \approx T_e$. Since the area under investigation extends from 40° to 25° N, the period of inertia oscillations varies between about 20 and 25 hours. For Lat. 30° N it is exactly 24 hours. Since the diurnal and semidiurnal tide waves, which are forced waves, have periods of 24 and 12.43 hours respectively, the diurnal waves will be increased by *resonance.*

THE TIDAL EFFECT IN OBSERVATIONS AT THE SCRIPPS PIER

It would be desirable to check these conclusions by means of anchor stations, for according to the results of those taken on the METEOR Expeditions over the West African shelf, 1937 and 1938, such tidal influence is probable (Defant 1937, 1948). But unfortunately no such anchor stations are available. However, for numerous years temperature recordings have been taken at the end of Scripps Pier at depths of 2 and 16 feet above bottom (water depth 18 feet). Leipper (1949), in discussing these observations, has pointed out the existence of large quasiperiodic variations in which the tidal periods seemed to be especially prevalent. In examining the tidal influence numerically, I have subjected the observations for August 28 through 31, 1927 (represented in fig. 2 of Leipper's paper) to harmonic analysis and have compiled the results in Table I (see also Fig. 1).

The tidal influence is very pronounced. The tide and temperature curves are almost completely reversed, and the phase differs by half a period. The variation in temperature with semidiurnal tide in the surface and bottom layers attains an amplitude of more than 3° C; with the diurnal wave in the surface layer it attains a magnitude of only 1° C. The half-hourly bathythermograms made at the end of

TABLE I. Harmonic Analysis of Observations Taken at Scripps Pier from August 18 through 31, 1927 (See Also Fig. 1)

	Mean value	*Diurnal wave (period = 24 h.)*	*Semidiurnal wave (period = 12 lunar hours)*
Tidal variation in ft.	6.5	$+ 1.32 \cos \frac{2\pi}{24} (t - 16.4^h)$	$+ 2.05 \cos \frac{2\pi}{12} (t - 6.7^h)$
Temp. °C 16′ above bottom:	17.80	$+ 0.31 \cos \frac{2\pi}{24} (t - 2.9^h)$	$+ 1.69 \cos \frac{2\pi}{12} (t - 0.6^h)$
at the bottom:	17.76	$+ 0.18 \cos \frac{2\pi}{24} (t - 12.8^h)$	$+ 1.74 \cos \frac{2\pi}{12} (t - 11.6^h)$

the pier during two days (fig. 20 of Leipper's paper) prove that the entire water mass in the vicinity of the coast is subjected to this tidal influence, the boundary layer rising and falling with an amplitude of over 7 feet. According to all these observations, periodic variations exist in both temperature and salinity in the entire water column and they follow the tides.

ELIMINATION OF TIDAL EFFECT FROM OBSERVATIONS OF THE MLR CRUISES

According to the foregoing considerations, it is most probable that the observations made off the California Coast include tidal influence, this influence being primarily responsible for the complicated structure of the dynamic topographies. The semidiurnal influences are weaker than the diurnal ones, and they are further suppressed by the selected distances between stations and the average ship speed. To obtain an undistorted dynamic topography of this surface, an effort should be made to eliminate the diurnal component also. A method for this is now given.

The method is much more complicated if some residues of the semidiurnal disturbance are left. The difficulty of completely eliminating the disturbances is dependent on three considerations. In the first place, the extent of these tidal influences varies according to localities, and consequently one must take into consideration many irregularities. Secondly, the distance between stations as well as their duration are subject to irregular variations which, although not great, change the *average* speed of the ship somewhat. The indicated anomaly of dynamic height at a station refers to a time interval of about 1 to 1½ hours, and this uncertainty as to time and locality enters fully into the observational values. In this one recognizes that the time values can

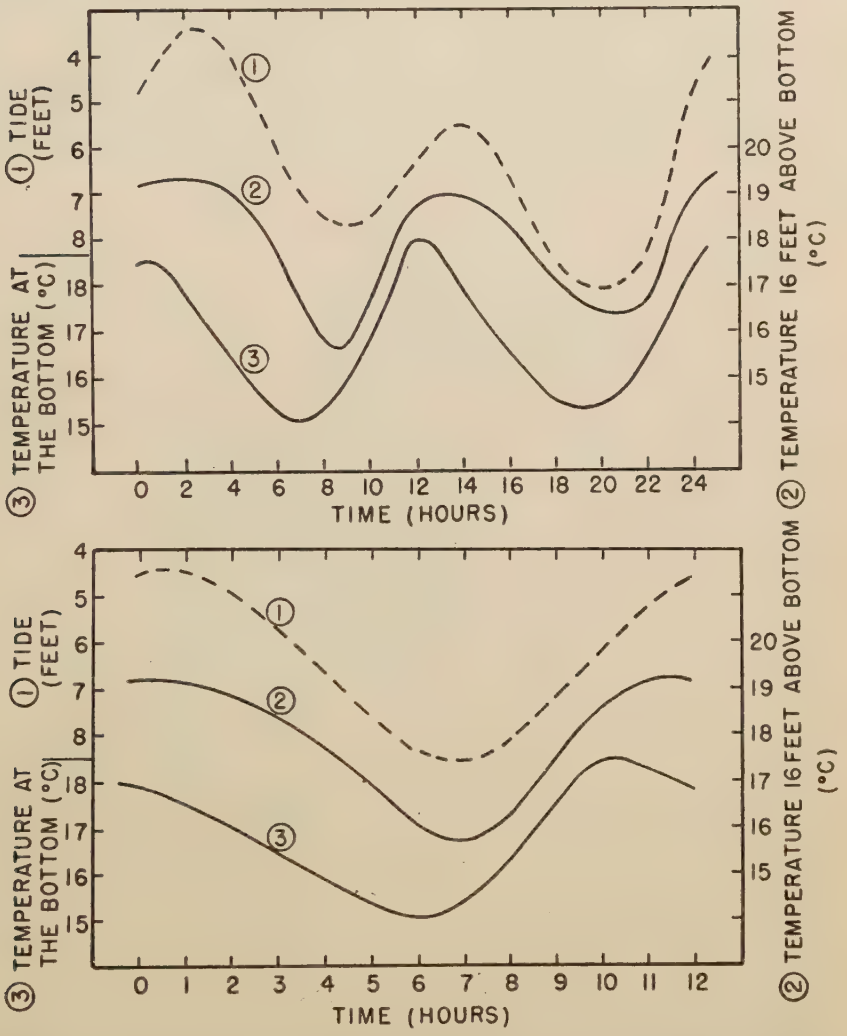
① TIDE (FEET)
③ TEMPERATURE AT THE BOTTOM (°C)
② TEMPERATURE 16 FEET ABOVE BOTTOM (°C)
TIME (HOURS)
① TIDE (FEET)
③ TEMPERATURE AT THE BOTTOM (°C)
② TEMPERATURE 16 FEET ABOVE BOTTOM (°C)
TIME (HOURS)

Figure 1. Above: Mean tidal curve for the period from August 28 through 31, 1927, and simultaneous temperature variations at the bottom and 16 ft. above the bottom at the end of the Scripps Pier at La Jolla, California. Below: Mean semidiurnal tide (period 12 lunar hours) and corresponding temperature variations for the same time at the end of the Scripps Pier at La Jolla, California, 16 ft. above the bottom.

have a margin of error of $\pm$ 1 hour. Thirdly, the tidal disturbances are superimposed on an average dynamic topography of the sea surface

which is unknown at first. These circumstances make it necessary to proceed by trial and error, but the following method has proved to be workable.

Fig. 2 shows the dynamic topography of the sea surface during the first cruise, including large eddies associated with the diurnal tide. The steps taken in separating the fundamental part from the tidal

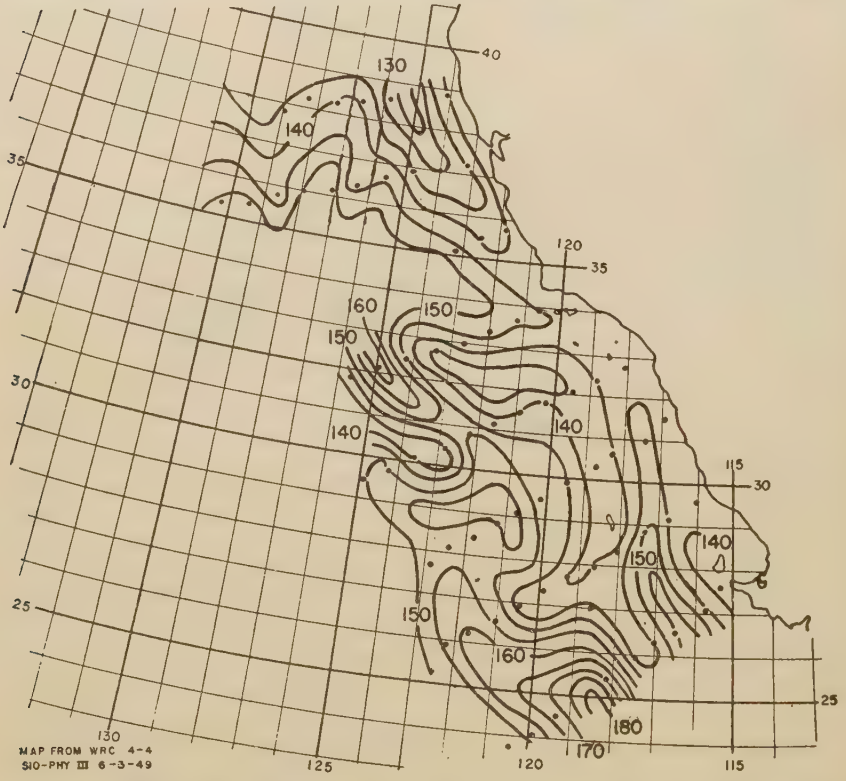

Figure 2. Marine Life Research Cruise 1 (Feb. 28 to Mar. 15, 1949): Dynamic height anomalies (0 over 1000 Decibars). Contour interval 5 dyn cm. The nearly normal lines to the coast are numbered consecutively from north to south, the southernmost line shown being the 1200 series.

influence will be shown by means of profiles 500, 800 and 1200. Tables II and III give all of the data of profiles 500 to 800 as well as the average difference in time ($\sim$ 6 hours) and the distance between stations ($\sim$ 40 n.m.) Figs 3 and 4, in their upper part, show the observed values of dynamic height along the profiles at various sta-

TABLE II. CRUISE 1. (FEBRUARY 28–MARCH 16, 1949): PROFILE 500

Station	*Date*	*Mean time GCT*	*Time-difference*	*Distance between stations in n.m.*	*Dyn. height Dyn. m.*	*Dyn. height from smooth curve*	*Difference Dyn. m.*	*Effective Time*
501	1. III	9.5^h			1.401	1.303	+ 0.098	+ 1.5^h
			5.8^h	46				
502		15.3			[1.280]	1.320	− .040	− 3.2
			5.8	45				
503	1. III	21.1			1.262	1.336	− .074	− 2.9
			6.8	40				
504	2. III	03.9			1.393	1.352	+ .041	+ 3.9
			6.8	45				
505	2. III	10.7			1.366	1.370	− .004	+ 1.3
			6.5	42				
506	2. III	17.2			[1.340]	1.387	− .047	− 5.2
			7.6	40				
507	3. III	00.8			1.379	1.396	− .017	+ 0.8

TABLE III. Cruise 1. (February–March 16, 1949): Profile 800

Station	*Date*	*Mean time GCT*	*Time-difference*	*Distance between stations in n.m.*	*Dyn. height Dyn. m.*	*Dyn. height from smooth curve*	*Difference Dyn. m.*	*Effective Time*
808	14. III	06.6^h			1.534	1.558	− 0.024	− 2.4^h
			7.9^h	38				
807		14.5			1.638	1.512	+ .126	+ 5.5
			6.2	39				
806		20.7			1.480	1.468	+ .020	+ 0.3
			5.5	34				
805	15. III	02.2			[1.370]	1.420	− .050	− 5.3
			7.4	40				
804		09.6			1.400	1.390	+ .010	+ 0.6
			6.6	40				
803		16.2			1.415	1.366	+ .049	+ 4.8
			5.6	46				
802		21.8			1.412	1.424	− .012	− 1.8
			5.4	39				
801	16. III	03.2			1.468	1.486	− .018	− 6.0

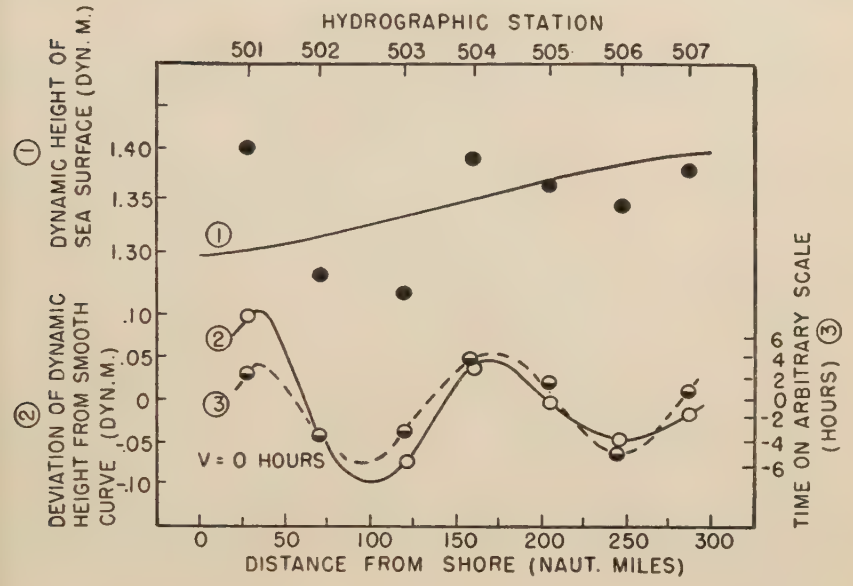

Figure 3. Cruise 1, Stations 501–507: Above: Dynamic heights at stations and smooth curve along the line. Below: Deviations of dynamic heights from the smooth curve (solid line) and effective times (dotted line) along the entire profile.

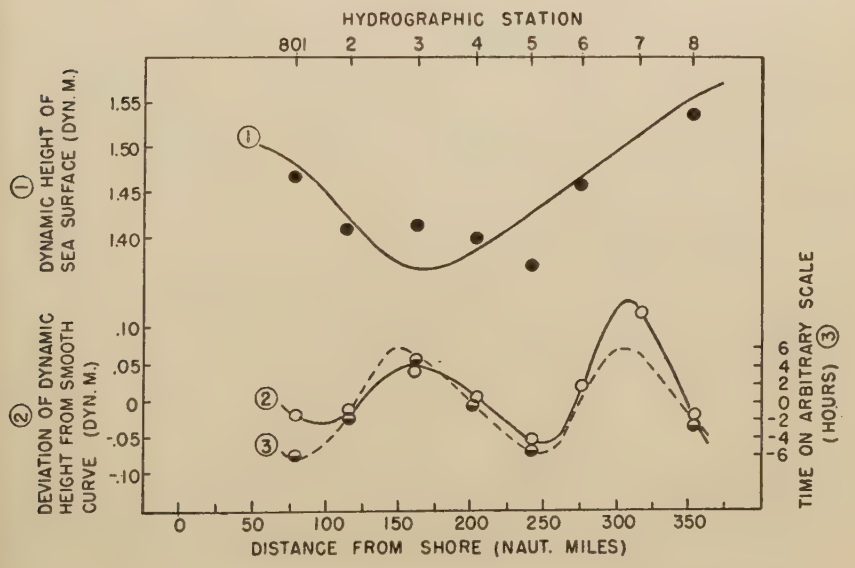

Figure 4. Same as Fig. 3 for stations 801–808.

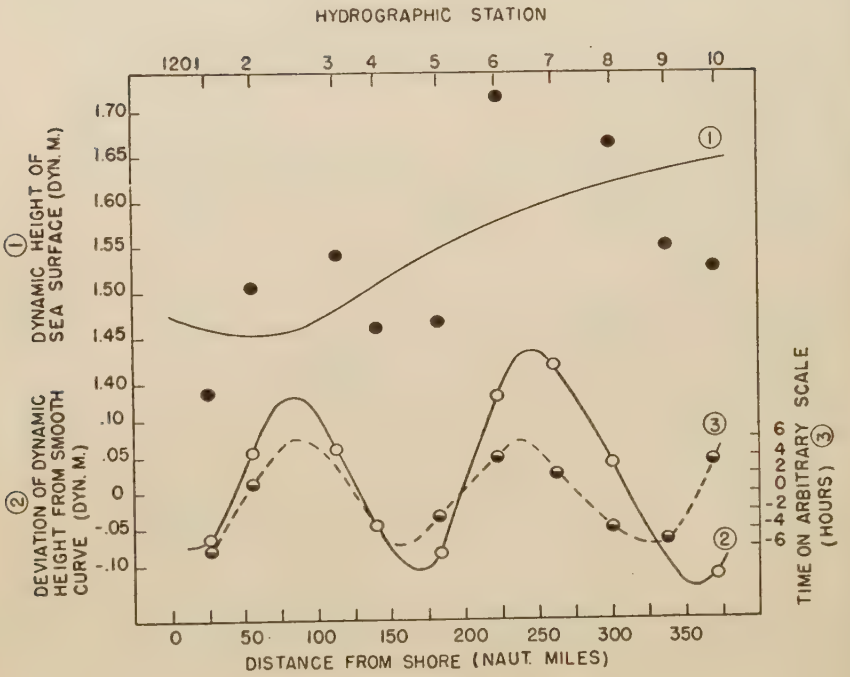

Figure 5. Same as Fig. 3 for stations 1201–1210.

tions at the correct distance from the coast. Through these values we draw a smooth mean curve which corresponds to the average dynamic topography that was prevailing when the profile was made. The deviations from this curve will show the tidal influence. To emphasize this tidal influence, it is advantageous to change the local time to an effective tidal time. We assume that the maximum positive effect of the tide always occurs at + 6 hours, the maximum negative effect at $18^h = -6$ hours, with no effect at 0 and 12 hours. At n hours before and after 6 hours the effect is equal, provided conditions are symmetrical. Therefore, this time n is considered as the effective time according to the following scheme:

Tidal time	0^h	1	2	3	4	5	6	12^h	13	14	15	16	17	18
	12^h	11	10	9	8	7		24^h	23	22	21	20	19	
Effective time	0^h	+1	+2	+3	+4	+5	+6	0^h	−1	−2	−3	−4	−5	−6

The effective time is a *relative* measure of tidal influence. The effective times of profiles 500 and 800 are contained in Tables II and

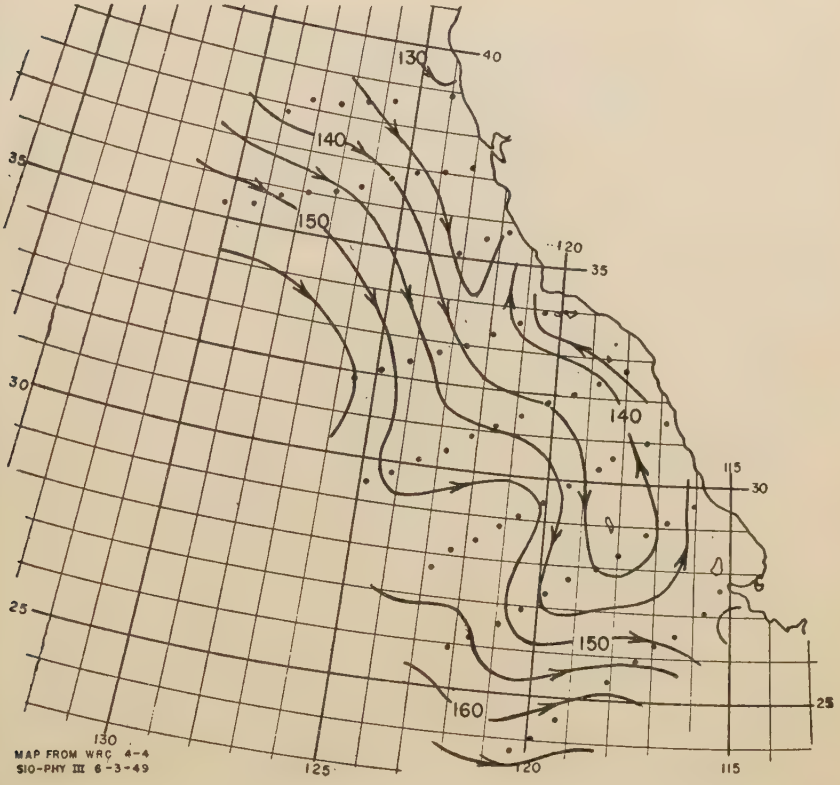

Figure 6. Cruise 1 (Feb. 28 to Mar. 15, 1949): Dynamic height anomalies (0 over 1000 Decibars) after elimination of tidal effect. Contour interval 5 dyn cm.

III. The scale of local time is shifted so that the effective time 6 hours corresponds to the maximum positive effect of tide. The drawing of the mean (basic) curve, the deviations of the station values from this mean curve, and the shift of the time scale, are mutually dependent, and one must seek the best compromise. This might be done quite objectively if the effect of the tide were constant with respect to time and locality, but since this is not the case we have proceeded by trial and error.

The full drawn curve in the lower part of Fig. 3 gives the distribution of deviations from the mean curve, whereas the dashed curve gives the effective times, here incidentally without a displacement of the time scale. The good agreement between both curves shows the relation

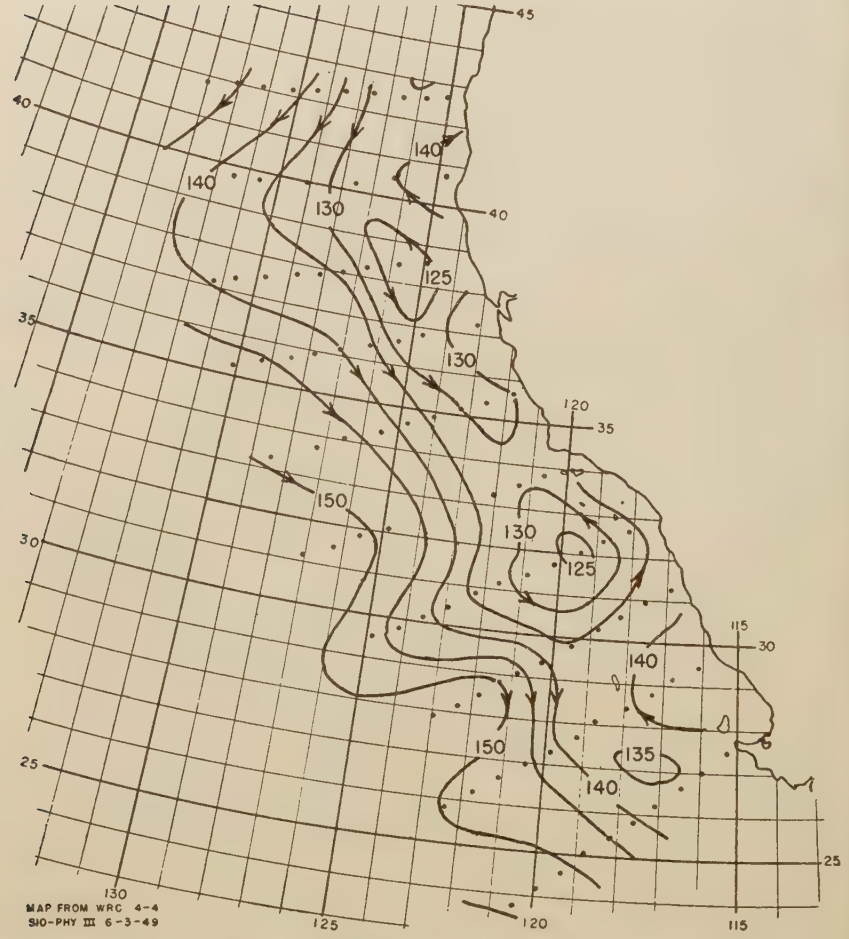

Figure 7. Cruise 2 (Mar. 28 to Apr. 12, 1949): Dynamic height anomalies (0 over 1000 Decibars) after elimination of tidal effect. Contour interval 5 dyn cm.

between deviations and tides. The profiles 800 and 1200 (Figs. 4 and 5) have been analyzed in the same manner, except that it was necessary to shift the time scale. Not all profiles show equally good agreement, and it is often necessary to adjust the basic curve repeatedly in order to reach the best compromise. In trying to make the curves of the deviations correspond to the curves of effective times, no attention should be given to the amplitude of the time curve, for the values are

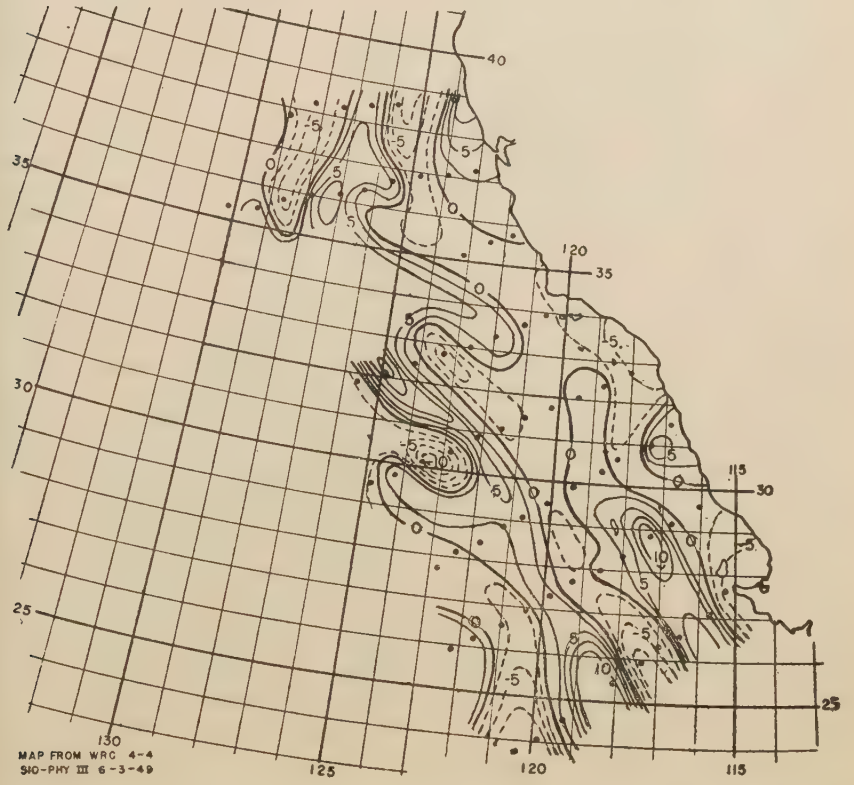

Figure 8. Distribution of deviations in dynamic heights caused by tides for Cruise 1 (0 over 1000 Decibars). Tidal effect: + above, − below the mean dynamic topography. Contour interval 2½ dyn cm. Full curves +, dashed curves −.

relative. Only the position of maxima and minima and the point of inflexion should coincide. In most cases this can be achieved, but the accuracy of the quantities, which have to be shifted, is ± 1 hour at most.

If there is a definite semidiurnal effect in the deviations of station values from the basic curve, then it is necessary to subject these values to harmonic analysis if we wish to designate this effect as a tidal effect and if we wish to separate semidiurnal and diurnal influences from one another. The work connected herewith increases considerably but it can hardly be avoided.

In this manner all of the profiles of a cruise can be analyzed so that

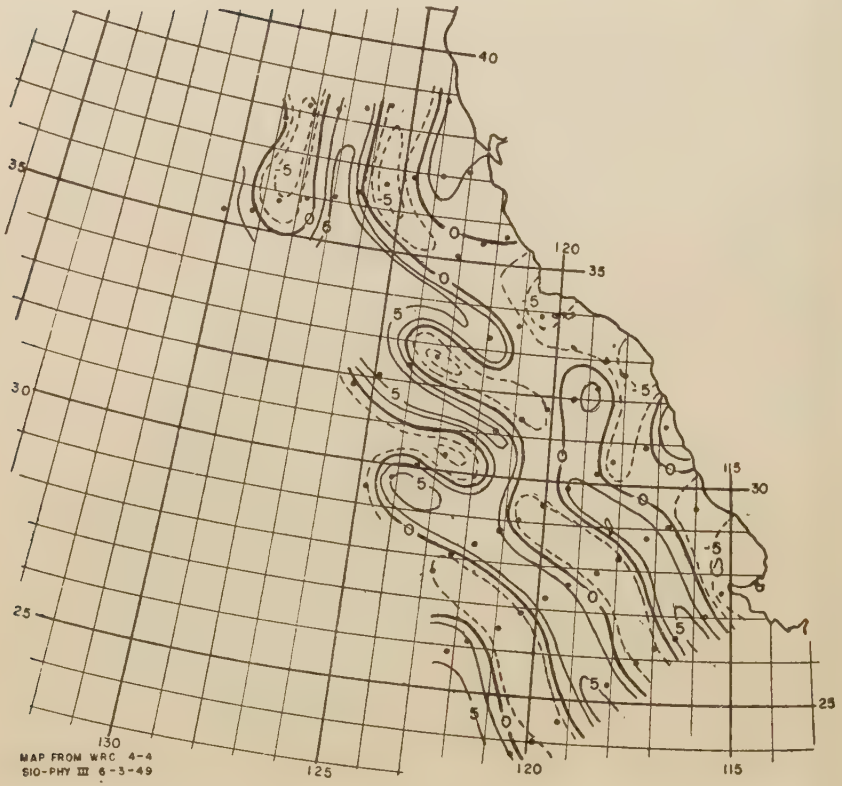

Figure 9. Time of stations (Cruise 1) expressed in effective time (6^h = maximal positive, -6^h = maximal negative effect). Contour interval $2\frac{1}{2}^h$.

one obtains the dynamic topography of the sea surface with tidal influences eliminated. The individual values of stations of the first cruise for the distribution of dynamic heights above 1000 decibars are shown in Fig. 6. In this figure one notices at once the extent of simplification. Off the entire California Coast, at a distance of 100–150 n.m., there is a trough where the physical ocean surface is low; toward the open ocean and toward the coast the surfaces rise fairly uniformly, which correspond to the California Current in a SSE direction on the one hand and to a coastal countercurrent to the NNW just off the coast on the other hand. The trough between both currents is probably connected with the phenomenon of upwelling and will be subject to variations.

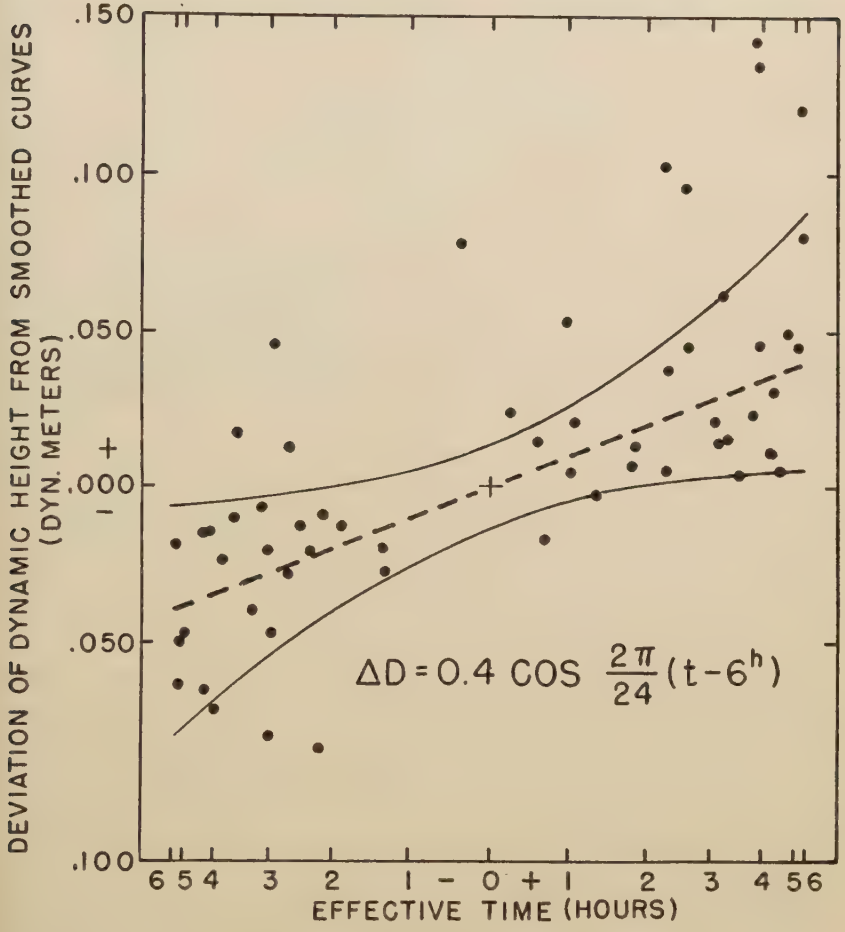
DEVIATION OF DYNAMIC HEIGHT FROM SMOOTHED CURVES (DYN. METERS)
.150
.100
.050
+ .000 -
.050
.100
$\Delta D = 0.4 \cos \frac{2\pi}{24}(t-6^h)$
6 5 4 3 2 1 - 0 + 1 2 3 4 5 6
EFFECTIVE TIME (HOURS)

Figure 10. Relation between deviations of dynamic heights from the mean dynamic topography and the effective times.

Once the dynamic charts of all cruises are freed from extraneous influences, the basic data will be available for study of the system of currents off the entire area during intervals between cruises, and it will be possible to go into problems regarding the causes of these variations. That such variations in the dynamic topography actually occur can be seen by a comparison with the dynamic topography of the second cruise (March 28–April 12, 1949), which is given in Fig. 7.

However, we will not go into any further discussion of these variations here.

It may still be of interest to examine the correlation that exists between the disturbances caused by conditions of survey and the effective times that determine the tidal influences. The best approach is to compare charts which indicate the geographical distribution of these two quantities (see Figs. 8 and 9). It will be seen that the appearance of the two charts is similar, and there is no better proof that these disturbances are caused by tides. Theoretically we can expect a relationship of the form $\Delta D = m \cos 2\pi/24\ (t - 6^h)$; such a relationship is actually found (Fig. 10). Approximately, it follows that $m = 4$ dyn cm. Therefore the disturbances caused by the tides can reach a maximum of 8 dyn cm, compared to a difference of 10 dyn cm between the trough and the left-hand side of the current in Fig. 5.

REFERENCES

Defant, Albert

1937. Die ozeanographischen Arbeiten auf der ersten Teilfahrt der Deutschen Nordatlantischen Expedition des "Meteor," Februar bis Mai, 1937. Ann. Hydrogr., Berl., *65*, Sept. Beiheft: 6–14.

1940. Die ozeanographischen Verhältnisse während der Ankerstation des *Altair* am Nordrand des Hauptstromstriches des "Golfstroms" nördlich der Azoren. Ann. Hydrogr., Berl., *68*, Nov. Beiheft, Lief 4: 3–35.

1948. Über interne Gezeitenwellen und ihre Stabilitätsbedingungen. Arch. Met. Geophys. Bioklim., (A) *1* (1): 39–61.

Helland-Hansen, Bjørn

1939. Untersuchungen über die oertlichen und zeitlichen Schwankungen des "Golfstromes" im Norwegischen Meer. Norsk geogr. Tidsskr., *7*.

Leipper, D. F.

1949. Sea temperature in shallow water. Thesis. Scripps Inst. Oceanogr., University of California.

Scripps Institution of Oceanography

1949. Physical and chemical data. Marine Life Research Program, Division III, Physical Oceanography, Division of Chemical Oceanography. Cruise reports 1–5. (mimeo.)

Sverdrup, H. U., M. W. Johnson and R. H. Fleming

1942. The oceans. Prentice-Hall, Inc., New York. 1087 pp.

THE RAY-PARTICLE ANALOGY[1, 2]

By

CARL ECKART

Scripps Institution of Oceanography

ABSTRACT

The similarity between the differential equations governing the motion of a particle and the rays in a wave field is recalled. The two become identical if the particle has unit mass and moves under the action of a potential energy $V = -1/c^2$, where c is the phase velocity of the waves.

In shallow water, the phase velocity of surface gravity waves is $c = (gh)^{1/2}$, where h is the water depth. This suggests the possibility of constructing an analogue computer for tracing the rays in regions of complex bottom topography. A relief map would be constructed, whose surface is at a distance beneath a datum plane that is everywhere inversely proportional to the water depth at the corresponding point. If a ball bearing is allowed to roll on this surface, it will trace out one of the rays, provided that simple precautions are observed in starting its motion.

This analogy can also be used for visualizing the rays in a qualitative fashion by merely inspecting a bottom contour map. Certain relatively unknown wave phenomena are shown to be easily deducible in this manner.

INTRODUCTION

Since the time of Hamilton, it has been known that there is a close analogy between the Newtonian motion of a particle and the refraction rays of light or other forms of wave motion. This analogy is quantitative if a suitable definition of the particle's velocity in terms of the index of refraction is used.

Let c be the phase velocity of the waves, u the velocity of the analogue particle. For simplicity, its mass will be taken to be unity. If the subscripts $_1$ and $_2$ refer to media of different characteristics, then Snell's law of refraction involves the index of refraction

$$n = c_2/c_1 = \sin\theta_2/\sin\theta_1 , \tag{1}$$

where θ_1 and θ_2 are the angles of incidence and refraction.

Our present problem is to determine the forces that must act on the analogue particle in order that its path in space be identical with the ray. If it is not acted on by any force when it is in a homogeneous medium, it will move in a straight line; since the ray is also straight,

[1] This work has been supported by the Beach Erosion Board, Corps of Engineers, Department of the Army.

[2] Contribution No. 469 from the Scripps Institution of Oceanography.

the problem is trivial. However, the direction must be altered when it passes from one medium to another. If the forces experienced during this transition are normal to the interface, its components of momentum parallel to the interface will be the same in both media. Consequently

$$u_1 \sin \theta_1 = u_2 \sin \theta_2 . \tag{2}$$

It remains to arrange matters so that u_1 and u_2 are determined only by the medium. This requires two assumptions: If the particle has a potential energy characteristic only of the medium, the conservation of energy yields

$$\tfrac{1}{2} u_1^2 + V_1 = \tfrac{1}{2} u_2^2 + V_2 = W ;$$

if the analogue particle is always given the same total energy, W, then u_1 and u_2 will be characteristic of the medium, as required.

Then Eq. (2) can be written

$$n = u_1/u_2 = \sin \theta_2/\sin \theta_1 .$$

Consequently, the motion of the analogue particle will trace out the ray if its speed u is inversely proportional to the phase velocity c.

In fact, the calculation just given is the pre-Fresnel theory of refraction, and it was used by Newton and others, including Hamilton, for the design of lenses. When Fresnel successfully used the wave theory of light to explain diffraction phenomena, Hamilton noted that both theories were consistent with all experiments on the refraction of light, despite the fact that they postulate different velocities of propagation. No direct measurements of the velocity had been made in any optically dense medium, and all indirect measurements were based on the index of refraction. Thus the transition from the one theory to the other involved only a revision of ideas, and no conflict with observed fact.

His attention having been attracted to the ray-particle analogy, Hamilton examined it for possible application to the dynamics of a particle. This led him to the discovery of the principle of least action, which is basic in modern dynamical theory (Hamilton, 1828–1837; Klein, 1926). It is of interest to note also that Louis de Broglie (1924) retraced this train of thought in the reverse direction and obtained results of the greatest importance for atomic physics.

This analogy between rays and the paths of particles has not been used in the theory of surface gravity waves. Without suggesting that it will be found to have any other significance than an analogy, on which it may be feasible to construct an analogue computer, it seems desirable to examine it in more detail.

THE GENERAL ANALOGY

According to Fermat's principle, the rays (i. e., orthogonals to the surfaces of equal phase) are curves in space along which the point of intersection (phase-point) with the moving phase surface travels with the velocity $c\,(x, y)$. If a ray joins the fixed points A and B in space, the time required for the phase-point to move from A to B is therefore

$$T = \int_A^B ds/c(x, y)\,, \tag{3}$$

where ds is the element of length on the ray. Moreover, for given A, B, and $c\,(x, y)$, T is an extremum (often a minimum) for the ray. That is, all paths of integration that differ only slightly from the ray yield values of T that are either all greater or all less than that for the ray.

Let the equation of the ray be given in the parametric form

$$\begin{aligned} x &= x\,(\tau)\,, \\ y &= y\,(\tau)\,, \end{aligned} \tag{4}$$

where τ is some parameter, which can be specified later in various ways. Then it follows from the above that the differential equations of the ray are

$$\begin{aligned} \frac{d}{d\tau}\left(\frac{1}{uc}\frac{dx}{d\tau}\right) - u\frac{\partial}{\partial x}\left(\frac{1}{c}\right) &= 0\,, \\ \frac{d}{d\tau}\left(\frac{1}{uc}\frac{dy}{d\tau}\right) - u\frac{\partial}{\partial y}\left(\frac{1}{c}\right) &= 0\,, \end{aligned} \tag{5}$$

where

$$u^2 = \left(\frac{dx}{d\tau}\right)^2 + \left(\frac{dy}{d\tau}\right)^2. \tag{6}$$

Since the parameter τ is arbitrary, it may be defined by the differential equation

$$u^2 c^2 = 2\,. \tag{7}$$

With this definition, the parameter τ is measured in units sec cm^{-2}, and Eq. (5) becomes

$$\begin{aligned} \frac{d^2x}{d\tau^2} - \frac{\partial}{\partial x}\left(\frac{1}{c^2}\right) &= 0\,, \\ \frac{d^2y}{d\tau^2} - \frac{\partial}{\partial y}\left(\frac{1}{c^2}\right) &= 0\,. \end{aligned} \tag{8}$$

These are quite analogous to those for a particle of unit mass moving under the action of the potential energy

$$V = -1/c^2 . \tag{9}$$

The total energy of the particle is therefore

$$W = \tfrac{1}{2}u^2 - 1/c^2 . \tag{10}$$

There are two minor exceptions to this analogy. 1) The independent variable is the parameter τ and not the physical time, and consequently the time (in τ-units) required by the analogue particle to move along the ray from A to B will not be given by Eq. (3). This corresponds to the fact that a measurement of the velocity of light would have decided between the two theories. 2) Because of Eq. (7), $u = \sqrt{2}/c$ and hence the total energy of the analogue particle must be zero and therefore cannot have arbitrary values. This corresponds to the fact pointed out in the Introduction that it was necessary to suppose that the analogue particle is always started with the same total energy.

THE FEASIBILITY OF AN ANALOGUE COMPUTER

The phase velocity c of surface gravity waves varies with the depth of water and with the period. For a given period the contours of equal velocity thus coincide with those of equal depth. Imagine a relief map constructed so that its depth below a horizontal datum plane is not water depth but rather (to some suitable scale) $1/gc^2$, where g is the acceleration of gravity. Further, imagine a particle of unit mass that is capable of sliding on this surface without friction and that is launched from rest by sliding down a frictionless trough from the datum level to a point on the surface. After the particle leaves the trough its motion will be governed by Eq. (7) and (8), and therefore it will trace the ray. It should be noted that, in this model, τ becomes the physical time and that time t of the wave theory does not appear.

Such a frictionless sliding particle may be approximated by a rolling sphere, provided its radius is so small that its rotational kinetic energy is negligible compared to its translational kinetic energy. The feasibility of using small ball-bearings for this purpose has been established in connection with analogue computers in other fields.

However, there are other difficulties. Because of the dispersion of deep water waves, it seems necessary to construct one relief map for each wave period to be studied; this might be overcome by tracing the rays graphically in those regions where the water is not so deep that refraction is negligible nor yet so shallow that the dependence of c on wave period is negligible. It would then be necessary to construct

only one relief map for the shallow water regions, where refraction is most marked and most difficult to determine by graphical methods.

In shallow water,

$$c^2 = gh\,,$$

where h is the water depth. Hence the ordinate of the relief map would be inversely proportional to the water depth. As the beach is approached, the map would have an ever increasing slope and the particle would leave the surface and fall freely through the air before the "water's edge" was reached. It is possible that a proper choice of design parameters can minimize the effect of this error until it is negligible as compared with other errors arising from the neglect of phenomena occurring in the surf zone.

Even if the physical construction of such analogue computers is not feasible, the analogy may still be used in visualizing the effect of bottom topography on the propagation of waves. For example, a submarine canyon will be represented on the relief map by a spur-like ridge pointing toward the shore. The action of the ridge in deflecting the analogue particles away from those parts of the beach close to the canyonhead will be obvious immediately. Also, the course of rays entering a harbor through a narrow channel can be easily visualized. In the analogue, the underwater ridge extending seaward from a promontory becomes a trough that guides the analogue particles so that they can hardly avoid striking the beach near its most seaward point.

Furthermore less well known phenomena can be readily visualized. Thus the shoal water over a bar would be represented by a depression on the relief map. Immediately it becomes clear that the analogue particle, if it enters the depression in a suitable manner, may execute several oscillations before escaping or may even describe a path that intersects itself several times. Furthermore, it becomes apparent that waves generated in shoal water, if they approach a continental shelf at a steep angle, may be totally reflected from the deep water regions (i. e., from the higher regions of the analogue relief-map). These effects, and the limitations of ray theory in dealing with them, are being discussed elsewhere.

REFERENCES

Hamilton, W. R.

1828. Theory of systems of rays. Trans. R. Irish Acad., *15:* 69–174.

1830. Supplement to an essay on the theory of systems of rays. Trans. R. Irish Acad., *16:* 4–61.

1837. Third supplement to an essay on the theory of systems of rays. Trans. R. Irish Acad., *17:* 1–144.

DE BROGLIE, LOUIS
1924. Recherches sur la théorie des quanta. Thêse, University of Paris.

KLEIN, FELIX
1926. Vorlesungen über die Entwicklung der Mathematik im 19 Jahrhundert. Grundlehr. Math. Wiss., *24* (1), chap. 5. Julius Springer, Berlin. 385 pp. (Also in, Gesammelte Mathematische Abhandlungen, Vol. 2: 601. Julius Springer, Berlin, 1922. 713 pp.)

A STUDY OF MIXING PROCESSES OVER THE EDGE OF THE CONTINENTAL SHELF[1]

By

ARTHUR R. MILLER

Woods Hole Oceanographic Institution

ABSTRACT

By means of T-S area diagrams, a method of analysis is developed for the study of closely spaced hydrographic data. In a transitional zone, such as that over the continental shelf off southern New England, this method is useful for following the continuity of the mixing process. Changes in salinity at the edge of the shelf are due, for the most part, to horizontal advection. There are indications of nonisentropic mixing on a smaller scale. From the turbulent features of the region, as indicated by instabilities, this condition is not unexpected.

INTRODUCTION

The edge of the continental shelf off the northeastern coast of the United States is a region where unlike water masses meet. In this paper a study of these waters is attempted by tracing their origin and following their transformation over the shelf.

The 100-fathom curve, coincident with the edge of the continental shelf, is considered to be the general boundary between coastal and oceanic water (Iselin, 1939). However, the actual boundary is poorly defined, since each water mass is found occasionally in the other's territory; this variability is fairly well known (Bigelow, 1933; Bigelow and Sears, 1935; Bumpus, 1948). The mean of the fluctuations follows approximately the 100-fathom contour, and for this reason the location is strategic for observing the exchange between coastal and oceanic waters. In general, according to Iselin (1939), a semipermanent circulation exists parallel to the shelf due to differences in density between the two water masses. The fresher coastal water, being normally the lighter of the two, tends to flow over the other, but it is deflected to the right by Coriolis' force. Along the northwestern Atlantic shelf a southwesterly drift usually prevails. At times, the difference in density is small and even vanishes. The winds are free then to shift large masses of water away from or into the area.

Another feature of the shelf circulation is the apparent existence of offshore-onshore components to the general drift, these being suggested

[1] Contribution No. 518 from the Woods Hole Oceanographic Institution.

by the evident salt exchange across the shelf. With depth, the salinity of the coastal water usually increases whereas that of the oceanic water decreases (Iselin, 1939). The offshore-onshore movement is accounted for in at least two different ways. Compensatory exchange may occur across the boundary as one mass moves out and another enters. Possibly this is of intermittent or sporadic occurrence depending on temporary local conditions. Small-scale mixing may occur at the boundary with a steady exchange of salt between the two masses.

METHOD OF SOLUTION

Were it not for the shallowness of the region, a logical tool for tracing the origin and transformation of waters over the shelf would be the widely used Temperature-Salinity correlation method (Helland-Hansen, 1918; Jacobson, 1929; Stockmann, 1946). In most cases the use of this method in shallow waters is inadvisable because, over a period of time, local factors such as evaporation, precipitation, and solar radiation influence the water (Tibby, 1941; Pollak, 1947). Nevertheless, in a limited area, in which mixing processes are proceeding rapidly relative to the disturbing influences of these factors, the method may supply useful information provided nearly synoptic data are employed.

DATA

The usefulness of the method has been tested by the treatment of observations sufficient in number to describe the water in the area. Hydrographic data across the edge of the continental shelf in the vicinity of Hudson Canyon were obtained during several traverses[2] made by the U. S. Fish and Wildlife Service vessel Albatross III in November, 1948 (Fig. 1). These observations were obtained by means of the Sea Sampler (Spilhaus and Miller, 1948), and they were closely spaced in time, distance and depth. For example, a 55-mile traverse was completed in five hours and was comprised of 10 hydrographic stations with an average of 10 observations at each station to depths of about 100 meters. All of the data were collected in one three-day interval.

A continuous bathythermograph trace, together with samples of sea water at each station, was obtained. Density figures were computed from temperatures read at the respective sampling depths (Spilhaus and Miller, 1948). The distribution of temperature, salinity, and

[2] Three sections were made during the cruise. Section III does not cross the shelf, and hence it will not be specifically referred to in this paper.

Figure 1. Chart showing positions of hydrographic stations off the coast of southern New England.

density (sigma–t) along two of the sections is shown graphically in Figs. 4a, 4b, 4c, 5a, 5b, 5c. The use of the bathythermograph trace in accurate hydrographic analysis is usually minimized to the extent that its chief worth is considered to be in the relative values of a single BT observation. Once confidence is gained in the consistent performance of an individual instrument, however, a sequence of BT observations becomes particularly valuable. Since the Sea Sampler had been calibrated recently, it was estimated that the temperature curves were accurate to $\pm 0.2°$ F. The water samples were titrated for salinity with an accuracy of $\pm 0.03‰$.

ANALYSIS

Before attempting to analyze the data, a basic theorem of the T-S correlation method is restated: "Water masses homogeneous in respect to temperature and salinity are represented by single points. Different water masses formed by mixing of two homogeneous water masses will be found in the diagram lying in a straight line" (Jacobsen, 1929). Straight-line mixing is the keynote of the following analysis.

Temperature-Salinity Correlations. Fig. 2 shows the observations plotted as a Temperature-Salinity diagram. The superimposed curve to the right of the observations represents the characteristic Slope Water curve for December (Iselin, 1936) near the area under observation. It defines the upper limits of salinity for water of a given temperature in the area.

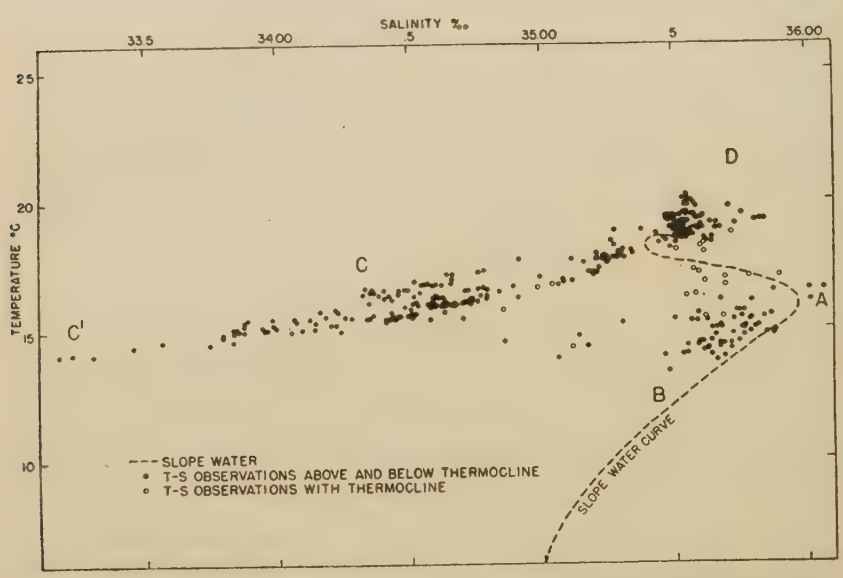

Figure 2. Distribution of observations on a T-S diagram. Dashed line is descriptive of slope water characteristics.

There are at least two different water types indicated by the T-S correlation. The well defined distribution of the warmer water (C′C D)[3] may be interpreted as the result of coastal water (C′C) mixing with the surface oceanic water (D). The source of the cooler

[3] C′C are observations taken well inshore from the edge of the shelf and are not of primary importance in the coastal-oceanic water exchange.

water (AB) is not as clear; from its distribution near the slope water curve, this subsurface water (AB) is assumed to be slope water somewhat modified by dilution.

The oceanic water observed in the shelf region at depths of less than 100 meters is separated into three water types. The cold portion, which is in agreement with Iselin's slope water curve, includes water that occurs normally between 200 and 600 meters (B) in the deeper slope water region (Iselin, 1936). For purposes of definition, parts of the slope water curve shown in Fig. 2 will be named as follows: The warm, saline portion (A) of the curve will be called Intermediate Slope Water, that is, water occurring immediately beneath the thermocline; the cooler, less saline portion (B) will be called Mid-depth Slope Water; the saline, surface water (D) will be called Surface Slope Water. The presence of all three types of water in the upper 100 meters over the shelf is not surprising when one refers to the upward slope of density (sigma–t) lines in profiles crossing the continental slope (Iselin, 1936; Montgomery, 1938).

The supposed sources of water over the edge of the shelf are now defined. The observations shown on the T-S diagram which lie between the slope water curve (AB) and the coastal water (C′C D) are as yet unexplained. Observations made within this area of the diagram, shown by open circles in Fig. 2, came from samples drawn from a sharply pronounced thermocline. From this fact one can deduce a limited transfer between the upper and lower water layers described by that part of the diagram. The remaining intermediate T-S points convey little information at this stage of analysis.

By study of the salinity profiles one can infer some water movement only to have it confused or refuted by the temperature profiles (Figs. 4a, 4b, 5a, 5b). The density (sigma-*t*) profiles (Figs. 4c, 5c) would clarify the situation somewhat if it were not for the unstable stratification (Spilhaus, Ehrlich and Miller, 1949). Apparently, then, a clear understanding of water movement due to mixing over the shelf is not to be gained by the study of these profiles. However, the uncertainty will be less obscure if we analyze the T-S observations in the manner described below.

The Quadrilateral Grid. A means of describing the T-S characteristics of the data by vertical profiles was found by considering the following postulates, which are based on the theorem which represents mixing processes by a straight line, as mentioned previously.

Consider an idealized situation where a given water type is described by a point in a T-S diagram which lies on a straight line between points representing two other water types. The latter types, when

mixed in quantities inversely proportional to the distance of their points from that of the given water type, result in a mixture *identical* with it. In this statement homogeneity of the water type is implied. However, if one associates water type with water mass, homogeneous water, in the absolute sense, would rarely be found in the ocean. On

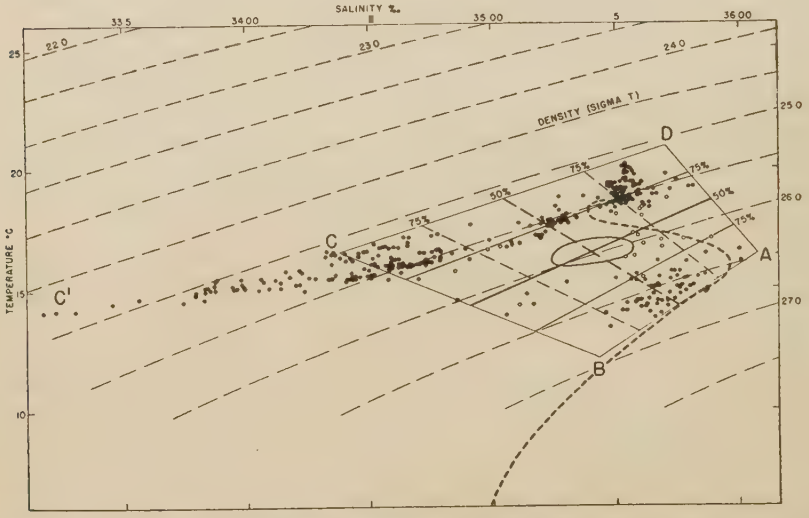

Eigure 3. The quadrilateral grid superimposed over the T-S observations in Fig. 2. Full lines and dashed lines within the grid divide it into 16 rectangular areas. The long dashed lines represent lines of equal potential density.

the other hand, relative homogeneity can be assumed if a water mass is sufficiently described in a T-S diagram by a cluster of observations about an imaginary point. It follows, then, that if the mixing water types can be described by discrete circles enclosing clusters, one obtains a *limited area* bounded by two lines tangent to the circles rather than a line between them.

True homogeneity is lost, but the sense of Jacobsen's postulate is retained in the following: If a given water type in a T-S diagram lies in such an *area* between two other water types, the latter types, when mixed in proper proportion, result in a mixture *similar* to it. From these postulates it is evident that our concept of mixing is not confined to one-dimensional lines. Within reasonable limits, an *area of mixing* is conceived in which two source waters are considered, with intermediary observations being proportional mixtures of these. This is a valid conception provided the intermediary observation has not

acquired its properties through some external influence other than mixing; in this case that influence is assumed to be negligible.

It is clear that an observation in a set of data which does *not* fall in the T-S area between two source waters is *not* a mixture of the two. But assuming that it is a mixture, a third and possibly a fourth water source may be involved. In a region where mixing occurs, one must find in the data those observations which represent more closely the source waters of that region. In this investigation we find four types of water whose characteristics could not be justified as a result of mixing within the area of investigation. These waters were the point sources to which the observations were related.

Four straight lines were drawn between A, B, C, and D (Fig. 3). The corners of the described quadrilateral represent water with definite characteristics, hereafter referred to as primary water *types*.[4] For instance, C represents coastal water; in like manner, D is surface slope water; A, intermediate slope water; and B, mid-depth slope water. All observations within the quadrilateral were assumed to be resultant mixtures of the four primary water types. This assumption is rather bold, for it is quite possible for alien waters to mix and form a type similar to one composed of the four bases. However, some indication of this intrusion would be apparent in the surrounding observations.

The next step was to find the proportions of the basic types in the observed samples. For this purpose the quadrilateral was subdivided proportionally to form a grid containing 16 rectangular areas. Along the line CB, which forms one side of the quadrilateral, observations falling on the segments closest to C contain proportionately more C water than B. Along the line CD the segments closest to C describe mixtures containing more C water than D. A mixture described in the three rectangular areas adjoining the above segments is predominantly C type water, that is, water in which C is greater than 50% of its volume. In like manner the other three types extend their influence over adjoining areas. In the four central rectangular areas the relative contributions of each water type is more ambiguous. It is probable that a given source is the major constituent in the closest central rectangle, but the argument is uncertain in a core about the center. This is not a serious drawback, however, for in actual distribution the volume of water described by this doubtful core is a small part of the whole.

By enclosing the set of observations in a grid constructed on a T-S

[4] Water *type* is used rather than *mass* so that stress will be put on the T-S description of the water rather than on the specific connotation of the word *mass*.

diagram, the assumption was made that all of the observations were products of the mixing of water types represented by the extreme corners of the grid. Since the positions of the grid lines are uniquely determined by the distributions of temperature and salinity along them, it is possible to transfer the grid with correct distortions to a diagram that shows the hydrographic section.

The distribution of the relative water type mixtures in two of the hydrographic sections was drawn in the following manner. By means of bathythermograph temperature curves, continuous T-S curves

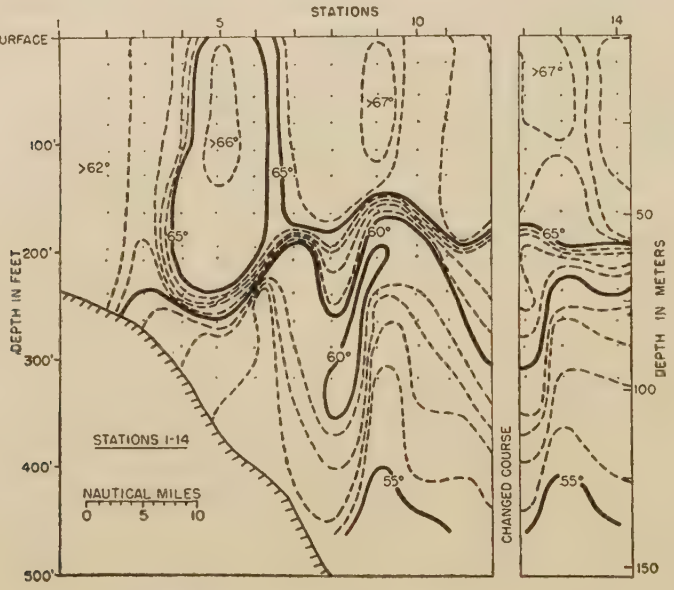

Figure 4a. Section I. Temperature.

for each station were constructed for graphic interpolation between the vertical salinity observations (Stommel, 1947). The depths at which each sample was collected were also marked on the curve. By superimposing each T-S curve on the quadrilateral grid, the depth at which it intersected each grid line was noted. (Comparison of the lines of intersection with the temperature curve was useful for obtaining accurate depth.) These depths were plotted in vertical sections whose coordinates were distance and depth. Finally, lines corresponding to the grid lines were drawn through their respective depths in the sections. The areas bounded by these lines represent water types with ranges of definition in accord with those of the master

grid. The final profiles for Sections I and II are shown in Figs. 4d, 5d.

It is easy to visualize the T-S description of the water in each section by imagining that the grid is placed on an elastic sheet which is pulled and pushed in such a way that the grid lines of definition finally take the shape represented in the figures. In this analogous operation it would be difficult to conceive the sequential relations being interrupted. A face on a rubber balloon is still a face no matter what the distortion.

The continuity of the method provides a means for detecting errors in observations. If observations do not fit the grid pattern, then they

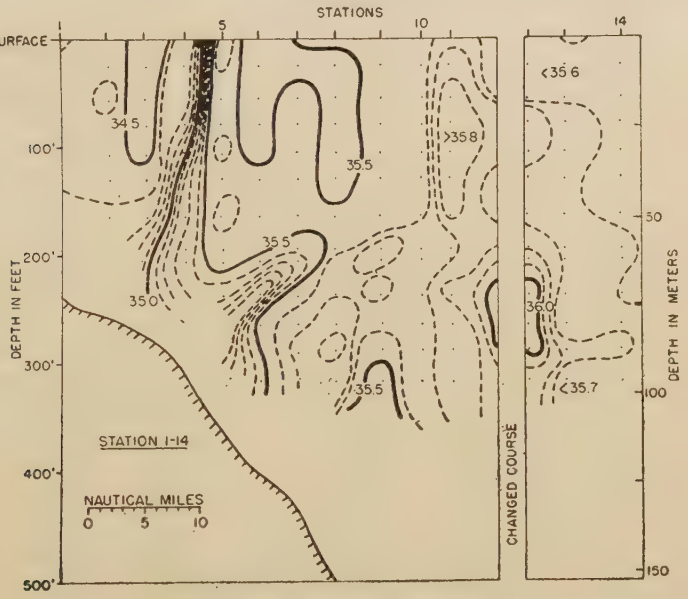

Figure 4b. Section I. Salinity.

should be questioned just as they would be in other methods of analysis. On the other hand, there were observations in the data whose authenticity was not confirmed by ordinary T-S analysis (Sverdrup, Johnson and Fleming, 1942). However, continuity of the grid pattern was fulfilled by including these observations. The finer details of the water type sections (Figs. 4d, 5d) are examples. (In all of the sections no data were omitted.) It would seem that the method has some analytical value in this respect.

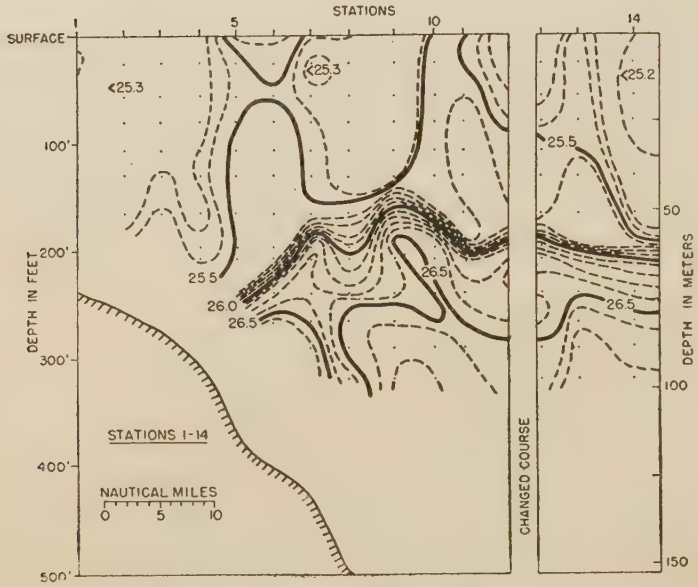

Figure 4c. Section I. Density (sigma-*t*)

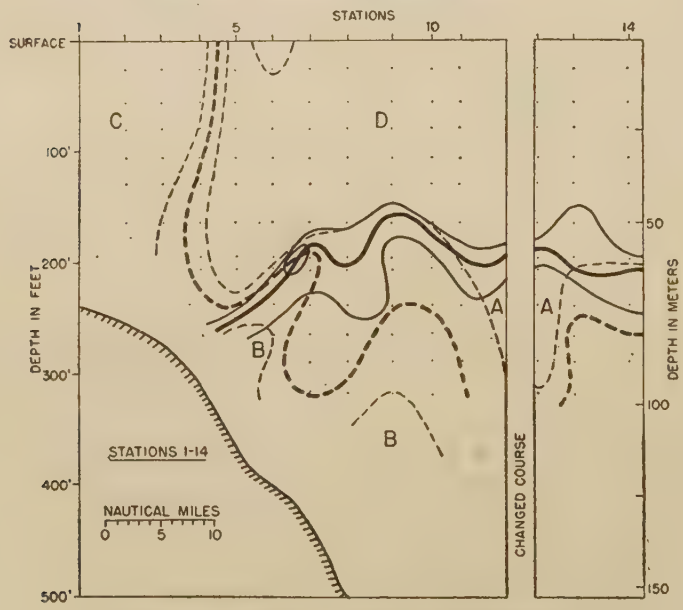

Figure 4d. Section I. Water type distribution.

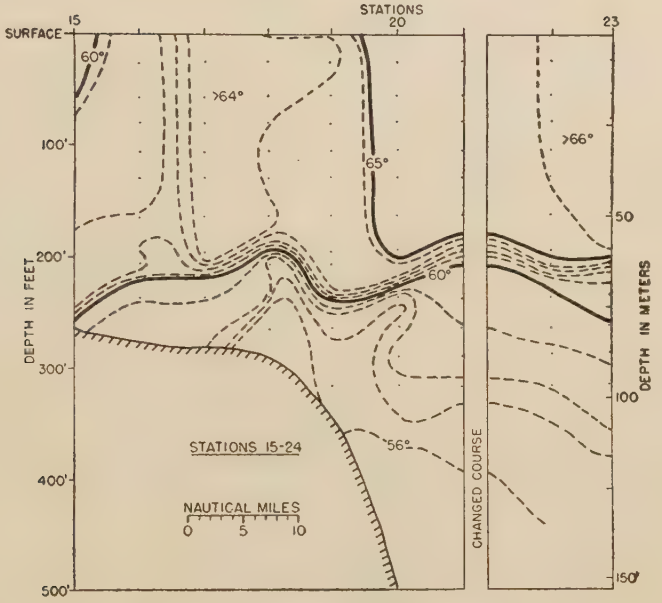

Figure 5a. Section II. Temperature.

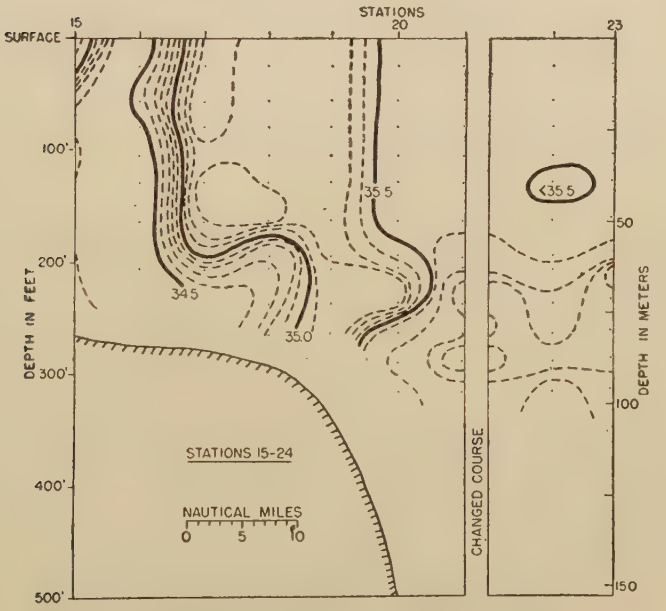

Figure 5b. Section II. Salinity.

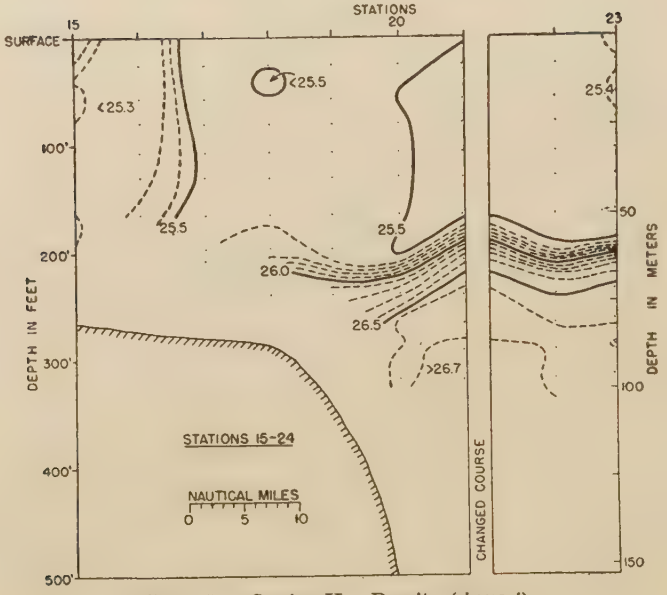

Figure 5c. Section II. Density (sigma-*t*).

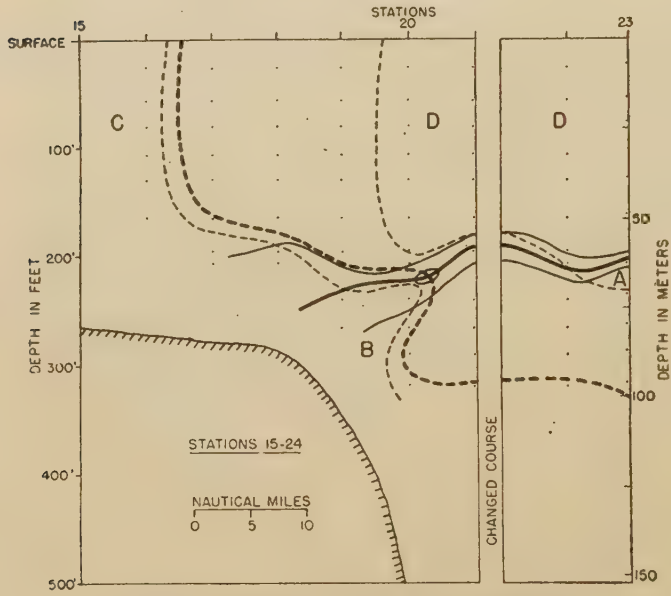

Figure 5d. Section II. Water type distribution.

CONCLUSIONS

By considering a set of observations as resultant mixtures of primary water types, a relation between the observations is established through their T-S characteristics. Those observations which are most similar to the basic water types are assumed to represent the source water in the region. This assumption is valid if the base has an extreme value of salinity or temperature, since it, in turn, must have its source outside the region that is being studied. By observing the character of the mixtures one is able to follow the mixing paths in a set of data.

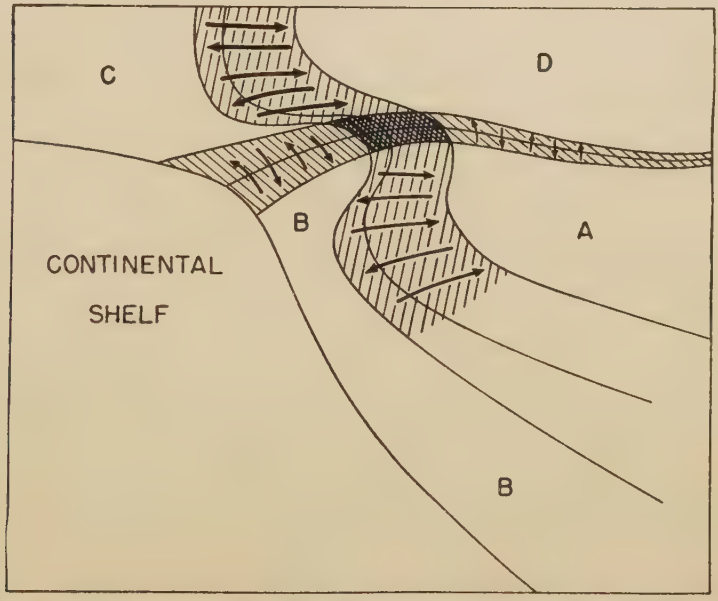

Figure 6. Schematic representation of the Water Type distribution near the edge of the continental shelf. Shaded areas are those in which intermediate mixtures occur; arrows show paths of exchange between water types.

Fig. 6 summarizes the water distribution for both sections. The shaded portions represent the areas of transitions between the water types. The transition from oceanic slope water to coastal water is accompanied by an apparent upwelling of the deep mid-depth slope water. This seems to occur in sufficient volume to effectively bar the intermediate slope water from taking an important part in the mixing process. This water, type A, occurs only at the most seaward hydrographic stations. The mixtures between A and B are not

necessarily local phenomena, since water with like characteristics is indicated in the seaward stations.

Major transfer takes place between the surface slope water and the coastal water. This is suggested by the relative volume of the mixed C and D water. It is a condition to be expected because the density differences are small between these two types. On the other hand, where the density differences are great, an appreciable exchange occurs between the "upwelled" water and the coastal water. This nonisentropic mixing suggests an internal energy source which may be localized at the edge of the shelf, for it does not appear to break up the sharp density gradient between the surface and intermediate slope waters where the density difference is smaller.

In this set of data it is seen that the boundary between oceanic and coastal waters is sharply defined and is in the neighborhood of the 50 fathom rather than the 100 fathom curve (Figs. 4d, 5d). Extending seaward from this boundary is a long, slender, subsurface tongue, which is a mixture of coastal, surface slope and mid-depth slope water. Hachey (1934) has shown a similar tongue in a laboratory experiment that demonstrates an intermediate movement of mixed water away from a mixing area. The fact that this tongue retains its identity over a distance of 5 to 10 miles is noteworthy. One would expect the turbulence and instability of the region to effectively destroy the thin layer in a short period of time. However, the tongue persisted over a three-day period for a distance of at least 40 miles along the edge of the continental shelf. It is probably a primary mixing effect which is maintained as long as there is sufficient water of a suitable type to replenish the particular mixture.

The juxtaposition of the steady state, as evidenced by the tongue, and the turbulence shown by instabilities, has a plausible explanation in an internal surf process such as that described by Defant (1948). In his laboratory tank experiments, where a two-layered medium was used, internal breakers were produced at the interface while the surface remained undisturbed. This experiment is analogous in some respects to the condition found over the edge of the shelf.

Although we have no direct internal wave measurements, we do have a combination of circumstances which point strongly to the occurrence of an internal surf process at the edge of the continental shelf. The nonisentropic mixing is a final outcome of the process and is better understood when one considers that we are dealing with a many-layered medium, the layers of which are converging on the edge of the shelf. An internal wave traveling in the direction of the shelf is affected by the slope and is upset at the edge so that its energy is expended in mixing water types of different density. In this manner

type B or mid-depth slope water becomes mixed with the surface layers.

The mixing mill at the edge of the shelf must be supplied with grist to grind, or otherwise it must run down. Also it must have a means to carry off the final product or else die out. Coastal water and surface slope water are the principal ingredients. It is a fair assumption that the mixed product is carried off in the general southwesterly drift. However, type B water must necessarily be replenished from deeper sources in order to maintain its effectiveness, and a certain amount of water must be carried off to compensate for the intrusion of type B water. It is suggested that the long tongue is the direct path by which excess water is drawn off.

It has been emphasized that type B has had its origin in greater depths offshore. Furthermore, it is assumed that it upwelled at the shelf. The assumption is likewise justified by oxygen analyses (not shown) which show that this water is low in oxygen content (about 3 ml/L). This water is raised to the 100 m. level, stirred at the edge of the continental shelf and added to the surface layers to become part of the coastal and surface oceanic circulation.

There are no indications to suggest that this upwelling is directly induced by the wind. The scope of this investigation is too limited to suggest a cause for upwelling other than that obtained in the general dynamics of oceanic circulation. The fact that it does occur is biologically significant because of the nutrient value of upwelled water.

ACKNOWLEDGMENT

The writer wishes to extend his thanks and appreciation to Alfred C. Redfield for his time, interest, and assistance in the preparation of this paper.

REFERENCES

Bigelow, H. B.
1933. Studies of the waters on the continental shelf, Cape Cod to Chesapeake Bay. I. The cycle of temperature. Pap. phys. Oceanogr., *2* (4): 1–135.

Bigelow, H. B. and Mary Sears
1935. Studies of the waters on the continental shelf, Cape Cod to Chesapeake Bay. II. Salinity. Pap. phys. Oceanogr., *4* (1): 1–94.

Bumpus, D. F.
1948. Hydrography of the western Atlantic. W. H. O. I. Tech. Rep., No. C-1: 1–31.

Defant, Albert
1948. Über interne Gezeitenwellen und ihre Stabilitätsbedingungen. Arch. Met. Geophys. Bioklim., (A) *1* (1): 39–61.

Hachey, H. B.
1934–35. Movements resulting from mixing of stratified waters. J. biol. Bd. Canad., *1* (2): 133–143.
Helland-Hansen, B.
1918. Nogen Hydrografiske Metoder. Forh. skand. naturf. Møte, 16: 357–359.
Iselin, C. O'D.
1936. A study of the circulation of the western North Atlantic. Pap. phys. Oceanogr., *4* (4): 1–101.
1939. Some physical factors which may influence the productivity of New England's coastal waters. J. Mar. Res., *2:* 74–85.
Jacobsen, J. P.
1929. Contribution to the hydrography of the North Atlantic. The Danish Dana Exped. 1920–22, Vol. *1*, No. 3. 98 pp.
Montgomery, R. B.
1938. Circulation in upper layers of southern North Atlantic deduced with use of isentropic analysis. Pap. phys. Oceanogr., *6* (2): 1–55.
Pollak, M. J.
1947. Hydrography of the western Atlantic; Hydrography of the subsurface slope water. W. H. O. I. Tech. Rep., No. 5: 1–15.
Spilhaus, A. F., A. Ehrlich, and A. R. Miller
1949. Hydrostatic instability at the edge of the continental shelf. Presented at 30th Ann. Meet. A. G. U. (to be published).
Spilhaus, A. F. and A. R. Miller
1948. The sea sampler. J. Mar. Res., *7:* 370–385.
Stockmann, W. B.
1946. A theory of *T-S* curves as a method for studying the mixing of water masses in the sea. J. Mar. Res., *6:* 1–24.
Stommel, Henry
1947. Note on the use of the *T-S* correlation for dynamic height anomaly computations. J. Mar. Res., *6:* 85–92.
Sverdrup, H. U., M. W. Johnson and R. H. Fleming
1942. The oceans. Prentice-Hall, Inc., N. Y. 1087 pp.
Tibby, R. B.
1941. The water masses off the west coast of North America. J. Mar. Res., *4:* 112–121.

NOTE TO AUTHORS

The pages of this Journal are open to all contributors, and manuscripts may be submitted to any member of the Board of Editors or to the Managing Editor. Publication will be made only in the English language, but copy may be submitted for consideration in other languages. Aid in translation of accepted manuscripts will be given when possible.

All manuscripts should be typewritten with double space, carefully corrected, with footnotes continuously numbered and set off in the body of the text. If an article is to appear as a contribution from another institution, it should be approved by that institution before submission; contribution numbers of such institutions are submitted with the return of galley proofs.

The author (or authors) of each article will receive a total of 50 free reprints (with covers). Additional reprints with or without covers may be ordered by authors or institutions at the cost of printing. Orders for reprints are given when galley proofs are returned.

Both galley and page proofs are submitted to the senior author of each article.

Tables should be prepared for clarity and as near as practicable to Journal pattern, without ruled lines if possible. Table footnotes should appear at the base of each Table.

Figures are required for consideration simultaneously with the manuscript. Original figures of inconvenient size for forwarding may be represented by photographs on first submission of a manuscript; originals are required for line cuts. Illustrations requiring half-tone reproduction should be avoided as far as possible, but they will be accepted when necessary. *It is very important that the proper size of characters and symbols should be used for the lettering of illustrations.* A diagram for determining suitable heights of letters for original drawings that will be reduced, together with an explanatory note, has been published in this Journal, Vol. III, No. 1: 89–91; reprints will be submitted to authors on request. Mechanical lettering is recommended. If facilities for lettering are not available to the author, it is preferable to receive illustrations with lettering indicated in pencil only, to be finished in ink in the editorial office. All illustrations will be subject to at least a minimum reduction at the rate of 1 : 1.2. Drawings which have been heavily patched and pasted must *not be rolled* for mailing. The legends for the figures, identified by corresponding figure numbers on the illustrations also, should be typed in sequence at the end of the manuscript.

A complete and *accurate list of references* in alphabetical order at the end of each article is essential. References may be indicated in the text by author's name (or names) and *year of publication*, or by italicized numbers which correspond to the numbers given in sequence in the list of references. Each reference should include the last name followed by at least two initials or first name; co-authors should be listed with the initials or first name preceding the last name. The date should be indented on the line below, followed by a complete title *verbatim* in lower case except for the first word. Publisher, city and pagination should be indicated for books; for periodicals (abbreviations from "World List of Scientific Periodicals," Oxford, as far as possible), the volume (italicized), number and pagination should be given.

Additional information regarding the preparation of manuscripts will be furnished by the Managing Editor.

TABLE OF CONTENTS

	Page
1. **Koji Hidaka**: Lateral mixing and wind-driven currents in an enclosed ocean	55
2. **E. Y. Dawson**: A note on the vegetation of a new coastal upwelling area of Baja California	65
3. **R. S. Dietz and E. C. LaFond**: Natural slicks on the ocean	69
4. **A. H. Woodcock**: Subsurface Pelagic *Sargassum*	77
5. **W. S. von Arx**: Some current meters designed for suspension from an anchored ship	93
6. **R. A. Geyer**: The occurence of pronounced salinity variations in Louisiana coastal waters	100
7. **Albert Defant**: On the origin of internal tide waves in the open sea	111
8. **Albert Defant**: Reality and illusion in oceanographic surveys	120
9. **Carl Eckart**: The ray-particle analogy	139
10. **A. R. Miller**: A study of mixing processes over the edge of the continental shelf	145

NOTICE

The PREVENTION OF DETERIORATION ABSTRACTS, published by the National Research Council (Prevention of Deterioration Center, Room 204), 2101 Constitution Avenue, Washington 25, D. C., are offered for subscription on a yearly basis. Abstracts are classified under the headings: Biological agents; Electrical and electronic equipment; Fungicides and other toxic compounds; Lacquers, paints, and varnishes; Leather; Lubricants; Metals; Miscellaneous; Optical instruments and photographic equipment; Packaging and storage; Plastics, resins, rubbers, and waxes; Textiles and cordage; and Wood and paper. One volume of approximately 2000 loose-leaf pages is published each year in monthly issues. Subject and author indexes are compiled annually to cover abstracts issued from July through June. The yearly rate of $50.00 includes two sturdy binders and index tabs.

An ADVANCE LIST, a monthly bibliography of all reports received in this field, is available for $10.00 a year.